SELECTION AND CHARACTERIZATION OF ANTIBODIES BLOCKING THE ENZYMATIC ACTIVITY OF THE TUMOUR ASSOCIATED CARBONIC ANHYDRASE IX

Dissertation

zur

Erlangung der naturwissenschaftlichen Doktorwürde
(Dr. sc. nat.)

vorgelegt der

Mathematisch-naturwissenschaftlichen Fakultät

der

Universität Zürich

von

Margarita Theresa Murri-Plesko

von

Winterthur (ZH)

Promotionskomitee

Prof. Dr. Christoph Renner (Vorsitz und Leitung der Dissertation)
Prof. Dr. Roland Wenger
Prof. Dr. Holger Moch

Zürich, 2011

ZUSAMMENFASSUNG

Solide Tumoren sind oft schlecht durchblutet. Dadurch haben sie eine verringerte Zufuhr an Sauerstoff und Nährstoffen, wodurch ihr Wachstum limitiert wird. Sauerstoffmangel führt zu Änderungen in der Genexpression – hauptsächlich des Hypoxie-induzierbaren Faktors (HIF) – welche es den Krebszellen erlauben, sich an einen tiefen Sauerstoffgehalt anzupassen. Eines dieser Zielgene ist Carboanhydrase IX (CA IX), ein Transmembranprotein mit extrazellulärer Domäne, welche die reversible Hydratisierung von Kohlenstoffdioxid zu Hydrogencarbonat und Protonen katalysiert. CA IX wird hauptsächlich im Tumorgewebe exprimiert und nur sehr selten in gesundem Gewebe, wie z.B. dem gastrointestinalen Trakt. Die katalytische Aktivität erleichtert das Wachstum von Tumoren durch Senkung des extrazellulären pHs und Neutralisierung des intrazellulären pHs. Dadurch ist CA IX einerseits ein vielversprechender Marker für Tumortargeting und andererseits ein mögliches Ziel für eine die CA IX Aktivität inhibierende Tumortherapie. In der Klinik werden mehrere synthetische Stoffe eingesetzt, welche die CA IX Aktivität inhibieren. Da diese aber auch mit anderen Carboanhydrase Isoformen interagieren, haben sie häufig schwere Nebenwirkungen, und ihr Einsatz in der Klinik ist limitiert. Daneben verwendet man Antikörper, die CA IX sehr spezifisch binden. Diese sind sehr hilfreich im Visualisieren von Tumoren, leider ist ihre therapeutische Wirkung jedoch umstritten. Das Ziel dieser Doktorarbeit war es daher, CA IX spezifische Antikörper mit Enzym-inhibitorischer Aktion zu etablieren, um effizientere Therapien gegen solide Tumoren zu entwickeln.

In dieser Arbeit wurden mit Hilfe des Phagendisplays zwölf Fab-Antikörper (MSC 1 – 12) selektioniert, die spezifisch an rekombinantes humanes CA IX binden. Keine unspezifische Bindung an andere Isoformen mit sehr grosser Homologie, namentlich CA II, CA XII oder CA XIV, wurde beobachtet, was die selektive Bindung an CA IX bestätigt. Zusätzlich waren zwei Antikörper, MSC 1 und MSC 3, kreuzreaktiv mit murinem CA IX. MSC 3 IgG färbte murines CA IX spezifisch in Tumorschnitten und kann daher in einem syngenen Mausmodell eingesetzt werden.

Fünf Antikörper, MSC 2, MSC 5, MSC 8, MSC 10 und MSC 12, waren in der Lage, die enzymatische Funktion von CA IX in einem biochemischen Assay auf Membranfragmenten teilweise zu inhibieren. Der vielversprechendste der Antikörper, MSC 8, inhibierte die CA IX Aktivität um 57 % als Fab-Antikörper und um 76 % als bivalenter IgG. Zudem inhibierte MSC 8 Fab die CA IX Aktivität auf intakten Einzelzellen um 48 % bzw. MSC 8 IgG um 61 %. Daneben bewirkte MSC 8 IgG die Internalisierung von CA IX, wodurch die CA IX Aktivität auf der Zelloberfläche weiter reduziert werden dürfte.

Daher könnte der humane CA IX spezifische IgG MSC 8 einen weitaus grösseren Nutzen haben als

zuvor entwickelte anti-CA IX Antikörper, indem Spezifität mit Inhibition der CA IX Enzym-Aktivität gekoppelt wird. Der therapeutische Effekt könnte weiter gesteigert werden, indem biologisch aktive Substanzen mit Hilfe dieser Antikörper spezifisch zu Zielzellen gebracht werden und durch Internalisierung direkt an ihren Wirkungsort gelangen.

ABSTRACT

The growth of solid tumours is limited by low supply of oxygen and nutrients due to poor vascularisation. Hypoxia leads to changes in gene expression mostly due to the hypoxia inducible factor (HIF), helping cancer cells to adapt to low oxygen levels. One of these target genes is carbonic anhydrase IX (CA IX), a transmembrane protein with an extracellular domain catalysing the reversible hydration of carbon dioxide to hydrogen carbonate and protons. CA IX expression is mostly limited to hypoxic tumour tissues. It is only rarely expressed in normal tissue, e.g. in the gastrointestinal tract. Its catalytic activity facilitates tumour growth by acidification of extracellular pH and neutralisation of intracellular pH. This makes carbonic anhydrase IX not only a promising marker for tumour targeting but also a potential target for tumour therapy by inhibiting CA IX enzymatic activity. Several chemical compounds inhibiting CA IX activity are used in the clinic. However, due to cross-reactivity with other carbonic anhydrase isoforms, they have severe side effects and their clinical use is very much limited. On the other hand, antibodies specifically targeting CA IX have proven to be very useful in tumour imaging, but their therapeutic effect is disputed. The aim of this thesis was therefore to establish CA IX specific antibodies blocking enzymatic activity in order to enhance efficacy of therapies against solid tumours.

In this thesis, twelve Fab antibodies, called MSC 1 – 12, specifically recognizing human CA IX were selected by phage display on recombinant human CA IX. No unspecific binding to any of the other highly homologous isoforms CA II, CA XII or CA XIV could be detected, confirming highly selective binding to CA IX. In addition, two of the antibodies, MSC 1 and MSC 3, were cross-reactive to murine CA IX. MSC 3 IgG specifically stained murine CA IX in tumour sections and can thus be used in syngeneic mouse models.

Five antibodies, MSC 2, MSC 5, MSC 8, MSC 10 and MSC 12, inhibited CA IX function partially in a biochemical assay on membrane fragments. The most potent of those antibodies, MSC 8, inhibited CA IX activity by up to 57 % as Fab antibody and 76 % as bivalent IgG. In addition, MSC 8 inhibited CA IX activity on intact single cells by 48 % and 61 % for MSC 8 Fab and MSC 8 IgG, respectively. In addition, MSC 8 IgG triggered CA IX internalisation which might further reduce CA IX activity on the cell surface.

Therefore, the fully human CA IX-specific IgG antibody MSC 8 may extend beyond the use of previously developed CA IX-antibodies by combining target-specificity with CA IX inhibitory activity. By delivering therapeutic moieties specifically to target cells and triggering internalisation of those compounds the here selected antibodies could further increase therapeutic efficacy.

TABLE OF CONTENTS

1 INTRODUCTION

The immune system is able to discriminate between self and non-self allowing immune cells to specifically target foreign structures and protect the body from invasion of pathogens. Nevertheless, there are diseases, where our immune system is impaired in its ability to protect the body. The most important of those diseases is cancer, the second most common cause of death in Europe and the US. Tumour cells are derived from normal tissue cells making it hard for the immune system to selectively target them. However, several proteins are upregulated and predominantly expressed in cancer cells. These antigens are called tumour associated antigens (TAA). In tumour therapy, TAA display important targets for selective treatment of tumours where surgery is not possible. Carbonic anhydrase IX targeted in this study is a TAA found in a variety of solid tumours due to its tight regulation by hypoxia, a hallmark of solid tumours.

1.1 HYPOXIA

Höckel and Vaupel define hypoxia as a "state of reduced oxygen (O_2) availability or decreased O_2 partial pressure (pO_2) below critical thresholds, thus restricting or even abolishing the function of organs, tissues or cells". Tissue hypoxia results from inadequate supply of oxygen and can be caused by reduced pO_2 of the blood (hypoxemic hypoxia), reduced ability of the blood to transport O_2 (anaemic hypoxia), reduced tissue perfusion (circulatory or ischemic hypoxia), deterioration of the diffusion geometry (diffusional hypoxia) or impaired ability of cells to use O_2 (histotoxic or cytotoxic hypoxia). Reduced oxygen levels impede oxidative phosphorylation in hypoxic areas leading to enhanced anaerobic respiration, followed by lactic acid fermentation and reduced ATP production (reviewed in (Hockel and Vaupel 2001)).

1.1.1 Hypoxia and cancer

In solid tumours, uncontrolled cell division leads to inadequate supply of tumour tissue with nutrients and oxygen due to increasing distance to blood vessels. With increasing distances from blood vessels, pO_2 decreases (**Figure 1.1 A**) (Helmlinger, Yuan et al. 1997). Growth of solid tumours is therefore limited by vascularisation (reviewed in (Carmeliet and Jain 2000)). In addition, tumour blood vessels are often highly disorganized leading to diffusional hypoxia and the transport capacity of the blood for O_2 is often reduced due to anaemia (reviewed in (Hockel and Vaupel 2001)). Even regions adjacent to blood vessels can show a hypoxic phenotype and very low extracellular pH (pH_e) (Helmlinger, Yuan et al. 1997), possibly due to elevated production of lactic acid. Additionally, also under normoxic conditions many tumours have a high rate of anaerobic

glycolysis followed by lactic acid fermentation. They often show a mixed metabolism with oxidative phosphorylation and anaerobic respiration at the same time, although exact mechanisms are not yet known (reviewed in (Stubbs, McSheehy et al. 2000)). In the 1930s, Warburg demonstrated that cancer cells have an elevated rate of lactate production, leading to the assumption that tumour cells would have an acidic intracellular pH (pH_i). However some 50 years later it became evident that pH_i was indeed neutral or even slightly alkaline, because lactate is not deposited intracellularly but exported - mainly through the H^+-monocarboxylate co-transporter. Accumulation of this metabolite and slow clearance due to poor vascularisation lead to acidification of the tumour stroma (reviewed in (Stubbs, McSheehy et al. 2000)). This decrease in pH_e following a decrease in pO_2 (**Figure 1.1 B**) (Helmlinger, Yuan et al. 1997) is not only caused by elevated production of lactic acid and slow clearance of the same, but also by other means, e.g. carbon dioxide (Dubois, Douma et al. 2007). In contrast to normal tissue, tumour cells show therefore a reversed pH gradient across the cell membrane with a rather high pH_i and a low pH_e (reviewed in (Stubbs, McSheehy et al. 2000)). The local glucose and oxygen availability both affect tumour acidity independently (Helmlinger, Sckell et al. 2002).

Tumour hypoxia augments the malignant potential of neoplasms – possibly due to genomic instability coupled to impaired repair mechanisms and to upregulation of transcription factors such as hypoxia inducible factor 1 (HIF-1) (reviewed in (Huang, Bindra et al. 2007)). Low pH_e might be an intrinsic feature of cancer phenotype facilitating tumour progression, tumourigenic transformation, chromosomal rearrangement, extracellular matrix break-down, migration and invasion, as well as induction of expression of cell growth factors and proteases (reviewed in (Stubbs, McSheehy et al. 2000)).

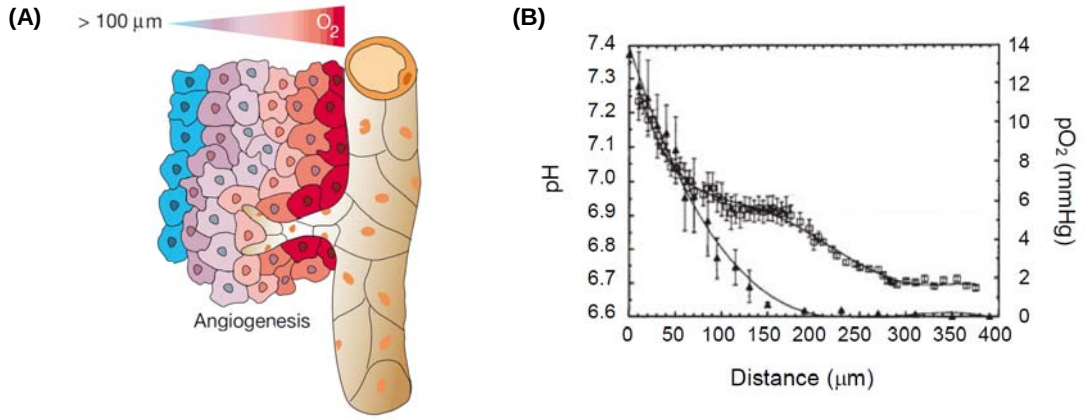

Figure 1.1: pO_2 and pH gradients with increasing distance from blood vessels. (A) Schematic representation of hypoxic tissue. Blood vessels supply cells with oxygen and nutrients. With increasing distance to blood vessels pO_2 therefore decreases. From (Carmeliet and Jain 2000). **(B)** Measurement of pO_2 and pH in the tissue. Both, pO_2 (filled triangles) and pH (open boxes) decrease with increasing distance from blood vessels. From (Helmlinger, Yuan et al. 1997).

It is not possible to state one single general threshold for hypoxia and the hypoxic state can not be predicted by size, stage or grade of a tumour. Usually, the oxygen state (median pO_2) of tumour tissues is reduced compared to the tissue of origin with recurring tumours having an even lower oxygen state than corresponding primary tumours (reviewed in (Hockel and Vaupel 2001)). A number of invasive as well as non-invasive techniques to analyze the oxygenation state of tumours are available (reviewed in (Hockel and Vaupel 2001)). Methods to quantify tumour hypoxia are very important in order to find optimal tumour therapies, since hypoxia as well as pH has an impact on therapy outcome. Radiotherapy depends on oxygen availability to generate free oxygen radicals damaging the DNA (**Figure 1.2**). Additionally, hypoxia-induced upregulation of heat-shock proteins might further protect tumour cells from effects of radiotherapy and therefore reduces therapeutic efficacy. Similarly, several anticancer agents depend on the availability of oxygen. Finally, hypoxia alters the potency of cytokines (reviewed in (Hockel and Vaupel 2001)). Low pH_e leads to chemoresistance possibly due to decreased uptake of weakly basic cancer drugs (Raghunand, He et al. 1999). Drug transport is mediated by active transport or passive diffusion, with weak electrolytes entering the cell by passive diffusion of the non-ionized form. Depending on the drug, a lower or higher pH_e favours building of the non-ionized form and thus drug-uptake (**Figure 1.3**). The ionized form is then thought to get stuck in the cytoplasm. Since uptake is pH-dependent, pH_i as well as pH_e could have an impact on chemoresistance (reviewed in (Stubbs, McSheehy et al. 2000)). Additionally, drug toxicity can depend on pH (reviewed in (Stubbs, McSheehy et al. 2000)). All this factors are possible causes why hypoxic tumours often lead to poor prognosis. Inhibition of factors regulating tumour pH might therefore augment effects of chemotherapy and reduce tumour progression by reducing metastases (Raghunand, He et al. 1999).

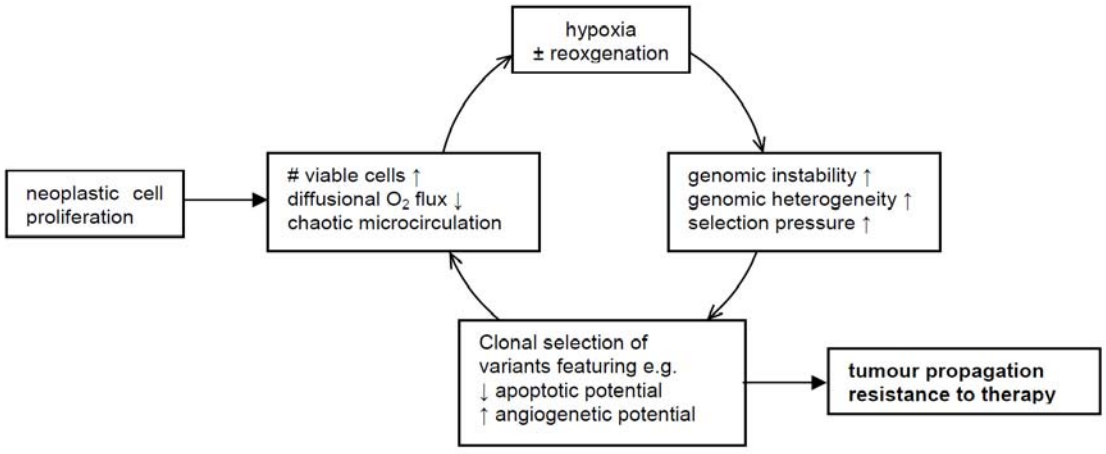

Figure 1.2: influence of hypoxia on malignant progression of tumours. Uncontrolled cell division leads to hypoxic conditions due to increased cell number and poor supply of oxygen. Hypoxia augments genomic instability and selection pressure leading to clonal selection of variants promoting tumour growth. Altered cells and hypoxia impede tumour therapy. From (Hockel and Vaupel 2001)

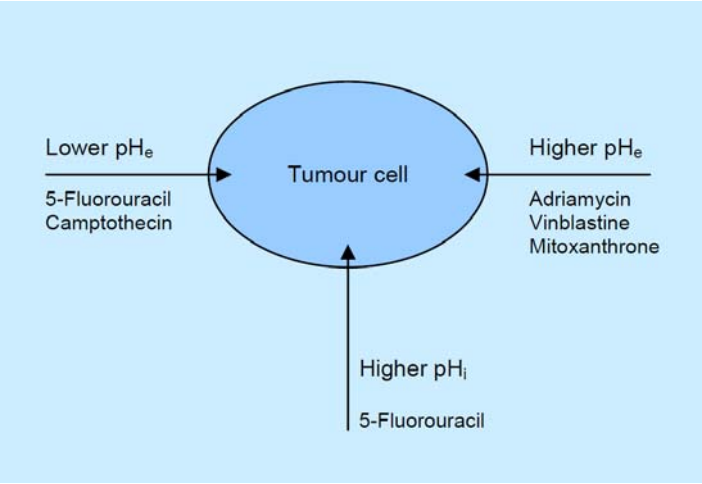

Figure 1.3: Modulation of tumour pH to increase uptake of chemotherapeutic drugs. The figure indicates the modulation (decrease or increase) of pH necessary to increase the uptake of the named drugs used in chemotherapy. The drugs are weak electrolytes. 5-Fluorouracil: uracil analogue; camptothecin: inhibitor of topoisomerase I; adriamycin (= doxorubicin) and mitoxantrone: DNA intercalating agents; vinblastine: mitose inhibitor. From (Stubbs, McSheehy et al. 2000)

1.1.2 Hypoxia inducible factor 1 (HIF-1)

The hypoxia inducible factor 1 (HIF-1) is a transcription factor regulating gene expression under hypoxic conditions. It is a heterodimer consisting of the two subunits HIF-1α and HIF-1β (Wang and Semenza 1995). The α-subunit is present in the cytosol and the β-subunit shown to be identical to the aryl hydrocarbon receptor nuclear translocator (ARNT) (Wang, Jiang et al. 1995) is constitutively expressed in the nucleus. HIF-1 is regulated by stabilization of its α-subunit (**Figure 1.4**) (Huang, Arany et al. 1996). Although constitutively expressed, under normoxic conditions HIF-1α is quickly degraded (Huang, Arany et al. 1996). Hydroxylation of its oxygen-dependent degradation (ODD) domain (Huang, Gu et al. 1998) by oxygen-dependent prolyl-4-hydroxylase domain proteins (PHDs) (Jaakkola, Mole et al. 2001) and subsequent binding of the von Hippel-Lindau tumour-suppressor protein (pVHL) (Maxwell, Wiesener et al. 1999; Jaakkola, Mole et al. 2001) results in ubiquitination by pVHL (Ohh, Park et al. 2000) and proteasomal degradation (Huang, Gu et al. 1998). Under hypoxic conditions on the other hand, hydroxylation of HIF-1α can not take place and pVHL can not bind (Jaakkola, Mole et al. 2001). The α-subunit is stabilized and can translocate into the nucleus where it binds the β-subunit, building the active transcription factor HIF-1 which binds to hypoxia responsive elements (HRE) of target genes (**Figure 1.5**) (reviewed in (Thiry, Dogne et al. 2006)). Target genes include among others glucose transporter GLUT-1 (Ebert, Firth et al. 1995) involved in glucose metabolism, vascular endothelial growth factor (Forsythe, Jiang et al. 1996) triggering neoangiogenesis (Shweiki, Itin et al. 1992) and carbonic anhydrase IX (Wykoff, Beasley et al. 2000), a protein involved in pH-regulation.

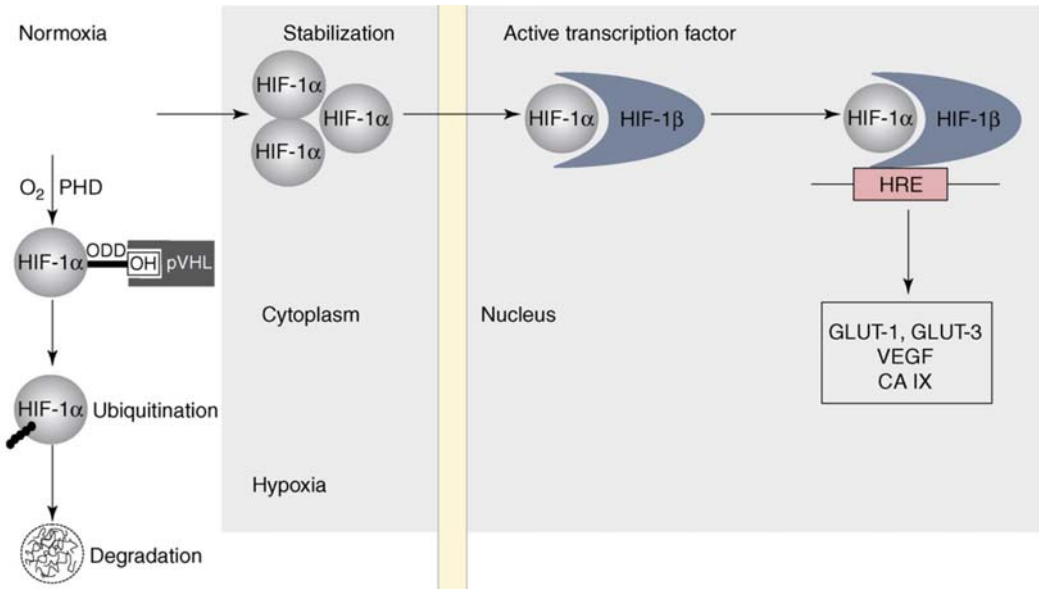

Figure 1.4: Induction of HIF-1 by hypoxia. Under normoxic conditions, ubiquitination by pVHL leads to proteosomal degradation of HIF-1α. Under hypoxic conditions pVHL can not bind and HIF-1α translocates to the nucleus where it binds HIF-1β building the active transcription factor HIF-1 which induces transcription of target genes. From (Thiry, Dogne et al. 2006)

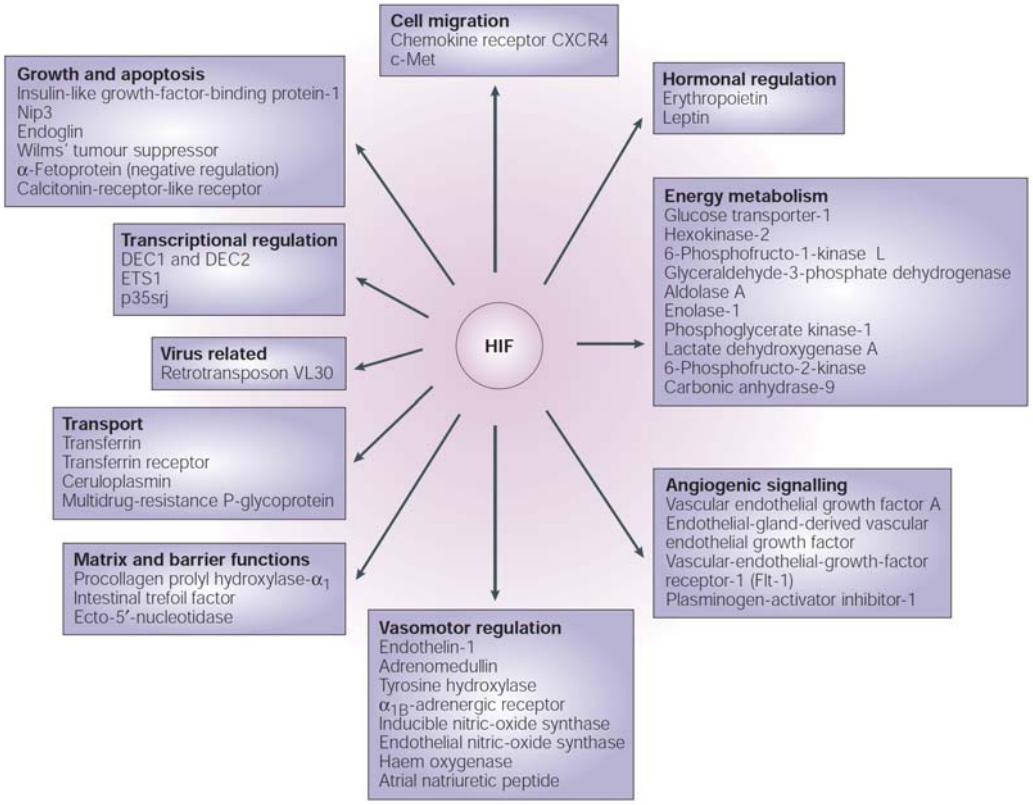

Figure 1.5: HIF target genes. Protein products of the genes are shown for which there is evidence of direct transcriptional activation by the hypoxia-inducible factor. Those proteins are involved in many functions important under conditions of low oxygen and in solid tumours, e.g. energy metabolism and angiogenetic signalling. From (Schofield and Ratcliffe 2004).

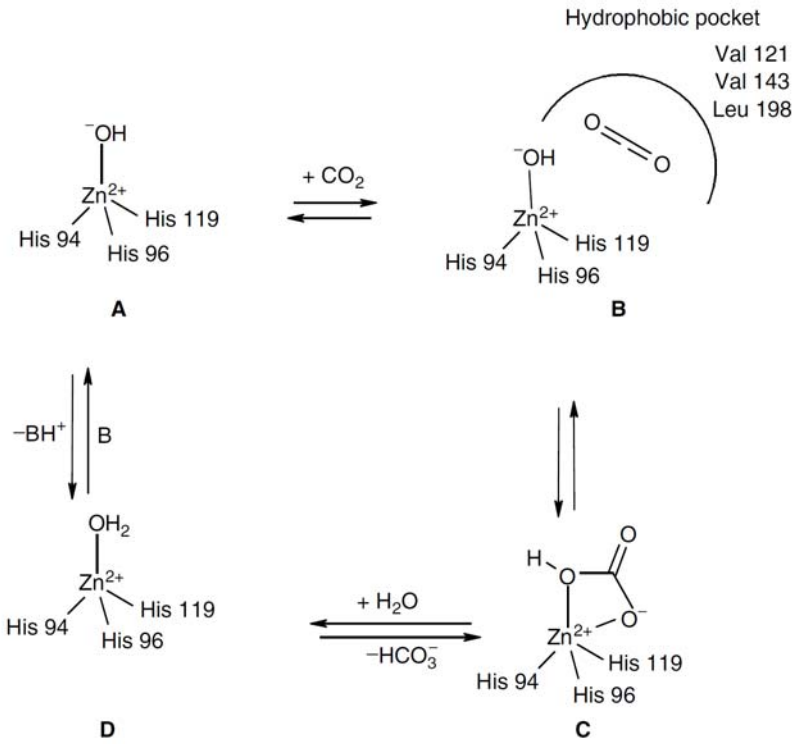

Figure 1.6: Mechanism of α-CA catalytic activity. (A) In the active form of the enzyme a hydroxide is bound to Zn^{2+}. **(B)** This strong nucleophile attacks a CO_2 molecule bound in a hydrophobic pocket in its neighbourhood, **(C)** leading to the formation of hydrogen carbonate coordinated to Zn^{2+}. **(D)** The hydrogen carbonate ion is then displaced by a water molecule. The enzyme contains now a water molecule coordinated to Zn^{2+}. A proton transfer reaction restores the original active form. This reaction can be assisted either by active site residues (e.g. His 64—the proton shuttle in CA II and CA IX) or by buffers. Numbers are given for CA II. From (Supuran 2004).

1.2 CARBONIC ANHYDRASES

One of the genes regulated by HIF-1 is carbonic anhydrase IX (CA IX). Like all animal kingdom carbonic anhydrases (CAs) characterized so far, CA IX belongs to the α-CAs (Hewett-Emmett and Tashian 1996). Carbonic anhydrases are metalloenzymes containing a Zn^{2+}-ion essential for catalytic activity (**Figure 1.6**). Enzymatic active carbonic anhydrases trigger the reversible hydration of carbon dioxide to hydrogen carbonate and protons (Sly and Hu 1995):

$$H_2O + CO_2 \rightleftharpoons HCO_3^- + H^+$$

Due to the conversion of carbon dioxide to hydrogen carbonate, carbonic anhydrases directly influence the hydrogen carbonate buffering system - an important buffering system in humans. Carbonic anhydrases therefore have a huge impact on physiological processes like acid-base regulation, respiration, electrolyte secretion, bone resorption and biosynthetic reactions using hydrogen carbonate as a substrate (reviewed in (Pastorekova, Parkkila et al. 2004; Supuran 2004)).

Table 1.1: Localization and activity of higher vertebrate carbonic anhydrases. Different isozymes differ in their subcellular localization and in their catalytic rate. Adapted from (Supuran 2004; Nishimori, Vullo et al. 2005)

Isozyme	catalytic activity	subcellular location
CA I	low	cytosol
CA II	high	cytosol
CA III	very low	cytosol
CA IV	high	membrane bound
CA VA	low	mitochondria
CA VB	high	mitochondria
CA VI	moderate	secreted into saliva
CA VII	high	cytosol
CARP VIII	acatalytic	cytosol
CA IX	high	transmembrane
CARP X	acatalytic	cytosol
CARP XI	acatalytic	cytosol
CA XII	low	transmembrane
CA XIII	moderate	cytosol
CA XIV	low	transmembrane

Of the 16 mammalian α-CA isoforms 13 are enzymatically active (CA I (Barlow, Lowe et al. 1987), CA II (Montgomery, Venta et al. 1987), CA III, CA IV (Zhu and Sly 1990), CA VA (Nagao, Platero et al. 1993), CA VB (Fujikawa-Adachi, Nishimori et al. 1999), CA VI, CA VII, CA IX, CA XII (Ivanov, Kuzmin et al. 1998; Tureci, Sahin et al. 1998), CA XIII (Lehtonen, Shen et al. 2004), CA XIV and CA XV which is not expressed in humans (Hilvo, Tolvanen et al. 2005)) and three appear to lack any catalytic activity and are therefore called carbonic anhydrase related proteins (CARP VIII, CARP X and CARP XI) (reviewed in (Supuran 2004)).

Carbonic anhydrase isoforms differ in their rate of catalytic activity and their subcellular localization (**Table 1.1**) (reviewed in (Supuran 2004)), with membrane associated carbonic anhydrases having an extracellular active site influencing various extracellular physiological processes like extracellular pH-regulation, as well as in their expression profiles (Pan, Leppilampi et al. 2006). In a particular mammalian tissue or organ, often multiple isozymes are co-expressed suggesting distinct functions for different isozymes, which might sometimes be redundant. Loss of one isozyme might therefore be compensated by another one (Pan, Leppilampi et al. 2006). In the stomach of CA II deficient mice, CA IX levels are indeed upregulated. Interestingly, in brain, colon or kidney this upregulation is not observed (Pan, Leppilampi et al. 2006).

CA II is the most widely expressed isozyme, present in all major mammalian organs (Pan, Leppilampi et al. 2006). Broad expression and high activity propose CA II to play a role in several fundamental biological processes (Parkkila, Parkkila et al. 1994; Sly and Hu 1995).

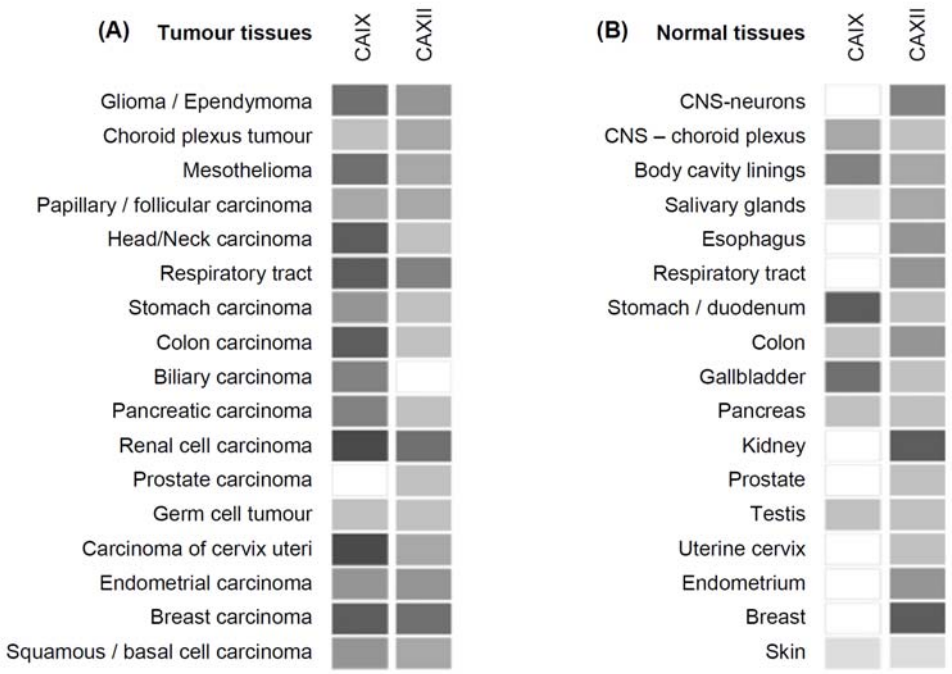

Figure 1.7: Expression of tumour-associated carbonic anhydrases. (A) CA IX and CA XII are both abundant in tumour tissue. **(B)** CA XII is broadly expressed in normal tissue, whereas CA IX expression is restricted to the gastrointestinal tract. Dark grey: high expression, light grey: low expression, white: no expression. From (Pastorekova and Pastorek 2004).

Two membrane-associated catalytically active isozymes, CA IX and CA XII, are abundant in many tumours (Pastorekova, Zavadova et al. 1992; Pastorek, Pastorekova et al. 1994; Tureci, Sahin et al. 1998; Wykoff, Beasley et al. 2000) due to their induction by hypoxia (**Figure 1.7 A**) (Ivanov, Kuzmin et al. 1998). In pVHL deficient cells, CA IX and CA XII both are expressed constitutively (Ivanov, Kuzmin et al. 1998; Wykoff, Beasley et al. 2000), but an influence of pVHL on the expression of other CA isoforms is not known so far. CA IX was the first carbonic anhydrase shown to be predominantly expressed in cancer tissue (reviewed in (Pastorekova and Pastorek 2004)) and its role is much better understood than the one of CA XII. CA IX is generally accepted as a sensitive and rather specific marker for conventional renal cell carcinomas (RCC) (Li, Cuilleron et al. 2003) and was suggested to serve as marker for hypoxia (Wykoff, Beasley et al. 2000).

CA IX and CA XII promote cell survival and growth through maintenance of pH_i (as described in detail in **1.3.3 CA IX function**) in cells exposed to hypoxic and acidic microenvironment. Their expression protects cells against cytoplasmic acidification and sustains ATP levels (Chiche, Ilc et al. 2009). Tumour growth in xenograft mice was significantly decreased after silencing of either *hif-1α* or its target genes *ca9* and *ca12*. Silencing of both target genes led to an 85% reduction of tumour growth as a result of reduced cell proliferation. In contrast, silencing of *ca9* only gave a

40% reduction and *ca12* alone did not lead to any significant decrease in tumour growth. CA IX and CA XII therefore work synergistically (Chiche, Ilc et al. 2009). Furthermore, i*n vivo* silencing of *ca9* can be partially compensated by increased CA XII expression while the reverse case has not been reported (Chiche, Ilc et al. 2009).

Although CA IX and CA XII both are associated with solid tumours, they are also expressed in a number of normal tissues (**Figure 1.7 B**). For CA IX, expression in normal tissue is restricted to the gastrointestinal tract, but CA XII is found in a broad range of normal tissue (Ivanov, Kuzmin et al. 1998; Tureci, Sahin et al. 1998; Pastorekova and Pastorek 2004).

1.3 CARBONIC ANHYDRASE IX (CA IX)

CA IX was the first carbonic anhydrase found to be associated with cancer. It was originally described in dense cultures (Pastorekova, Zavadova et al. 1992) and only later prevalence under hypoxic conditions became evident (Wykoff, Beasley et al. 2000).

1.3.1 CA IX structure

The full length cDNA of CA IX was first cloned by Pastorek et al. in 1994 (Pastorek, Pastorekova et al. 1994). Two years later, the CA IX gene was sequenced and characterized by Opavsky et al. (Opavsky, Pastorekova et al. 1996).

The CA IX protein sequence consists of 459 amino acids (aa) and has a calculated molecular weight of 49.7 kDa (Opavsky, Pastorekova et al. 1996). CA IX consists of 4 different domains: a short N-terminal signal peptide (SP, aa 1-37), a proteoglycan-like domain (PG domain, aa 53-111) unique to CA IX and involved in cell adhesion processes (Zavada, Zavadova et al. 2000), an extracellular carbonic anhydrase domain (CA domain, aa 135-391) with catalytic activity, a single hydrophobic transmembrane domain (TM domain, aa 415-436) and an intracellular C-terminal domain (IC domain, aa 436-459) necessary for proper function of CA IX (Hulikova, Zatovicova et al. 2009) (**Figure 1.8**) (Pastorek, Pastorekova et al. 1994; Opavsky, Pastorekova et al. 1996; Pastorekova and Pastorek 2004; Morgan, Pastorekova et al. 2007).

Figure 1.8: Domain organization of CA IX. CA IX consists of a short signal peptide (SP), a proteoglycan-like (PG) domain, the extracellular carbonic anhydrase (CA) domain with catalytic activity, a single transmembrane (TM) domain and an intracellular (IC) domain. From (Thiry, Dogne et al. 2006)

Table 1.2: Homology of the CA domain of CA IX compared to the CA domain of different isozymes. The CA IX catalytic domain is highly homologous to the CA domains of other isozymes. Data from (Opavsky, Pastorekova et al. 1996)

Isozyme	Homology to CA IX
CA I	31.9 %
CA II	35.8 %
CA III	31.7 %
CA IV	30.7 %
CA VI	40.8 %

The CA domain of CA IX is highly homologous to the CA domains of other carbonic anhydrases (**Table 1.2**) (Opavsky, Pastorekova et al. 1996), with the zinc-binding histidyl residues as well as the other residues in the active site being conserved (Pastorek, Pastorekova et al. 1994). Also the C-terminal part shows high homology to other carbonic anhydrases in contrast to the N-terminal part (Pastorek, Pastorekova et al. 1994). Indeed, CA IX is the only carbonic anhydrase isoform known so far to posses a PG domain, showing 38 % homology to the keratin sulphate attachment domain of the proteoglycan aggrecan (Doege, Sasaki et al. 1991; Opavsky, Pastorekova et al. 1996).

In SDS-PAGE analysis, CA IX migrates as a double band of 54 kDa and 58 kDa (Pastorekova, Zavadova et al. 1992; Pastorek, Pastorekova et al. 1994), the origin of which is unknown. Both polypeptides originate from the same mRNA (Pastorek, Pastorekova et al. 1994). Although CA IX contains a *N*-glycosylation site (Asn^{346}) within the CA domain (Hilvo, Baranauskiene et al. 2008) (for sequence and numbering see **5.1.2 CA IX amino acid sequence**), the double band does not origin from different glycosylation patterns (Pastorek, Pastorekova et al. 1994; Hilvo, Baranauskiene et al. 2008).

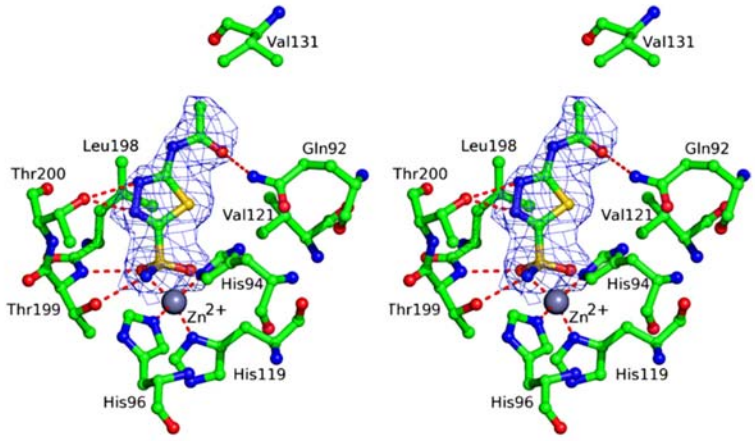

Figure 1.9: Stereoview of the active site region of CA IX bound by acetazolamide. Acetazolamide inhibits CA IX function by binding to the Zn^{2+}-ion in the active site necessary for catalytic activity. From (Alterio, Hilvo et al. 2009).

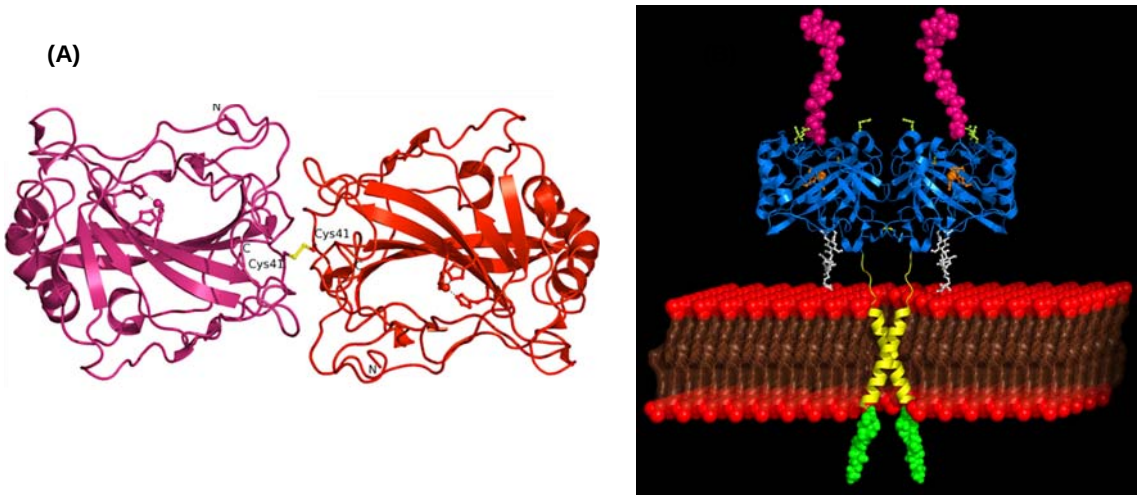

Figure 1.10: X-ray structure of the dimeric catalytic domain. (A) The X-ray structure of the catalytic domain of CA IX shows formation of a CA IX dimer. **(B)** The proposed structure of the full length CA IX dimer is based on the X-ray structure of the dimeric catalytic domain (blue). The hypothetical arrangement of the PG domains (magenta), the transmembrane helices (yellow), the cytoplasmic domains (green) and the glycan moieties (white) attached to the catalytic domain (blue) is schematically reported. From (Alterio, Hilvo et al. 2009).

Recombinant protein obtained by a mammalian expression system in addition demonstrated the occurrence of an *O*-linked glycosylation site (Thr^{115}) containing oligosaccharides highly similar to those in the proteoglycan domain of other proteins involved in cell adhesion processes and tumour progression (Hilvo, Baranauskiene et al. 2008). CA IX contains three putative phosphorylation sites at the cytoplasmic tail, possibly leading to intracellular signalling (reviewed in (Thiry, Dogne et al. 2006)). CA IX is very stable (Pastorek, Pastorekova et al. 1994) with a half life of approximately 38 h (Rafajova, Zatovicova et al. 2004).

In 2009, Alterio et al managed to co-crystallize the catalytic domain of CA IX with acetazolamide, a broad range carbonic anhydrase inhibitor (**Figure 1.9**), showing that CA IX forms dimers linked by disulfide bonds (**Figure 1.10**) (Alterio, Hilvo et al. 2009). There is one intramolecular disulfide bond (Cys^{156} - Cys^{336}), as well as two cysteins (Cys^{174} and Cys^{409}) able to form intermolecular disulfide bonds (Hilvo, Baranauskiene et al. 2008). Since up to date there does not exist any full length crystal structure of CA IX, it can not be excluded, that the transmembrane domain or the intracellular tail is necessary for correct multimerization and that the full length protein might form other multimers. Previous studies based on SDS-PAGE under non-reducing conditions showed several bands around 150 kDa suggesting a trimeric form (Pastorekova, Zavadova et al. 1992; Svastova, Hulikova et al. 2004).

Recent studies indicate that under hypoxia there exists a special hypoxic conformation of CA IX which is the catalytically active conformation. CA IX activity thus depends not only on protein upregulation via HIF-1 but also on the formation of the active conformation by the absence of

oxygen per se (Dubois, Douma et al. 2007). Studies using a chemical compound specifically recognizing the active conformation of CA IX suggest that formation of the active conformation does not require de novo protein synthesis but displays a fast oxygen mediated effect. The active conformation is reached within 15 min of hypoxic exposure and is gradually lost after re-oxygenation with a half-life time of approximately 30 min (Dubois, Douma et al. 2007).

1.3.2 CA IX expression

The gene coding for CA IX is conserved in a single copy in the human genome on chromosome 9p12-13 (Grabmaier, Vissers et al. 2000) as well as in different vertebrate species (Pastorek, Pastorekova et al. 1994; Opavsky, Pastorekova et al. 1996). CA IX is often expressed in tumour tissues but only rarely in normal tissues (**Figure 1.11**) (Pastorek, Pastorekova et al. 1994; Wykoff, Beasley et al. 2000). The most abundant expression of CA IX in normal tissue is found within the epithelial cells of normal gastric mucosa (Pastorek, Pastorekova et al. 1994). It is located at the basolateral surface possibly involved in maintaining gastric mucosa integrity and balance between cell differentiation and proliferation.

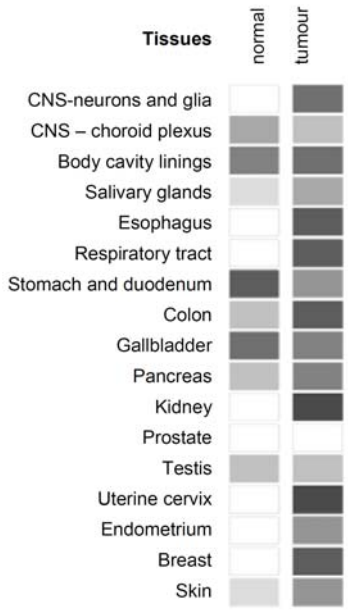

Figure 1.11: Expression of CA IX in normal and tumour tissue. In normal tissue CA IX expression is restricted to the gastrointestinal tract, whereas it is highly abundant in tumour tissue. Dark grey: high expression, light grey: low expression, white: no expression. Adapted from (Pastorekova and Pastorek 2004).

Upregulation of CA IX in cancer tissue is not due to mutations in the gene (Grabmaier, Vissers et al. 2000) but to hypoxic conditions. CA IX contains a HRE-Element and is thus upregulated by hypoxia through HIF-1 as shown in **1.1.2 Hypoxia inducible factor 1 (HIF-1)**. Since HIF-1 is downregulated by pVHL, pVHL deficient tumours e.g. RCC containing a mutation in the gene encoding pVHL (Gnarra, Tory et al. 1994) express CA IX constitutively and with uniform distribution (Wykoff, Beasley et al. 2000). In contrast CA IX is heterogeneously und mostly perinecrotic distributed in non-pVHL deficient tumours where expression is regulated by HIF-1α and hypoxia (Wykoff, Beasley et al. 2000). Interestingly, in tissues expressing CA IX this expression is decreased or even lost during carcinogenesis (reviewed in (Pastorekova and Pastorek 2004)).

Beside its upregulation under low oxygen levels (true hypoxia) by HIF-1, a second pathway of CA IX regulation is suggested, occurring at intermediate oxygen levels as found in dense cultures due to depletion and limited diffusion (Kaluz, Kaluzova et al. 2002). It is supposed that density-mediated upregulation is independent of HIF-1α stabilization since HIF-1 levels are not changed in conditions of dense cultures. Nevertheless a minimal level of HIF-1α activity is required, as shown by the necessity of HRE for density-mediated CA IX expression (Kaluz, Kaluzova et al. 2002). Density-mediated upregulation is independent of anchorage, growth factors contained in serum, pH or glucose concentration. The only known factor in cell-density mediated upregulation is phosphatidylinositol 3-kinase (PI3K), although the exact mechanism is not yet known (Kaluz, Kaluzova et al. 2002). Tumours with deregulated PI3K activity might therefore express CA IX constitutively. Effects of hypoxia and density-mediated CA IX expression are additive suggesting that they are due to independent mechanisms (Kaluz, Kaluzova et al. 2002).

Since CA IX expression is influenced by HIF-1, PHD-inhibitors like dimethyloxaloylglycine (DMOG) (Asikainen, Ahmad et al. 2005) or iron-chelators, e.g. desferrioxamine (DFO) (Wang and Semenza 1993) complexing the iron in the catalytic centre of PHDs, lead to upregulation of CA IX *in vitro* by indirect stabilization of HIF-1α. Activation by metal ions like cobalt chloride is achieved by a yet unknown mechanism that might depend on PHDs (Yuan, Hilliard et al. 2003; Schofield and Ratcliffe 2004), on inhibiting binding of pVHL to hydroxylated HIF-1α (Yuan, Hilliard et al. 2003) or on reactive oxygen species and PI3K activity (Triantafyllou, Liakos et al. 2006).

There have been differing reports on influence of the PI3K/Akt pathway on HIF activity and corresponding downstream CA IX gene regulation (Arsham, Plas et al. 2002; Pore, Jiang et al. 2006; Shafee, Kaluz et al. 2009). Correlations might be cell type specific, although a certain level of PI3K/Akt activity was proposed to be necessary for HIF-1 down-stream target activity (Shafee, Kaluz et al. 2009).

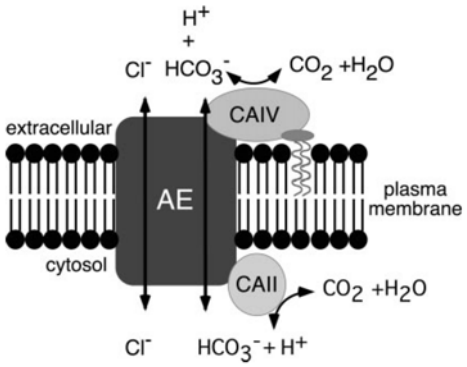

Figure 1.12: A hydrogen carbonate transport metabolon. Schematic model of a transport metabolon consisting of an anionic exchanger (AE), CA II and CA IV. The transport metabolon enhances hydrogen carbonate flux across the cell membrane. Extracellular CA IV provides hydrogen carbonate which is transported in the cytosol by AE where it is consumed by intracellular CA II. The reaction can also take place in the reverse direction facilitating hydrogen carbonate efflux. From (Sterling, Alvarez et al. 2002)

1.3.3 CA IX function

CA IX influences pH (see **1.2 Carbonic anhydrases**). It is one of the most active carbonic anhydrase isozymes (Hilvo, Baranauskiene et al. 2008) with a catalytic rate constant k_{cat} of $3.8 \cdot 10^5$ s^{-1} and k_{cat}/K_m of $5.5 \cdot 10^7$ $M^{-1}s^{-1}$ (reviewed in (Thiry, Dogne et al. 2006)) and an extracellular catalytic domain (Opavsky, Pastorekova et al. 1996). Thus, Svastová et al suggested a role of CA IX in the control of pH_e (Svastova, Hulikova et al. 2004). It seems plausible that low pH_e in tumours is associated not only with production of lactic acid due to high glycolysis but also with carbon dioxide hydration (Helmlinger, Sckell et al. 2002) catalyzed by CA IX (Dubois, Douma et al. 2007).

There is evidence that CA IX has also an impact on pH_i (Chiche, Ilc et al. 2009), possibly by association with anionic exchangers or Na^+/HCO_3^- co-transporters building a so called hydrogen carbonate transport metabolon (Morgan, Pastorekova et al. 2007). This transport metabolon facilitates the transport of hydrogen carbonate across the membrane (Morgan, Pastorekova et al. 2007). CA IX leads to production of extracellular hydrogen carbonate, which then might be transported into the cytosol by anionic exchangers or Na^+/HCO_3^- co-transporters. In combination with intracellular CA II, hydrogen carbonate in the cytosol might be converted to carbon dioxide which can diffuse across the plasma membrane. This transport metabolon might therefore sustain a hydrogen carbonate influx across the membrane and thus neutralizes the cytosolic acid load produced in many tumour cells by anaerobic glycolysis.

CA II and CA IV have been described earlier to participate in such a hydrogen carbonate transport metabolon (**Figure 1.12**) (Vince and Reithmeier 1998; Sterling, Reithmeier et al. 2001; Sterling,

Alvarez et al. 2002; Loiselle, Morgan et al. 2004; Alvarez, Vilas et al. 2005). The first evidence for a hydrogen carbonate transport metabolon involving CA IX came from Morgan et al. Direct interaction of CA IX with several AE could be shown, with the CA domain of CA IX necessary for assembly of the transport metabolon (Morgan, Pastorekova et al. 2007).

Beside its influence on pH regulation, CA IX has important functions in cell-adhesion processes (Zavada, Zavadova et al. 2000; Svastova, Zilka et al. 2003). In polarized Madin Darby canine kidney (MDCK) epithelial cells, CA IX co-localizes with E-cadherin at sites of cell-cell adhesion. Association of CA IX with β-catenin, α-catenin and E-cadherin diminishes binding of E-cadherin to β-catenin, thereby disrupting cell contacts and reducing cell-cell adhesion capacity (Svastova, Zilka et al. 2003). For cell-adhesion, full-length protein is required. Zavada et al. showed that the binding site of CA IX for cell-receptors lies within the PG-domain and is identical to the epitope of the antibody M75 (discussed in detail in **1.4.2 Antibodies against CA IX**) (Zavada, Zavadova et al. 2000).

In addition to these two generally accepted functions in pH-regulation and cell-adhesion, several additional functions for CA IX have been proposed by Wang and coworkers. They suggested CA IX to have chaperone-like functions, complexing antigens at 37 °C, to serve as immunoadjuvans and to stimulate an adaptive immune response against tumour antigens. They therefore proposed CA IX to have an analogous role in activating the immune system as heat shock proteins but under hypoxic conditions rather than heat shock. They further showed CA IX to bind to dendritic cells in a receptor-specific manner and to be processed primarily through the proteosomal pathway leading to cross-presentation (Wang, Wang et al. 2008).

1.4 CA IX AS TARGET IN TUMOUR THERAPY

CA IX is expressed in many tumours but only rarely in normal tissue. Additionally, CA IX function was shown to promote tumour growth and progression by influencing pH and cell adhesion (see **1.3.3 CA IX function**). Therefore, it is an interesting target for tumour therapy. Such new therapies are needed since some solid tumours, e.g. metastatic RCC, are resistant to conventional therapy (reviewed in (Motzer, Russo et al. 1997; Lilleby and Fossa 2005)).

1.4.1 Chemical drugs inhibiting CA IX function

There exist many chemical compounds inhibiting CA IX catalytic activity. Most of them belong to one of two main classes: metal complexing anionic compounds or sulfonamides binding to the Zn^{2+}-ion in the active site of carbonic anhydrases (**Figure 1.13 A**) (Abbate, Casini et al. 2004; Weber,

Casini et al. 2004; Di Fiore, De Simone et al. 2005; Menchise, De Simone et al. 2005; Alterio, Vitale et al. 2006; Di Fiore, Pedone et al. 2006) (reviewed in (Pastorekova, Parkkila et al. 2004)). Mann and Keilin were the first ones giving evidence that sulfonamides inhibit carbonic anhydrases (Mann and Keilin 1940). This was the beginning for the discovery of many different sulfonamides inhibiting CA IX function. Most of them are not selective for CA IX but recognise also other isoforms, although with different affinities (Weber, Casini et al. 2004; Di Fiore, De Simone et al. 2005; Menchise, De Simone et al. 2005; Alterio, Vitale et al. 2006; De Simone, Vitale et al. 2006; Di Fiore, Pedone et al. 2006). Unspecific binding and inhibition of other isozymes with important functions for normal cell growth are major drawbacks of chemical drugs targeting CA IX. There exist several strategies to achieve selectivity. One strategy is the restriction of drug activation in hypoxic regions. This is thought to minimize cross-reactivity to other isoforms expressed in normal tissue. Restriction can be achieved by hypoxia-activatable prodrugs, e.g. bulky dimeric sulfonamides not able to bind the active site of carbonic anhydrases. These bulky sulfonamides are stabilized with disulfide bonds, which are reduced under conditions found in tumours leading to the corresponding thiols inhibiting CA IX activity (De Simone, Vitale et al. 2006). Another strategy to avoid cross-reactivity with other carbonic anhydrase isoforms expressed under hypoxic conditions is to screen compounds for selective inhibition of CA IX over other isoforms, e.g. CA II (De Simone, Vitale et al. 2006). A third approach for selectivity of inhibitors is to make them membrane-impermeant, e.g. by a positive charge (Scozzafava, Briganti et al. 2000; Menchise, De Simone et al. 2005). Even though a lot of effort is taken to make chemical inhibitors specific for CA IX, there is still a lot of work needed.

The first carbonic anhydrase inhibitors were used before it was even known that there exist so many isozymes with important physiological function. Nevertheless, sulfonamides became widely accepted because of generally favourable outcome, e.g. as anti-glaucoma agents and diuretics. The sulfonamide acetazolamide is one of the best studied classical carbonic anhydrase inhibitors used in clinics (under the trademark diamox; **Figure 1.13 B**). It was originally used as antiglaucoma agent. Acetazolamide has a lot of side effects because it inhibits various isozymes and needs to be applied systemically. Many other carbonic anhydrase inhibitors have the same drawbacks (reviewed in (Pastorekova, Parkkila et al. 2004)).

Some carbonic anhydrase inhibitors are even not selective for carbonic anhydrases (Abbate, Casini et al. 2004; Weber, Casini et al. 2004; Di Fiore, Pedone et al. 2006). They are also used in the therapy of a number of neurological and neuromuscular syndromes, e.g. epilepsy and ataxia (reviewed in (Pastorekova, Parkkila et al. 2004)).

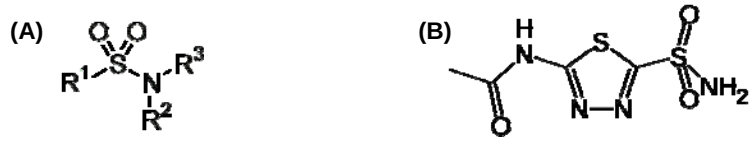

Figure 1.13: Sulfonamides. (A) Sulfonamides are commonly used carbonic anhydrase inhibitors containing a sulfonamide group. **(B)** The sulfonamide acetazolamide is a broad range carbonic anhydrase inhibitor used in clinics.

1.4.2 Antibodies against CA IX

Monoclonal antibodies (MAbs) specifically reacting with TAA are important tools for detection and therapy of cancers. By selectively targeting tumour cells they have potential applications in tumour visualization as well as delivery of therapeutic moieties, e.g. radioisotopes, drugs or toxins (reviewed in (Kuroki, Huang et al. 2006)). Independently, two antibodies against TAA in different tumours were identified: M75 against a cervical-carcinoma associated antigen (Pastorekova, Zavadova et al. 1992) and G250 against a RCC-associated antigen (Oosterwijk, Ruiter et al. 1986). Only later, these TAA were shown to be CA IX.

The antibody M75 was described by Pastorekova et al. It was first found as antibody against the quasi-viral agent MaTu, shown to be a two-component system consisting of the viral protein MX (p58X) from vesicular stomatitis virus and endogenous MN later shown to be identical to CA IX (Pastorekova, Zavadova et al. 1992). M75 recognizes a linear epitope in the PG domain of CA IX which is unique to the CA isoform IX. The epitope of M75 consists of a sixfold tandem repeat of six aa (aa 61–96) forming 4 identical (GEEDLP) and two slightly different (SEEDSP and REEDPP) tandem repeats with a minimal serologically active sequence provided by PGEEDLP (Zavada, Zavadova et al. 2000). Recognition of a linear epitope enables M75 to recognize both native and denatured antigen and makes it useful for a broad range of applications. ^{125}I-labelled M75 can be used for tumour visualization. It specifically accumulates in HT29 xenografts in nude athymic mice despite predominant CA IX expression in perinecrotic regions with low accessibility (Chrastina, Zavada et al. 2003). HT29 provides a general model for hypoxic tumours. M75 therefore is a promising tool for targeting of hypoxic tumours (Chrastina, Zavada et al. 2003).

The antibody G250 was selected by Oosterwijk et al. by using the antibody hybridoma technology with specificity for a RCC-associated antigen (Oosterwijk, Ruiter et al. 1986). The G250 antigen was later shown to be identical to CA IX (Grabmaier, Vissers et al. 2000). The G250 antigen is expressed in most RCC as well as in a couple of non-RCC carcinomas (Oosterwijk, Ruiter et al. 1986). The epitope of G250 is not known. It is supposed to be a sterical epitope limiting the use of G250 in some molecular biology methods where recognition of the denatured protein is required.

G250 (Bleumer, Knuth et al. 2004) as well as ^{131}I-G250 (Divgi, Bander et al. 1998; Steffens, Boerman et al. 1999; Brouwers, Mulders et al. 2005) was tested in phase I and II clinical trials (**Table 1.3**). Currently, there is in an ongoing phase III clinical trial for tumour therapy .To avoid induction of human anti-mouse antibodies, a chimeric variant of G250 was constructed (Velders, Litvinov et al. 1994). G250 is used under the trademark rencarex® (WX-G250) by Wilex. The antibody is well tolerated (Bleumer, Knuth et al. 2004) but therapeutic efficacy is controversial (Divgi, Bander et al. 1998; Steffens, Boerman et al. 1999; Bleumer, Knuth et al. 2004; Brouwers, Mulders et al. 2005). However, ^{131}I-G250 is a useful clinical tool for tumour imaging (Oosterwijk, Bander et al. 1993; Divgi, Bander et al. 1998) and ^{124}I-cG250 antibody is successfully used as a PET tracer to identify clear-cell renal carcinoma with a 100% positive predictive value (Divgi, Pandit-Taskar et al. 2007).

Since *in vitro* CA IX can be upregulated by IFN-α and IFN-γ in some cell lines (Brouwers, Frielink et al. 2003), a combination therapy with interferons is thought to enhance therapeutic efficacy. Additionally IL-2 does upregulate G250 mediated antibody dependent cellular cytotoxicity (ADCC) *in vitro* (Liu, Smyth et al. 2002). Therefore, several studies tried to combine the ability of G250 for tumour targeting with immuno-modulating agents (e.g. IL-2 in clinical trials (Bleumer, Oosterwijk et al. 2006; Davis, Liu et al. 2007)) or with toxic moieties (e.g. TNF in preclinical studies (Bauer, Oosterwijk-Wakka et al. 2009)).

Table 1.3: Clinical studies using G250. Overview showing some of the clinical studies using G250 as unlabelled or 131I labeled antibody alone or in combination with IL-2. Many clinical studies using G250 have been performed but its clinical relevance is discussed. CR: complete response, SD: stable disease, PD: progressive disease, PR: partial response. Adapted from (Stillebroer, Mulders et al. 2010)

Reference	Therapy	CR/PR/SD/PD	CR/PR/SD/PD duration	Special features
(Bleumer, Knuth et al. 2004)	unlabeled cG250	1 CR; 1 PR; 8 SD; 26 PD	1-20^{+} weeks	phase II
(Bleumer, Oosterwijk et al. 2006)	unlabeled cG250 + low dose IL-2	2 PR; 6 SD; 27 PD	24^{+} weeks	phase II
(Davis, Liu et al. 2007)	unlabeled cG250 / ^{131}I-cG250 + low dose IL-2	1 SD; 8 PD	16-22^{+} weeks	pilot study
(Divgi, Bander et al. 1998)	^{131}I-mG250	17 SD; 16 PD	2-3 months	phase I / II
(Steffens, Boerman et al. 1999)	^{131}I-cG250	1 PR; 1 SD; 10 PD	3 and 9^{+} months	phase I
(Brouwers, Mulders et al. 2005)	^{131}I-cG250	5 SD; 22 PD	3-12 months	two high dose treatments

1.5 AIM OF THE THESIS

Many solid tumours are difficult to treat. Especially renal cell carcinomas (RCC) are often resistant to radiotherapy. Therefore, new therapies are needed. One approach is to specifically target tumour associated antigens (TAA). CA IX is a promising TAA for tumour targeting and therapy, since it is predominantly expressed in tumour tissue and has an impact on tumour growth through its catalytic activity regulating tumour pH. Several sulfonamides and anionic compounds are available, inhibiting CA IX activity. Their major drawback is unspecific binding and broad inhibition of many different carbonic anhydrase isozymes. In contrast, antibodies are very specific. Up to date, mainly two antibodies (M75 and G250) are used to target CA IX in tumour tissue. Unfortunately, both of them are not able to inhibit CA IX activity and their clinical use is controversial. In order to achieve new promising therapies, it is important to combine the inhibition potential of chemical drugs with the specificity of antibodies.

The aim of this work was to combine target specificity of antibodies with biological activity against CA IX enzymatic activity. The goal was to select new antibodies against CA IX and characterize them in more detail. A major focus was to examine the physiological effect of the here selected antibodies and to find antibodies inhibiting CA IX activity. To have a simple test system, cross-reactivity of such antibodies with the murine isoform of CA IX was furthermore intended.

2 MATERIAL AND METHODS

2.1 MATERIAL

2.1.1 Primers

Primers were used for DNA fingerprint (fingerprint_fwd; fingerprint_back) and sequencing (pCES fwd_LC; pCES rev_HC) of pCES1 derived constructs as well as for colony PCR (pEE 12.4_1901_rev) and cloning (all other primers) of pEE 12.4 derived constructs (**Table 2.1**).

Table 2.1: Primers. The sequence of primers used in this work is listed. Orange: overlap with pCES1 leading to a universal primer for cloning from this vector, red: overlap with specific sequence of variable domains, blue: overlap between two subsequent primers, underlined: restriction sites indicated in the corresponding primer name (DraIII or RsrII). HC: heavy chain, LC: light chain.

Primer designation	Primer sequence
fingerprint_back	5' - agc gga taa caa ttt cac aca gg - 3'
fingerprint_fwd	5' - ttt gtc gtc ttt cca gac gtt agt - 3'
HC_Dra_3'	5' - agg cgc aga ggc cgg cca cgg tgt gcc atc tta ccg ctt gag acg gtg ac - 3'
HC_Dra_5'_MSC 8	5' - tcc act cct gtg tct tct cta cag gcg tcc aca gcc agg tgc agc tac - 3'
HC_Dra_5'_MSC 11	5' - tcc act cct gtg tct tct cta cag gcg tcc aca gcg agg tcc agc tgg - 3'
HC_Dra_5'	5' - cca tcg aag cca gtc acc cag tga agg ggg ctt cca tcc act cct gtg tc - 3'
LC_Rsr_3'	5' - agg atc ttt aat taa cgg acc gct act cac gta gga cgg tca gct tgg tc - 3'
LC_Rsr_3'_MSC 11	5' - agg atc ttt aat taa cgg acc gct act cac gct tga tct cca cct tgg tc - 3'
LC_Rsr_5'_MSC 3	5' - t gtc ttc tct aca ggc gtg cac agc cag tct gtc gtg acg cag c - 3'
LC_Rsr_5'_MSC 8	5' - t gtc ttc tct aca ggc gtg cac agc cag gct gtg ctg act cag c - 3'
LC_Rsr_5'_MSC 11	5' - t gtc ttc tct aca ggc gtg cac agc gaa att gtg ttg acg c - 3'
LC_Rsr_5'	5' - cag tca agg ggg cgg acc gct tcc atc cac tcc tgt gtc ttc tct aca gg
pCES fwd_LC	5' - agc gga taa caa ttt cac aca gg - 3'
pCES rev_HC	5' - gga agt agt cct tga cca - 3'
pEE 12.4_1901_rev	5' - cgg cga cat ttt caa tat gc - 3'

2.1.2 Antibodies

Primary and secondary antibodies used in this work are listed in **Table 2.2** and **Table 2.3**, respectively.

Table 2.2: Primary antibodies. Primary antibodies used in this work are shown. The target of the antibodies as well as their source is indicated. In the rest of the work antibodies are referred to by their short name.

antibody designation	short name	target	source
mAb anti-c-myc [9-E10]	anti-Myc	Myc-tag	Novus Biologicals
Penta-His™ antibody, mouse monoclonal IgG1	anti-His	His-tag	QIAGEN
ESC 11 IgG	ESC 11 IgG	muFAP and huFAP	produced in-house *)
CA IX (M-100), rabbit polyclonal IgG	M-100	murine CA IX	Santa Cruz
chG250	chG250	human CA IX	kindly provided by E. Oosterwijk
M75	M75	human CA IX	kindly provided by E. Oosterwijk
anti-hCarbonic Anhydrase II, purified rat monoclonal IgG_{2A}	anti-CA II	human CA II	R&D Systems
anti-mTNF-α, mTNF-α affinity purified goat IgG	anti-muTNF	murine TNF-α	R&D Systems
anti-hTNF-α, TNF-α affinity purified goat IgG	anti-huTNF	human TNF-α	R&D Systems
Hypoxyprobe™-1 Kits 4.3.11.3. mAb	hypoxy-probe	pimonidazole	hpi
ChromePure human IgG, whole molecule	huIgG	-	Jackson ImmunoResearch

*) E. Fischer, manuscript in preparation

Table 2.3: Secondary antibodies. Secondary antibodies used in this work are shown. The target of the antibodies as well as their source is indicated. In the rest of the work antibodies are referred to by their short name.

antibody designation	short name	target	source
R-Phycoerythrin-conjugated Streptavidin	Strep-PE	Biotin	Jackson ImmunoResearch
Streptavidin-POD conjugate	Strep-POD	Biotin	Roche
DyLight™ 549-conjugate Streptavidin	Strep-DyLigth 549	Biotin	Jackson ImmunoResearch
Cy™5-conjugated AffiniPure $F(ab')_2$ fragment goat anti-human IgG, $F(ab')_2$ fragment specific	anti-huFab-Cy5	human $F(ab')_2$	Jackson ImmunoResearch

Polyclonal rabbit anti-goat immunoglobulins/ biotinylated	anti-goat-biotin	goat IgG	Dako Cytomation
R-Phycoerythrin-conjugated AffiniPure $F(ab')_2$ fragment goat anti-human IgG, $F(ab')_2$ fragment specific	anti-huFab-PE	human $F(ab')_2$	Jackson ImmunoResearch
Biotin-SP-conjugated AffiniPure $F(ab')_2$ fragment goat anti-human IgG, $F(ab')_2$ fragment specific	anti-huFab-biotin	human $F(ab')_2$	Jackson ImmunoResearch
Peroxidase-conjugated AffiniPure Goat Anti-Human IgG, $F(ab')_2$ Fragment Specific	anti-huFab-POX	human $F(ab')_2$	Jackson ImmunoResearch
polyclonal goat anti-mouse immunoglobulins/HRP	anti-m-HRP	mouse IgG	Dako Cytomation
Biotin-SP-conjugated AffiniPure Rabbit Anti-Mouse IgG (H+L)	anti-m-biotin	mouse IgG (H+L)	Jackson ImmunoResearch
Biotin-SP-conjugated AffiniPure $F(ab')_2$ Fragment Goat Anti-Rabbit IgG, $F(ab')_2$ Fragment Specific	anti-rabbit-biotin	rabbit $F(ab')_2$	Jackson ImmunoResearch
goat anti-rabbit IgG-HRP	anti-rabbit-HRP	rabbit IgG	SantaCruz
Biotin-SP-conjugated AffiniPure Donkey Anti-Rat IgG (H+L)	anti-rat-biotin	rat IgG (H+L)	Jackson ImmunoResearch

2.1.3 Plasmids

Two plasmids were used: pCES1 and pEE12.4. The pCES1 plasmid (kindly provided by Dyax, MA, USA) displays the Fab antibody library used (see **2.2.2 Selection of antibodies by phage display**). It can be used to express phages presenting Fab antibodies coupled to the gene III protein on their surface (see **2.2.3 Phage production**) or to produce soluble Fab antibodies (see **2.2.7 Fab production**) (de Haard, van Neer et al. 1999). A schematic representation of pCES1 is shown in **Figure 2.1**. At the 3' end a hexa-histidine-tag followed by a *myc*-tag is attached to simplify detection and purification of Fab antibodies. The plasmid contains an ampicillin-resistance cassette.

The plasmid pEE 12.4 (LONZA Biologicals, Basel, Switzerland) is designed for expression of IgGs in myeloma cell lines. It contains the glutamine synthetase (GS) gene and an ampicillin-resistance cassette as selection marker.

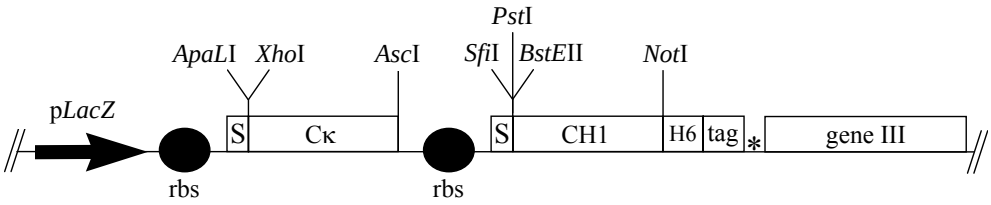

Figure 2.1: Phagemid vector pCES1 for display of antibody Fab fragments. Schematic representation of pCES1. The operon is under the control of the LacZ promotor (p*LacZ*). Rbs: ribosomal binding site, S: signal sequence, H6: hexa-histidine-tag, tag: *myc*-tag, *: amber stop codon enabling production of Fab antibodies. Cloning sites indicated are unique in pCES1. From (de Haard, van Neer et al. 1999).

The plasmids selected and cloned in this work are all derived from pCES1 or pEE 12.4 (**Table 2.4**). pCES1-MSC 1-12 were selected by phage display and used to produce phages displaying Fab antibodies MSC 1 - 12 or to produce Fab antibodies MSC 1-12. pEE 12.4 MSC 3, pEE 12.4 MSC 8, pEE 12.4 MSC 11, pEE 12.4 MSC 3-huTNF, pEE 12.4 MSC 3-muTNF, pEE 12.4 MSC 11-huTNF and pEE 12.4 MSC 11-muTNF were cloned in this work and used for expression of the corresponding IgG or $F(ab)_2$-TNF constructs.

Table 2.4: Plasmids. List of plasmids selected by phage display (derived from pCES1) and plasmids cloned in this work (derived from pEE 12.4). All plasmids contain the ampicillin-resistance cassette as selection marker. Plasmids derived from pEE 12.4 contain in addition the GS gene as selection marker for cell culture. For cloning strategies, see **2.2.14 Cloning of IgGs and TNF-constructs.** HC: heavy chain, LC: light chain.

plasmid designation	description
pCES1-MSC 1-12	pCES1 containing the variable domains of HC and LC of the selected Fab antibodies MSC 1 - 12
pEE 12.4	plasmid for expression of IgGs in myeloma cell lines
pEE 12.4 MSC 3	pEE 12.4 containing the variable domains of HC and LC of MSC 3
pEE 12.4 MSC 8	pEE 12.4 containing the variable domains of HC and LC of MSC 8
pEE 12.4 MSC 11	pEE 12.4 containing the variable domains of HC and LC of MSC 11
pEE 12.4 MSC 3-muTNF	pEE 12.4 containing the variable domains of HC and LC of MSC 3, with the Fc region replaced by murine TNF
pEE 12.4 MSC 3-huTNF	pEE 12.4 containing the variable domains of HC and LC of MSC 3, with the Fc region replaced by human TNF
pEE 12.4 MSC 11-muTNF	pEE 12.4 containing the variable domains of HC and LC of MSC 11, with the Fc region replaced by murine TNF
pEE 12.4 MSC 11-huTNF	pEE 12.4 containing the variable domains of HC and LC of MSC 11, with the Fc region replaced by human TNF

Table 2.5: Bacterial media. The composition of the indicated bacterial media is listed. For cloning LB medium was used, for phage display and expression of Fab antibodies 2xTY media were used.

Bacterial media	**composition**	
LB	10 % (w/v)	Bacto™ Tryptone
	5 % (w/v)	yeast extract
	10 % (w/v)	NaCl
LB agar plates		LB
	1.5 % (w/v)	Difco™ Agar
2xTY	16 % (w/v)	Bacto™ Tryptone
	10 % (w/v)	yeast extract
	5 % (w/v)	NaCl
2xTY-AG		2xTY
	0.1 mg/ml	ampicillin
	2 % (w/v)	glucose
2xTY-AK		2xTY
	0.1 mg/ml	ampicillin
	25 µg/ml	kanamycin
2xTY-AG agar plates		2xTY-AG
	1.5 % (w/v)	Difco™ Agar

2.1.4 Bacteria, phages and bacterial media

Premade Z-competent *E.coli* cells (TG-1; Zymo Research) were used for phage display (see **2.2.2 Selection of antibodies by phage display**) and expression of Fab antibodies (see **2.2.7 Fab production**). For cloning of IgGs and TNF-constructs, One Shot® TOP10 Competent cells (TOP10; Invitrogen) were used. Bacterial media are indicated in **Table 2.5**.

M13K07 (New England Biolabs) containing a kanamycin resistance cassette was used as helper phage (see **2.2.2 Selection of antibodies by phage display** and **2.2.3 Phage production**).

2.1.5 Cell lines and cell culture media

Experiments were performed on human cell lines stably transfected with a plasmid encoding CA IX or with empty vector (HCT 116-CA IX / HCT 116-EV; SKRC 17 MW1 cl4 / SKRC 17), on pVHL deficient renal clear cell carcinomas expressing CA IX at different levels (SKRC 1, SKRC 52 and SKRC 59) and on HeLa cells upregulating CA IX expression under hypoxia (see **2.2.1 Cell culture**), upon stimulation with hypoxia mimicking agents (see **2.2.1 Cell culture**) and under

conditions of high density. HEK 293 cells were used for transient transfections (see **2.2.15 Transient and stable transfection**). Human cell lines with the respective culture medium (**Table 2.6**) are given in **Table 2.7**.

Murine cell lines used are listed in **Table 2.8**. C51 and CT26 upregulate CA IX expression upon induction under hypoxic conditions or after incubation with hypoxia mimicking agents (see **2.2.1 Cell culture**). Wehi S cells were used for TNF-assays (see **2.2.22 TNF assay**). NSO cells were used for stable transfection (see **2.2.15 Transient and stable transfection**). The stable transfections produced in this work express human IgG or $F(ab)_2$-TNF constructs.

Table 2.6: Cell culture media. The composition of cell culture media is indicated.

culture media	composition	
D10		DMEM
	10 % (v/v)	FBS
	100 U / 100 µg/ml	penicillin-streptomycin
D10 β-m		D10
	50 µM	β-mercaptoethanol
Dfreeze	90 % (v/v)	FBS
	10 % (v/v)	DMSO
Dsel		DMEM w/o glutamine
	10 % (v/v)	dialyzed FBS
	2 % (v/v)	GS-supplement (50x)
	10 µM	MSX
	100 U / 100 µg/ml	penicillin-streptomycin
R10		RPMI
	10 % (v/v)	FBS
	100 U / 100 µg/ml	penicillin-streptomycin
R10_6.3		RPMI w/o sodium hydrogen carbonate
	10 % (v/v)	dialyzed FBS
	30 mM	MES
	1 % (v/v)	HT-supplement (100x)
	1 % (v/v)	antibiotic antimycotic solution (100x)
	set pH to 6.3	
R10_7.3		RPMI w/o sodium hydrogen carbonate
	10 % (v/v)	dialyzed FBS
	30 mM	HEPES
	1 % (v/v)	HT-supplement (100x)
	1 % (v/v)	antibiotic antimycotic solution (100x)
	set pH to 7.3	

Table 2.7: Human cell lines. Different cancer cell lines were used to express CA IX (transfected cell lines, pVHL-deficient cell lines and cell lines upregulating CA IX under hypoxic conditions) and cultured using the indicated media. For transient transfections HEK 293 cells were used.

Human cell lines	culture media	description	origin
HCT 116-CA IX	D10	human colon carcinoma	P. Swietach
HCT 116-EV	D10	human colon carcinoma	P. Swietach
HEK 293	D10 + 0.2 mg/ml G418	human embryonic kidney	ATCC
HeLa	D10	human cervical cancer	ATCC
MCF-7	D10	human breast cancer cell line	Ludwig Cancer Institute
SKRC 1	R10	human renal clear cell carcinoma	Ludwig Cancer Institute
SKRC 17	R10	human renal clear cell carcinoma	E. Oosterwijk
SKRC 17 MW1 cl4	R10 + 0.4 mg/ml G418	human renal clear cell carcinoma	E. Oosterwijk
SKRC 52	R10	human renal clear cell carcinoma	Ludwig Cancer Institute
SKRC 59	R10	human renal clear cell carcinoma	Ludwig Cancer Institute

CHO-MSC 3 and CHO-MSC 8 cells were produced by stable transfection of CHO cells at the Ludwig Cancer Institute in Melbourne, Australia, for large scale production of MSC 3 and MSC 8 IgG (**Table 2.9**).

Table 2.8: Murine cell lines. C51 and CT26 cell lines were used to express CA IX under hypoxic conditions and cultured using the indicated media. For stable transfections NSO cells were used leading to NSO-derived cell lines. TNF-sensitive Wehi S cells were used in TNF-assays.

Murine cell lines	culture media	description	origin
C51	D10	murine colon carcinoma	M. Rudin
CT26	D10 β-M	murine colon carcinoma	H. Nishikawa
NSO	D10	murine myeloma	LONZA
NSO-MSC 11	Dsel	NSO producing MSC 11 IgG	produced in this work
NSO-MSC 11-muTNF	Dsel	NSO producing MSC 11-muTNF	produced in this work
NSO-MSC 3-muTNF	Dsel	NSO producing MSC 3-muTNF	produced in this work
Wehi S	R10	murine fibrosarcoma	Ludwig Cancer Institute

Table 2.9: Hamster cell lines. For large scale production of IgG, CHO cells were stably transfected with pEE 12.4 MSC 3 and pEE 12.4 MSC 8.

Hamster cell lines	culture media	description	origin
CHO	D10	chinese hamster ovary cells	Ludwig Cancer Institute
CHO-MSC 3	Dsel	CHO producing MSC 3 IgG	produced in Melbourne
CHO-MSC 8	Dsel	CHO producing MSC 8 IgG	produced in Melbourne

2.1.6 Chemicals and kits

Chemicals and kits used are listed in **Table 2.10**.

Table 2.10: Chemicals and kits. Chemicals and kits are listed with the respective companies. In brackets commonly used abbreviations or chemical formulas are indicated.

Chemicals / Kits	purchased from
1 kb ladder	New England Biolabs
100 bp ladder	New England Biolabs
acetazolamide (ATZ)	Sigma-Aldrich
acetic acid, 99 %	Sigma-Aldrich
acrylamide - Rotiphorese® Gel 30 (37, 5:1)	Roth
agarose	Promega
ammonium chloride (NH_4Cl)	Sigma-Aldrich
ammonium persulfate (APS)	Sigma-Aldrich
ampicillin sodium salt (Amp)	Sigma-Aldrich
antibiotic antimycotic solution (100x)	Sigma-Aldrich
Bacto™ Tryptone	BD Biosciences
BCA™ Protein Assay Reagent	Thermo Scientific
BD Cytofix/Cytpoperm™	BD Biosciences
BD Perm/Wash™	BD Biosciences
bovine serum albumin (BSA)	Thermo Scientific
Brilliant Blue R	Sigma-Aldrich
bromphenol blue sodium salt	Merck
BstNI	New England Biolabs
calcium chloride ($CaCl_2$)	Sigma-Aldrich
CaptureSelect Fab kappa affinity matrix	BAC
cobalt chloride ($CoCl_2$)	Fluka
collagen type I	BD Biosciences
Complete, EDTA free (Proteinase inhibitor)	Roche
crystal violet	Roth
DHPE-fluorescein	Invitrogen

dialysed fetal bovine serum (dialysed FBS)	Sigma-Aldrich
Difco™ 2xYT (Yeast Extract Tryptone) Medium	BD Biosciences
Difco™ Agar, granulated	BD Biosciences
dimethyl sulfoxide (DMSO)	Sigma-Aldrich
dimethyloxaloylglycine (DMOG)	Frontier Scientific
disodium hydrogen phosphate (Na_2HPO_4)	Roth
DL-dithiothreitol (DTT)	Sigma-Aldrich
DMEM	Invitrogen
DMEM w/o glutamine	Invitrogen
DraIII	New England Biolabs
Dynabeads® Protein G	Invitrogen
ECL™ Western Blotting Detection Reagents	GE Healthcare
ethanol (EtOH)	Merck
ethidium bromide (EtBr), 10 mg/ml	Sigma-Aldrich
ethylenediaminetetraacetic acid (EDTA)	Sigma-Aldrich
EZ4U	Biomedica
fetal bovine serum (FBS)	Invitrogen
FseI	New England Biolabs
FuGENE HD Transfection Reagent	Roche
G418	Sigma
glucose	DeltaSelect
glycerol	Roth
glycine	Sigma-Aldrich
GS-supplement (50x)	Invitrogen
HBS-P^+ 10x	GE Healthcare
Hepes	Invitrogen
HT-supplement (100x)	Invitrogen
hydrochloric acid (HCl), fuming (37 %)	Roth
imidazole	Sigma-Aldrich
isopropanol	Kantonsapotheke Zürich
isopropyl-β-D-tiogalactopyranosid (IPTG)	Roche
kanamycin disulfate salt (Kan)	Sigma-Aldrich
magnesium chloride ($MgCl_2$)	Sigma-Aldrich
MES	Roth
methanol	Kantonsapotheke Zürich
Methionine sulphoximine (MSX)	Sigma-Aldrich
milk powder	Roth
normal goat serum (NGS)	Vector Laboratories
NotI	New England Biolabs
Octyl β-D-glucopyranoside (β-OG)	Sigma-Aldrich
OptiMEM	Invitrogen
Orange G	Sigma-Aldrich
paraformaldehyde, 4% in PBS (4 % PFA)	Kantonsapotheke Zürich
penicillin-streptomycin	Invitrogen

Peroxidase Substrate Solution A and B	KPL
Phusion™ Hot Start High–Fidelity DNA Polymerase	Finnzymes
poly L-Lysine	Sigma-Aldrich
polyethylene glycol 6000 (PEG)	Sigma-Aldrich
potassium chloride (KCl)	Roth
potassium D-gluconate	Sigma-Aldrich
potassium dihydrogen phosphate (KH_2PO_4)	Sigma-Aldrich
Precision Plus Protein™ DUAL COLOR Standards	Biorad
ProLong® Gold antifade reagent with DAPI	Invitrogen
PvuI	New England Biolabs
QIAGEN Plasmid Midi Kit	QIAGEN
QIAprep Miniprep Kit	QIAGEN
QIAquick Gel Extraction Kit	QIAGEN
rAPid Alkaline Phosphatase	Roche
Rapid DNA Ligation Kit	Roche
Recombinant Human Carbonic Anhydrase II (rhCA II)	R&D Systems
Recombinant Human Carbonic Anhydrase IX (rhCA IX)	R&D Systems
Recombinant Human Carbonic Anhydrase XII (rhCA XII)	R&D Systems
Recombinant Human Carbonic Anhydrase XIV (rhCA XIV)	R&D Systems
Recombinant Mouse Carbonic Anhydrase IX (rmCA IX)	R&D Systems
REDTaq™ ReadyMix™ PCR Reaction Mix	Sigma-Aldrich
RPMI	Invitrogen
RPMI w/o sodium hydrogen carbonate	Sigma-Aldrich
RsrII	New England Biolabs
sodium chloride (NaCl)	Fluka
sodium dodecylsulfate (SDS), 20 % solution	Ambion
sodium hydrogen carbonate ($NaHCO_3$)	Sigma-Aldrich
sulphuric acid (H_2SO_4), 2 N	Roth
SuperSignal® West Femto Maximum Sensitivity Substrate	Thermo Scientific
Talon® metal affinity resin	Clontech Laboratories
Temed	Bio-Rad
Triethylamine	Sigma-Aldrich
Tris Ultra	Roth
Triton X-100	Sigma-Aldrich
Trypan blue solution (0.4 %)	Sigma-Aldrich
Tween 20	Fluka
Yeast extract	Sigma-Aldrich
β-mercaptoethanol	Sigma-Aldrich

2.1.7 Buffer

Composition of buffers is given in **Table 2.11**.

Table 2.11: Buffer. Composition of the buffers is indicated.

1 kb ladder	20 % (v/v)	1 kb ladder
	20 % (v/v)	5x DNA loading buffer
	10 % (v/v)	dH_2O
100 bp ladder	20 % (v/v)	100 bp ladder
	20 % (v/v)	5x DNA loading buffer
	10 % (v/v)	dH_2O
agarose gel, 0.8 – 3 %	2 % (v/v)	50x TAE
	0.8 – 3 % (w/v)	agarose
Amm-NT	1 mM	$CaCl_2$
	1 mM	$MgCl_2$
	4.5 mM	KCl
	10 mM	Glucose
	12 mM	$NaHCO_3$
	100 mM	NaCl
aerate for 1 h with 5 % CO_2 / 95 % N_2	30 mM	NH_4Cl
B-NT	1 mM	$CaCl_2$
	1 mM	$MgCl_2$
	4.5 mM	KCl
	10 mM	Glucose
	12 mM	$NaHCO_3$
aerate for 1 h with 5 % CO_2 / 95 % N_2	130 mM	NaCl
Coomassie destain	45 % (v/v)	methanol
	10 % (v/v)	acetic acid (99 %)
	45 % (v/v)	dH_2O
Coomassie staining solution	45 % (v/v)	methanol
	10 % (v/v)	acetic acid (99 %)
	0.25 % (w/v)	Brilliant Blue R
	45 % (v/v)	dH_2O
crystal violet solution	0.05 % (w/v)	crystal violet
	20 % (v/v)	EtOH
DNA loading buffer, 5x	50 % (v/v)	1x TAE
	50 % (v/v)	Glycerol
	0.4 % (w/v)	Orange G

HBS-P^+	10 mM	Hepes
	0.15 M	NaCl
	0.05 % (v/v)	Surfactant P20
Hepes-NT, pH 7.4	1 mM	$CaCl_2$
	1 mM	$MgCl_2$
	4.5 mM	KCl
	10 mM	Glucose
	10 mM	Hepes
set pH to 7.4	130 mM	NaCl
homogenization buffer	15 mM	NaCl
	35 mM	KCl
	105 mM	potassium D-gluconate
	20 mM	Hepes
	20 mM	MES
isopropanol/HCl		Isopropanol
	0.4 N	HC
Lämmli buffer	0.28 M	Tris Ultra
	0.5 M	DTT
	30 % (v/v)	glycerol
	1 % (v/v)	SDS (20 %)
	0.0012 % (w/v)	bromphenol blue
	5.5 % (v/v)	β-mercaptoethanol
lysis buffer	150 mM	NaCl
	50 mM	Tris-HCl, pH 7.4 (1 M)
	10 mM	$MgCl_2$
	0.70 %	β-OG
MES-NT, pH 6.4	1 mM	$CaCl_2$
	1 mM	$MgCl_2$
	4.5 mM	KCl
	10 mM	Glucose
	10 mM	MES
set pH to 6.4	130 mM	NaCl
MPBS, 2 – 4 %		PBS
	2 – 4 % (w/v)	milk powder
MPBST	150 mM	NaCl
	10 mM	Na_2HPO_4
	1.5 mM	KH_2PO_4
	0.1 – 0.3 % (v/v)	Tween 20
	2 % (w/v)	milk powder

PBS	150 mM	NaCl
	10 mM	Na_2HPO_4
	1.5 mM	KH_2PO_4
PBST, 0.1 - 0.3 %	150 mM	NaCl
	10 mM	Na_2HPO_4
	1.5 mM	KH_2PO_4
	0.1 – 0.3 % (v/v)	Tween 20
PEG/NaCl	20 % (w/v)	PEG
	1.5 M	NaCl
running buffer	25 mM	Tris Ultra
	0.1% (v/v)	SDS (20 %)
	200 mM	Glycine
running gel, 10 % (v/v)	42 % (v/v)	dH_2O
	33 % (v/v)	acrylamide (30 %)
	25 % (v/v)	1.5 M Tris/SDS, pH 8.8
	0.01 % (v/v)	APS
	0.0005 % (v/v)	Temed
running gel, 12 % (v/v)	35 % (v/v)	dH_2O
	40 % (v/v)	acrylamide (30 %)
	25 % (v/v)	1.5 M Tris/SDS, pH 8.8
	0.01 % (v/v)	APS
	0.0005 % (v/v)	Temed
running gel, 8 % (v/v)	48 % (v/v)	dH_2O
	27 % (v/v)	acrylamide (30 %)
	25 % (v/v)	1.5 M Tris/SDS, pH 8.8
	0.01 % (v/v)	APS
	0.0005 % (v/v)	Temed
SDS loading buffer (non-reducing gel)	0.28 M	Tris Ultra
	30 % (v/v)	glycerol
	1 % (v/v)	SDS (20 %)
	0.0012 % (w/v)	bromphenol blue
stacking gel, 5 % (v/v)	61 % (v/v)	dH_2O
	13 % (v/v)	acrylamide (30 %)
	25 % (v/v)	0.5 M Tris/SDS, pH 6.8
	0.01 % (v/v)	APS
	0.0007 % (v/v)	Temed
TAE, 50x	2 mM	TRIS Ultra
	0.25 mM	acetic acid (99 %)
	0.5 mM	EDTA

transfer buffer	25 mM 190 mM 20 % (v/v)	Tris Ultra Glycine methanol
Tris/NaCl, pH 7.5	25 mM 0.15 M set pH to 7.5	Tris Ultra NaCl
Tris/SDS, 0.5 M, pH 6.8	0.5 M 0.4 % (v/v) adjust pH to 6.8	Tris Ultra SDS (20 %)
Tris/SDS, 1.5 M, pH 8.8	1.5 M 0.4 % (v/v) adjust pH to 8.8	Tris Ultra SDS (20 %)
Tris-HCl, pH 7.4	1 M adjust pH to 7.4	Tris Ultra

2.2 METHODS

2.2.1 Cell culture

All cells were grown at 37 °C in a 5 % CO_2 incubator in the media indicated in **Table 2.7**, **Table 2.8** and **Table 2.9**. Cells were passaged by detachment after incubation with PBS containing 1 mM EDTA for 5 – 20 min. Cell numbers were determined after staining cells with trypan blue using a Neubauer haemocytometer (Omnilab). For freezing, cells were resuspended in 1 ml freezing medium (Dfreeze) and transferred to CryoTube^{TM} Vials (Nunc). Vials were stored for 2 d in a cell freezing box containing isopropanol at –80 °C before transfer to liquid nitrogen (-180 °C).

For expression of CA IX, cells were induced chemically or in a hypoxic chamber. For chemical induction cells were incubated with 1 mM (HeLa) or 2 mM (C51 and CT26) dimethyloxaloylglycine (DMOG; stock: 1 M in DMSO) for 48 h at 37 °C in a 5 % CO_2 incubator. Alternatively, cells were induced with 200 µM $CoCl_2$ for 48 h. For hypoxic induction cells were incubated for 48 h in an Invivo$_2$ 400 hypoxic chamber (Ruskinn Technology) at 0.2 % O_2, 5 % CO_2.

2.2.2 Selection of antibodies by phage display

For selection of CA IX specific antibodies, a non-immunized phage library expressing Fab antibodies was used (see **2.1.3 Plasmids**) (de Haard, van Neer et al. 1999). 10^{13} phages were precipitated by adding 1/5 volume PEG/NaCl and incubation for 1 h on ice, centrifuged for 15 min at 4'000 rpm and blocked in 1 ml 2 % MPBS for 1 h at room temperature. During phage block, Dynabeads® Protein G for preabsorption and subsequent phage display were prepared.

Dynabeads® Protein G were washed three times with Tris/NaCl, pH 7.5. rhCA IX was immunoprecipitated using M75 in a total volume of 300 µl Tris/NaCl, pH 7.5 for 1 h at 4 °C and the CA IX/M75-complex was incubated for 1 h at 4 °C with Dynabeads® Protein G. For preabsorption, M75 antibody alone was incubated with Dynabeads® Protein G. Dynabeads® Protein G complexes were removed from the suspension using a magnetic rack and washed four times with Tris/NaCl, pH 7.5.

Blocked phages were added to M75/Dynabeads® Protein G and preabsorbed for 2 h at room temperature. M75/Dynabeads® Protein G were removed from the suspension using a magnetic rack and the phage containing supernatant was transferred to CA IX/M75/Dynabeads® Protein G and incubated for 1 h at room temperature. Phages bound to CA IX/M75/Dynabeads® Protein G were

washed 10x with MPBST, 10x with 0.3 % PBST and 3x with PBS using a magnetic rack, and subsequently eluted with 1 ml 100 mM triethylamine for 10 min at room temperature. CA IX/M75/Dynabeads® Protein G were removed from the suspension using a magnetic rack and phage containing supernatant was neutralized by adding 500 µl Tris-HCl, pH 7.4.

E. coli TG-1 were grown in 2xTY medium to an OD_{600} of 0.5. 1 ml neutralized phages was added to 5 ml TG-1 and 4 ml 2xTY and incubated for 30 °C in a water bath at 37 °C. The TG-1/phage suspension was centrifuged for 10 min at 4'000 rpm and the pellet containing infected TG-1 was resuspended in 1.2 ml 2xTY. The bacteria suspension was plated on two 10 cm 2xTY-AG agar plates and bacteria were amplified over night at 30 °C. On the next day TG-1 were collected by scraping from the plates, resuspended in 2 TY-AG and an aliquot was frozen with 15 % glycerol at -80 °C. 5-15 µl of the suspension were inoculated in 50 ml 2xTY-AG at 37 °C with shaking until an OD_{600} of 0.5. Phages were produced using M13K07 as helper phage in a ratio of 20:1 phage to bacteria. TG-1/M13K07 suspension was incubated for 30 min at 37 °C in a water bath, centrifuged for 10 min at 4'000 rpm and the pellet was resuspended in 25 ml prewarmed 2xTY-AK and grown over night at 30 °C on an orbital shaker.

Four rounds of selection with decreasing antigen concentration were performed (round 1: 90 µg M75, 30 µg rhCA IX and 400 µl Dynabeads® Protein G; round 2: 65 µg M75, 15 µg rhCA IX and 250 µl Dynabeads® Protein G; rounds 3 and 4: 45.5 µg M75, 10 µg rhCA IX and 150 µl Dynabeads® Protein G).

2.2.3 Phage production

Colonies of *E.coli* TG-1 containing pCES1 encoding the appropriate Fab antibody were inoculated in 100 µl 2xTY-AG in flat-bottomed 96-well-plates and grown over night at 30 °C on a orbital shaker. On the next day 2 µl were transferred to a round-bottomed 96-well-plate containing 120 µl 2xTY-AG per well. The plate was sealed with an AirPore™ Tape Sheet (QIAGEN) to minimize evaporation of medium and incubated at 37 °C for 2 h (until OD ≈ 0.5). 40 µl 2xTY-AG containing $2 \cdot 10^9$ plaque forming units (pfu) M13K07 helper phage were added to each well and incubated for 30 min at 37 °C. The plate was centrifuged for 10 min at 1700 rpm and all supernatant was removed. Cells were resuspended in 120 µl 2xTY-AK and grown o/n at 30 °C while shaking. On the next day the plate was centrifuged at for 10 min at 1700 rpm and supernatant was used for downstream assays like flow cytometry.

To the original flat-bottomed plate glycerol was added to a final concentration of 15 % and the plate was frozen at –80 °C.

Table 2.12: PCR conditions for fingerprint. Temperature and time for denaturation, annealing and elongation are given. 40 cycles were performed in order to generate many copies of DNA leading to strong bands in agarose gel electrophoresis, which is especially important for DNA fingerprint, were many small bands are produced.

	temperature	time	
initial denaturation	94 °C	10 min	
denaturation	94 °C	45 s	40 cycles
annealing	50 °C	45 s	
elongation	72 °C	90 s	
final elongation	72 °C	10 min	

2.2.4 DNA fingerprint

Colonies were screened by PCR using the REDTaq™ ReadyMix™ PCR Reaction Mix according to the manufacturer's instruction. PCR conditions are shown in **Table 2.12**. For fingerprint of Fab antibody sequences in pCES1 primers fingerprint_fwd and fingerprint_back were used for PCR, followed by digestion with BstNI for 3 h at 60 °C. Fingerprint of pEE12.4 to confirm correct insertion of HC and LC was performed using the corresponding cloning primers for variable domain amplification and the amplified DNA was cut with an appropriate multi-cutting restriction enzyme. Bands were analyzed on a 3 % agarose gel.

2.2.5 Agarose gel electrophoresis

Sample DNA was mixed with 5x DNA loading buffer and separated on a 0.8 – 3 % agarose gel in 1x TAE at 80 – 100 V. For DNA samples obtained by PCR with REDTaq™ ReadyMix™ PCR Reaction Mix no 5x loading buffer was needed. 0.5 µg 100 bp or 1 kb ladder was used as size standard. DNA was visualized under UV using ethidium bromide in a BioDoc-It Imaging System (UVP).

2.2.6 Monoclonalisation of bacteria expressing Fab antibodies

If necessary, bacteria expressing Fab antibodies were monoclonalised by several rounds of isolation of plasmid DNA using the QIAprep Miniprep Kit and subsequent transformation into *E. coli* TG-1 according to the manufacturers' instructions.

2.2.7 Fab production

Fab antibodies were produced in *E. coli* TG-1. Overnight cultures of TG-1 were inoculated 1:100 in 1 l 2xTY-AG and grown at 37 °C. At an OD_{600} of 0.6-0.9 cultures were induced with 1 mM IPTG for 4 h at 30 °C. Cells were centrifuged for 15 min at 4000 rpm and the pellet was frozen at – 20 °C. Soluble Fab antibodies were released from the periplasmic fraction by incubation in 25 ml PBS pH 8 containing Complete, EDTA free (Proteinase inhibitor) at 4 °C over night. Crude fractions from Fab antibody production were centrifuged 20 min at 8000 g and Fab antibodies containing supernatant was incubated with 1 ml Talon® metal affinity resin for 1 h at 4 °C, washed with 0.1 % PBST, and loaded onto an empty column. The column was washed with 3x column volume 0.1 % PBST and Fab antibodies were eluted with PBS, containing 100 mM imidazole. Fab antibodies were dialyzed over night at 4 °C against PBS and analyzed by SDS-PAGE followed by coomassie staining.

2.2.8 Protein concentration by BCA protein assay or photometry

Protein concentration was measured with the BCA™ Protein Assay Reagent according to the manufacturer's instruction. 5 µl sample was incubated with 100 µl detection reagent for 30 min at 37 °C. Absorption at 562 nm was measured in a Wallac Victor^2 1420 Multilabel Counter (PerkinElmer). BSA was used as standard.

Alternatively, concentration of purified Fab antibodies was measured in a spectrophotometer (Eppendorf) at 280 nm using the Lambert-Beer equation:

$$A = \varepsilon \cdot l \cdot c$$

where A is the absorbance, ε the extinction coefficient of the protein, l the path length and c the concentration. Extinction coefficients for Fab antibodies were calculated using the ProtParam tool from ExPASy Proteomics Server (Swiss Institute of Bioinformatics) (**Table 2.13**).

2.2.9 Whole cell protein extraction

SKRC 17 MW1 cl4 and SKRC 17 cells from a confluent 75 mm^2 cell culture flask were pelleted and incubated in 1 ml lysis buffer containing Complete, EDTA free (Proteinase inhibitor) according to the manufacturer's instruction for 20 min at 4 °C while vortexing regularly. The sample was centrifuged for 5 min at 13'000 rpm, protein containing supernatant was stored at - 20 °C and later used for Western blot experiments.

Table 2.13: Extinction coefficients. Extinction coefficients for Fab antibodies MSC 1 – 12 were calculated using the ProtParam tool from ExPASy Proteomics Server (Swiss Institute of Bioinformatics).

protein (Fab antibody)	extinction coefficient [M^{-1} cm^{-1}]
MSC 1	78'560
MSC 2	75'915
MSC 3	74'425
MSC 4	68'465
MSC 5	81'415
MSC 6	81'415
MSC 7	75'915
MSC 8	93'905
MSC 9	74'426
MSC 10	72'935
MSC 11	66'405
MSC 12	78'040

2.2.10 SDS-PAGE followed by coomassie staining or immuno blotting

30 µl or 2 µg sample (for maximal signal or comparison of different probes, respectively) were heated with 1/6 volume Lämmli buffer for 5 min at 95 °C and loaded on an SDS-polyacrylamide gel. For non-reducing conditions, SDS loading buffer (w/o DTT and β-mercaptoethanol) was used. Precision Plus Protein™ DUAL COLOR Standards was used as molecular weight standard. Proteins were collected in a 5 % (v/v) stacking gel at 45 mA and subsequently separated according to their molecular weight in a running gel (12 % for reducing conditions, 8% for non-reducing conditions) at 65 mA using running buffer.

The SDS-polyacrylamide gel was stained with coomassie staining solution for 1 h at room temperature and afterwards destained in coomassie destain until background was minimal. Gels were scanned using a CanoScan LiDE 70 (Canon).

Table 2.14: Staining protocol for Western blot analysis. Targets were detected using the indicated staining procedure.

target	1st antibody	2nd antibody	3rd antibody
human CA IX	M75 (1:1'000)	anti-m-HRP (1:1'000)	-
human CA IX	MSC 1 – 12 Fab antibody (20 µg/ml)	anti-Myc (1:1'000)	anti-m-HRP (1:1'000)
human Fab / IgG	anti-huFab-POX (1:10'000)	-	-
muTNF	anti-muTNF (1:1'000)	anti-goat-biotin (1:5'000)	Strep-POD (1:10'000)
huTNF	anti-huTNF (1:1'000)	anti-goat-biotin (1:5'000)	Strep-POD (1:10'000)

Alternatively, the SDS-polyacrylamide gel was soaked in transfer buffer and transferred for 30 min at 10 V to a Protran® nitrocellulose transfer membrane (0.45 µm pore size, Whatman®) using a Trans-blot® SD semi-dry transfer cell (Bio-Rad). Membranes were blocked with 4 % MPBS for 1 h at room temperature and stained against the designated targets with the indicated antibodies added in PBS for 1 h at room temperature (**Table 2.14**). After each antibody, membranes were washed three times with 0.1 % PBST. Bands were detected in a ChemiDoc-It Imaging System with BioChemi HR Camera (UVP) using ECL™ Western Blotting Detection Reagents or SuperSignal® West Femto Maximum Sensitivity Substrate.

If no resolution of proteins according to molecular weight was necessary, a DotBlot was performed. 30-100 µl sample was loaded directly on nitrocellulose transfer membranes using a loading applicator. Membranes were stained according to the procedure in Western blot analysis.

2.2.11 Flow cytometry

Fab antibodies and IgGs were analyzed for binding specificities using flow cytometry on antigen expressing human and murine cell lines. Bound Fab antibody was detected with anti-Myc, followed by anti-m-biotin and Strep-PE. Surface bound IgG was detected using anti-huFab-PE (for huIgG) or anti-m-biotin followed by Strep-PE (for muIgG). As control, human samples were stained with M75 (1:100) followed by an anti-m-biotin and Strep-PE and murine samples with M-100 (1:100) followed by an anti-rabbit-biotin and Strep-PE. All antibodies were used at a dilution of 1:200 if not stated otherwise. Incubation was performed in a volume of 100 µl for 30 min and samples were washed once with PBS between different antibodies. Analysis was performed on a FACScan cytometer (BD Biosciences). Geometric mean fluorescence intensity (GMFI) was determined using FlowJo 7.5 and signals were normalized to the staining cascade, with the staining cascade set to one and the samples shown as n-fold GMFI.

For titrations, HeLa or SKRC 52 cell lines were induced in 75 cm^2 flasks under hypoxic conditions (0.2 % O_2, 5 % CO_2.) for 24 h. Antibodies were added at concentrations ranging from 0 µg/ml to 1 mg/ml and incubated for 2 h in an Invivo$_2$ 400 hypoxic chamber (Ruskinn Technology). Alternatively, antibodies were added to normoxic cells and incubated at normoxic conditions for 2 h. Cells were scraped, 10'000 cells per sample were fixed for 30 min in 2 % PFA and stained using anti-huFab-PE. Geometric mean fluorescence intensity (GMFI) was determined using FlowJo 7.5 and signals were given as percentage of maximal binding. Concentration of half maximal binding (EC_{50}) was determined.

2.2.12 ELISA

96-well-microtiter-plates (MaxiSorp Nunc) were coated with 100 ng protein (rhCA IX, rmCA IX, rhCA II, rhCA XII or rhCA XIV, respectively) over night at 4 °C, blocked with 2 % MPBS for 1 h at room temperature, incubated with 20 µg/ml Fab antibody MSC 1-12 for 1 h at room temperature and detected with anti-Myc (1:1'000), followed by anti-m-HRP (1:1'000). As loading control, samples were stained with anti-His (1:100), followed by anti-m-HRP (1:1'000). For specific isoforms, the corresponding antibodies were used: M75 (1:100) for human CA IX followed by anti-m-HRP (1:1'000), M-100 (1:100) for murine CA IX followed by anti-rabbit-HRP (1:1'000) and anti-CA II (1:100) for CA II followed by anti-rat-biotin (1:100) and Strep-POD (1:5'000). Peroxidase Substrate Solutions A and B were mixed at a ration of 1:1. 100 µl of solution was added to each well. As soon as a clear colour change was visible, the reaction was stopped with 50 µl 2 N H_2SO_4 and absorbance at 450 nm was measured in a Wallac Victor^2 1420 Multilabel Counter (PerkinElmer). Signals were normalized to the staining cascade and significance was evaluated using a two tailed, paired T-test.

2.2.13 Surface Plasmon Resonance binding assays

Binding analysis of Fab antibodies to rhCA IX or rmCA IX was performed on a BIAcore T100 instrument (GE Healthcare, Uppsala, Sweden). CA IX was immobilized at low density on a CM5 sensor chip (Biacore AB) using amine coupling chemistry, in accordance to the manufacturer's instructions. Fab antibodies at different concentrations (5 to 240 nM) in HBS-P$^+$ buffer were injected at a flow rate of 30 µl/min at 25°C to analyse binding kinetics. No washing was performed, since the coated protein showed to be instable after any tested washing procedure. For the same reason, chips were coated at low density. Analysis of the binding curves and the determination of rate constants were done using non-linear analysis with BIAcore T100 Evaluation Software V 2.0. Double-referenced association and dissociation phase data were locally fit to a 1:1 binding model, assuming bulk contribution.

2.2.14 Cloning of IgGs and TNF-constructs

Variable domains of heavy chain (HC) and light chain (LC) from pCES1 were amplified by two subsequent PCR reactions (**Table 2.15**) using Phusion^{TM} Hot Start High-Fidelity DNA Polymerase according to the manufacturer's instructions (**Table 2.16**). For MSC 3 HC the DNA sequence was codon optimized for a eukaryotic expression system and ordered at geneart. For cloning of F(ab)$_2$-TNF constructs the TNF insert was cut out from ESC 14-huTNF or ESC 14-muTNF, respectively

(Wüest et al., unpublished data). Inserts and pEE 12.4 backbone were digested with DraIII, RsrII or FseI/NotI for heavy chain, light chain or $F(ab)_2$-TNF constructs, respectively. The pEE 12.4 backbone was dephosphorylated using rAPid Alkaline Phosphatase according to the manufacturer's instructions. Insert and pEE 12.4 backbone were both purified via extraction from an agarose gel (see **2.2.5 Agarose gel electrophoresis**) using the QIAquick Gel Extraction Kit and ligated using the Rapid DNA Ligation Kit according to the manufacturer's instructions. Constructs were transformed into One Shot® TOP10 Competent cells according to the manufacturer's instruction. Cloning was analyzed by DNA fingerprint (see **2.2.4 DNA fingerprint**) and confirmed by sequencing at Microsynth. Positive clones were grown in LB containing 0.1 mg/ml ampicillin over night at 30 °C. Bacteria suspension was frozen in 15 % glycerol and stored at –80 °C. Plasmids were prepared using QIAprep Miniprep Kit or QIAGEN Plasmid Midi Kit.

Table 2.15: Primers used for cloning of IgG. The primers used for the first and second PCR for amplification of the variable domains of the heavy and light chain of selected antibodies are indicated. Sequences of primers are given in Table 2.1.

cloning of …	PCR I	PCR II
MSC 3 LC	LC_Rsr_5'_MSC 3 & LC_Rsr_3'	LC_Rsr_5' & LC_Rsr_3'
MSC 8 HC	HC_Dra_5'_MSC 8 & HC_Dra_3'	HC_Dra_5' & HC_Dra_3'
MSC 8 LC	LC_Rsr_5'_MSC 8 & LC_Rsr_3'	LC_Rsr_5' & LC_Rsr_3'
MSC 11 HC	HC_Dra_5'_MSC 11 & HC_Dra_3'	HC_Dra_5' & HC_Dra_3'
MSC 11 LC	LC_Rsr_5'_MSC 11 & LC_Rsr_3'_MSC 11	LC_Rsr_5' & LC_Rsr_3'_MSC 11

Table 2.16: PCR conditions for amplification of variable domains of HC and LC. Temperature and time for denaturation, annealing and elongation are given. For the first PCR 10 cycles were performed followed by a second PCR using 15 cycles. PCR products were not purified between the two PCR reactions.

	temperature	time	
initial denaturation	98 °C	30 s	
denaturation	98 °C	10 s	PCR I: 10 cycles / PCR II: 15 cycles
annealing	57 °C	10 s	
elongation	72 °C	10 s	
final elongation	72 °C	5 min	

2.2.15 Transient and stable transfection

HEK 293 cells were transiently transfected using FuGENE HD Transfection Reagent according to the manufacturer's instructions, using 8 µl FuGENE HD Transfection Reagent and 2 µg DNA. Cells were grown in OptiMEM to reduce influence of albumin in downstream Western blot experiments. Supernatants were tested after 2-4 d in Western blot and flow cytometry.

For stable transfection, 40 µg DNA was linearized with PvuI for 3 h at 37 °C, followed by heat inactivation of PvuI for 20 min at 80 °C. Digestion was confirmed by electrophoresis on a 0.8 % agarose gel (see 2.2.5). 10^7 NSO cells were washed with 20 ml DMEM and resuspended in 700 µl DMEM. DNA was added to the cells, mixed gently and cells were electroporated in a gene pulser® II (Biorad) with a single pulse of 250 V, 400 µFd. Cells were then added to 200 ml DMEM. 50 µl/well cell-suspension was plated in forty 96-well-plates and incubated at 37 °C. Next day, 150 µl Dsel selection medium were added to each well. NSO cells do not express GS and therefore can not survive without addition of glutamine. Cells transfected with pEE 12.4 containing the GS gene thus can be positively selected. After 4 weeks plates were tested for single clones. Supernatants from single clones were tested for IgG production in DotBlot and subsequently in Western blot and flow cytometry. Stable cell lines producing MSC 11 IgG, MSC 3-muTNF and MSC 11-muTNF were generated.

2.2.16 IgG purification

Supernatants of transient or stable transfections were sterile filtered and incubated with 0.5 ml CaptureSelect Fab kappa affinity matrix per litre for 3 h at 4 °C on a rotator. Samples were centrifuges for 3 min at 1500 rpm and washed three times with PBS. IgGs were extracted from the beads by incubation with 4 bead volumes of PBS, containing 0.1 M glycine for 1-2 min. After centrifugation at 1500 rpm for 3 min, the supernatant was transferred to a new Eppendorf tube and was purified by a second centrifugation step. pH of the supernatant was neutralized using 1 M Tris, pH 8 (1/10 sample volume) and dialyzed o/n at 4 °C. Samples were aliquoted and shock-frozen in liquid nitrogen before storage at –80 °C.

MSC 3 IgG and MSC 8 IgG were produced and purified by the Ludwig Cancer Institute in Melbourne, Australia.

2.2.17 Inhibition of CA IX activity on membrane fragments

To inhibit CA IX activity in membrane fragments, measurements were performed according to Swietach et al (Swietach, Wigfield et al. 2008). In brief, confluent HCT 116-CA IX and HCT 116-

EV cells were scraped to ice cold water and centrifuged for 7 min at 5000 rpm. Cells were resuspended in ice cold homogenization buffer and subjected to two rounds of freeze-thawing followed by centrifugation and resuspension of the pellet in fresh homogenization buffer. 660 µl membrane fragment suspension was added to a 2 ml well-stirred vessel cooled to 2 °C. A narrow pH electrode was used to monitor pH. 330 µl of CO_2-saturated water (produced by aeration of dH_2O with 5 % CO_2 / 95 % N_2 for at least 1 h at 2 °C) were added to start the carbonic anhydrase-catalyzed reaction. pH time-courses were measured. The spontaneous hydration rate was determined on membrane–free buffer. Effect of selected antibodies was determined by adding 20 µg/ml Fab antibodies or IgGs to the membrane fragments. As control, 20 µg/ml G250, 20 µg/ml anti-CA II or 100 µg/ml acetazolamide (stock: 100 mg/ml in DMSO) were used. For MSC 8 Fab and MSC 8 IgG, a dose response experiment was performed using concentrations from 0.1 µg/ml to 100 µg/ml or from 0.1 µg/ml to 200 µg/ml, respectively. The reaction constant was calculated from the pH time-course using a fitting algorithm developed by Swietach et al (Swietach, Patiar et al. 2009) and normalized to HCT 116-EV (zero) and activity using HCT 116-CA IX membrane fragments (one).

2.2.18 Inhibition of CA IX activity on intact single cells

CA IX activity was inhibited on intact single cells according to Swietach et al. (Swietach, Patiar et al. 2009). HCT 116-CA IX cells were plated on a poly-L-Lysine coated chamber, fitted on an inverted Nikon microscope. Cells were exposed to medium containing 50 µM DHPE-fluorescein for 10 s. The dye was excited at 484 nm by a monochromator and emission was detected at 520 ± 20 nm with a photomultiplier. Cells were either preincubated for 1 h with Fab fragments and IgG at a concentration of 20 µg/ml or Fab antibodies were added to the superfusate at a concentration of 1 µg/ml. As control, 100 µg/ml acetazolamide (ATZ, stock: 100 mg/ml in DMSO) were added to the superfusate. Cells were superfused with 2 ml/min B-NT or Amm-NT. For calibration, Hepes-NT, pH 7.4 and Mes-NT, pH 6.4 were used. Data were acquired at 100 Hz using Spike software. The area under the curve was calculated as a measurement for carbonic anhydrase IX activity and normalized to ATZ.

2.2.19 Immunofluorescence of tumour tissue

Sections of C51 tumours (kindly provided by S. Lehmann and M. Rudin, Zürich, Switzerland) were fixed in 4 % PFA for 10 min and stained with hypoxy-probe (1:100) and unpurified supernatants of transiently transfected HEK 293 cells expressing MSC 3 IgG and MSC 11 IgG at a dilution of 1:20,

followed by anti-huFab-Cy5 (1:100). Incubations were performed in a volume of 300 µl in PBS containing 2 % NGS and 2 % Triton X-100. Between different antibodies, sections were washed three times for 10 min in PBS. Sections were embedded using ProLong® Gold antifade reagent with DAPI. Pictures were taken on an inverse SP2 Leica microscope with 40x magnification.

2.2.20 Internalization of CA IX detected by immunofluorescence

Cover slips were coated with 100 µg/ml collagen type I in PBS for 1 h at 4 °C. 5'000 cells were seeded o/n. CA IX expression was chemically induced using DMOG as described in **2.2.1 Cell culture**. Cells were stained with 20 µg/ml anti-CA IX antibodies (MSC 3, MSC 8) or negative control (ESC 11) for 1 h at 4 °C or 37 °C, respectively. Cells were fixed and permeabilized with BD Cytofix/Cytpoperm™ for 30 min at 4 °C. Bound IgG was detected with anti-huFab-biotin (1:200) followed by Strep-DyLigth549 (1 µg/ml, 1:1'800). Antibodies were dissolved in BD Perm/Wash™ and incubated for 1 h at 4 °C. Between different antibodies, cover slips were washed twice with BD Perm/Wash™. Cover slips were embedded with ProLong® Gold antifade reagent with DAPI. Pictures were taken on an inverse SP2 Leica microscope with 40x magnification.

2.2.21 Proliferation assay

To test inhibition of proliferation by selected antibodies, 10'000 SKRC 52 cells were seeded in 96-well plates and next day different concentrations of Fab antibodies (up to 1 µM) were added. Alternatively 100'000 HeLa cells or MCF-7 cells were seeded in a 6-well plate, incubated for 24 h in an Invivo$_2$ 400 hypoxic chamber (Ruskinn Technology) at 1 % O_2 and next day 1 µM Fab antibody was added. To test inhibition by IgG, 1'000 HeLa, SKRC 17 and SKRC 17 MW1 cl4 or SKRC 52 cells were seeded in a 96-well plate and incubated for 1-5 days in an Invivo$_2$ 400 hypoxic chamber (Ruskinn Technology) at 0.2 % O_2 with up to 0.5 µM IgG. 1-10 days after addition of Fab antibodies or IgGs, proliferation was determined using the EZ4U kit according to the manufacturer's instruction, by staining with crystal violet or by counting the cells. For crystal violet staining, cells were washed with PBS and incubated for 10 min at room temperature with crystal violet solution. Plates were washed in dH_2O and dried. Crystal violet was dissolved in isopropanol/HCl and absorbance was measured at 560 nm in the Wallac Victor^2 1420 Multilabel Counter (PerkinElmer). To assess significance a paired two-tailed T-test was performed.

To test proliferation under conditions of low pH and low hydrogen carbonate, 1000 SKRC 17, SKRC 17 MW1 cl4 or SKRC 52 cells were seeded in 6-well-plates. After attachment of the cells to the plate, medium was changed to RPMI w/o hydrogen carbonate at pH 6.3 or 7.3 (R10_6.3 or

R10_7.3, respectively) and 20 µg/ml IgG or 100 µM acetazolamide (stock: 100 mM in DMSO) were added. Cells were incubated in an incubator at ambient CO_2-partial pressure for 24 h. Medium was changed to normal RPMI and cells were grown for another 7 d at 5 % CO_2. Colonies were counted.

2.2.22 TNF assay

10'000 Wehi S cells were seeded in 96-well-plates in a volume of 100 µl. After attachment of the cells to the plate, 100 µl supernatant of HEK 293 cells transiently transfected with $F(ab)_2$-TNF constructs and serial dilutions of the same were added and incubated over night in the incubator. On the next day, cells were stained using the EZ4U kit according to the manufacturer's instruction (with only 10 µl of substrate added to 200 µl cell culture). Absorbance was measured at 450 nm in the Wallac Victor^2 1420 Multilabel Counter (PerkinElmer) after 2 h. Significance was assessed using a paired, two-sided T-test.

3 RESULTS

3.1 SELECTION OF RHCA IX SPECIFIC FAB ANTIBODIES BY PHAGE DISPLAY

3.1.1 Phage display

Fab antibodies specific to recombinant human CA IX (rhCA IX) were selected from a large human Fab antibody library by phage display. Four rounds of selection were performed on decreasing concentrations of antigen. After each selection round, phage pools were tested for specific binding to CA IX in flow cytometry on chemically induced HeLa cells (**Figure 3.1 A**). After selection round one, no enrichment of phages specifically recognizing CA IX was detectable, whereas rounds two and three both led to an increase in CA IX specific phages. Selection round four did not further increased binding of the phage pool to HeLa cells expressing CA IX compared to round three. After phage display, single clones were picked and phages were produced. Since every selection round leads to the loss of potential binders, phages after round three (88 clones) and four (264 clones) were used for subsequent screening by flow cytometry on CA IX expressing cells. 16 % of the tested phages from round three were able to bind to CA IX, whereas after four rounds of selection the fraction was augmented to 23 % (**Figure 3.1 B**). In total, 75 potential binders were identified.

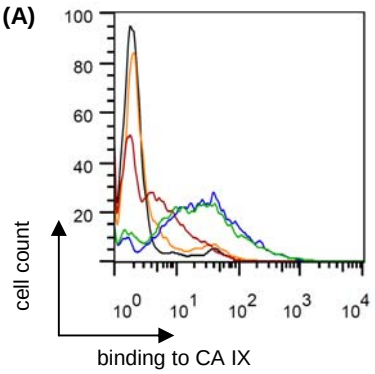

(B)

	# of clones tested	# of binders	% of binders
3rd round	88	14	16 %
4th round	264	61	23 %

Figure 3.1: Analysis of phages after selection rounds three and four in flow cytometry. (A) Flow cytometry of phage pools. Phage pools after selection rounds one (orange), two (red), three (blue) and four (green) were tested on HeLa cells induced with 1 mM DMOG and compared to the staining cascade (black). **(B)** Flow cytometry of single phage clones. Single clones after rounds three and four were tested for the percentage of binding to CA IX expressed on HeLa cells induced with 1 mM DMOG.

3.1.2 Preliminary analysis of selected Fab antibodies

The potential binders were used for DNA fingerprint and grouped according to their restriction patterns. Fingerprint led to the identification of 22 groups containing distinct restriction patterns, with each group consisting of one to 16 clones with identical restriction pattern. One clone of each group was used to produce Fab antibodies that were tested for specific binding by flow cytometry. Binding of Fab antibodies was tested on HeLa cells chemically induced to express CA IX and compared to not induced HeLa cells. Additionally, specific binding of Fab antibodies was tested on CA IX expressing SKRC 17 MW1 cl4 cells compared to the parental SKRC 17 cells. This screen allowed identifying potential binders specifically recognizing CA IX but no other antigen possibly present during the first screen by flow cytometry which was performed on CA IX positive cells only. Some potential binders bound also to the negative cell lines and, thus, were excluded from further experiments. Furthermore, some binders were excluded, since binding to the positive cell line observed in the first screen could not be confirmed. All groups excluded apart from one consisted of only one clone. The last group excluded contained two clones with identical restriction pattern.

According to this second screen, only twelve groups selected against CA IX were analysed further. One clone of each group was once more subjected to DNA fingerprint analysis (**Figure 3.2 A**). All twelve clones showed a distinct restriction pattern, confirming uniqueness of the selected groups. The number of clones per group was determined (**Figure 3.2 B**). Seven groups contained several clones with four groups consisting of more than eight clones, indicating enrichment of phages during phage display. One clone of each group was sequenced and, if necessary, clones were monoclonalised. Sequencing led to the identification of twelve distinct clones named MSC 1 – 12.

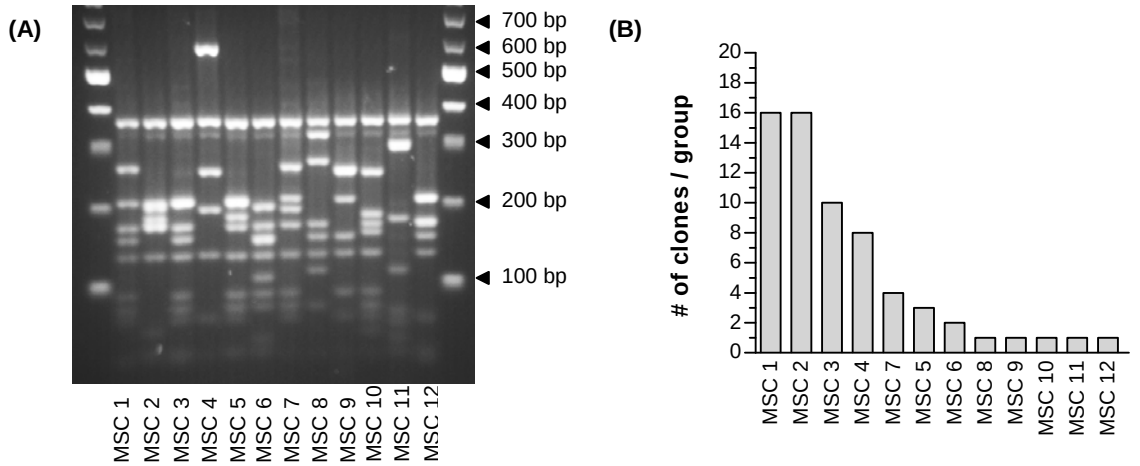

Figure 3.2: Fingerprint MSC 1 – 12. (A) Uniqueness of the twelve selected groups named MSC 1 – 12 was confirmed in DNA fingerprint using BstNI as multi-cutting restriction enzyme. **(B)** The number of clones with identical restriction pattern in each group MSC 1 – 12 was determined.

3.2 CHARACTERIZATION OF MSC 1 – 12

3.2.1 Production of Fab antibodies

Fab antibodies MSC 1 – 12 were produced and analyzed in SDS-PAGE followed by coomassie staining (**Figure 3.3**). As control, two Fab antibodies ESC 11 and ESC 14 (raised by E. Fischer and T. Wüest, unpublished data) recognizing Fibroblast Activation Protein (FAP) were produced and analyzed by SDS-PAGE, too. Coomassie staining confirmed production of all Fab antibodies. Heavy chain and light chain of the Fab antibodies were expressed at the expected size (around 25 kDa) and purity of the Fab antibodies was approved.

3.2.2 Induction of CA IX expression in human cell lines

CA IX expression can be achieved by stable transfection of cell lines with the *ca9* gene, by using pVHL deficient cell lines or by inducing cells to express CA IX, either by chemical induction or by hypoxic induction in a hypoxic chamber. In pre-tests optimal conditions for CA IX expression were determined and chemical induction using $CoCl_2$ and DMOG was compared. Chemical induction was optimal to upregulate CA IX in HeLa cells with 200 µM $CoCl_2$ for 48 h (**Figure 3.4 A**) or with 1 mM DMOG for 48 h (**Figure 3.4 B**). Induction in the hypoxic chamber was optimal at 0.2 % O_2 for 48 h (**Figure 3.4 C**). Chemical induction with DMOG led to a sharper peak in the histogram showing CA IX expression than the chemical induction with $CoCl_2$. This sharper peak corresponds to a more homogeneous expression of CA IX and thus further experiments were performed using DMOG.

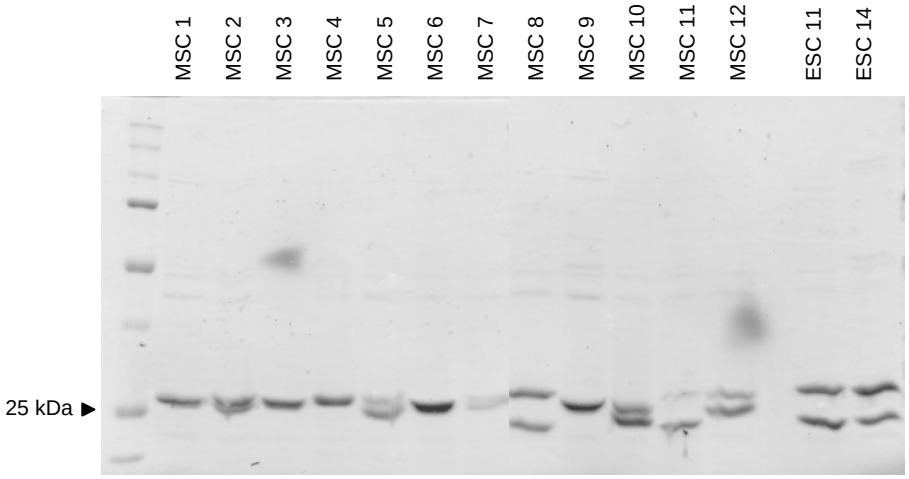

Figure 3.3: Coomassie of Fab antibodies MSC 1 – 12. Purity of Fab antibodies MSC 1 – 12 as well as control antibodies ESC 11 and ESC 14 was confirmed in SDS-PAGE and subsequent coomassie staining.

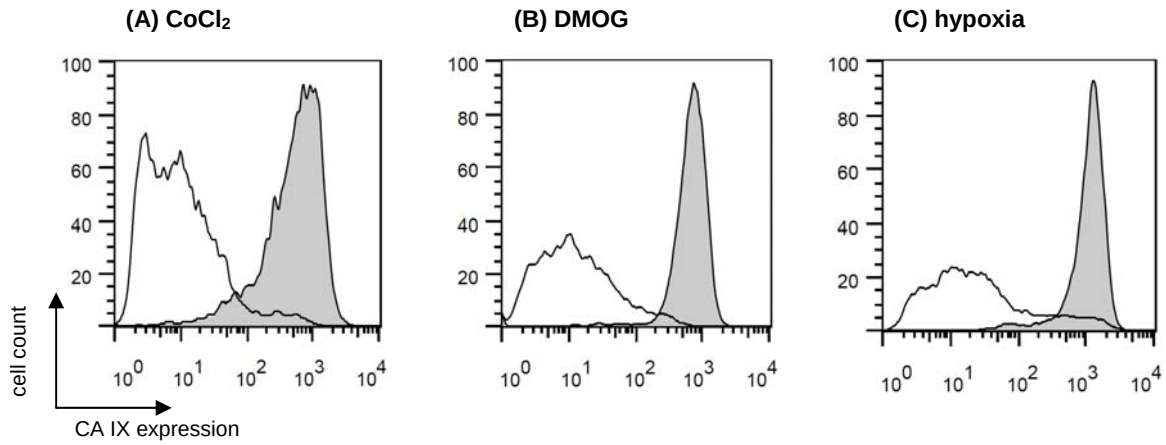

Figure 3.4: Induction of CA IX expression in HeLa cells. Optimal conditions for induction of CA IX expression in HeLa cells were found for **(A)** chemical induction with 200 µM $CoCl_2$, **(B)** chemical induction with 1 mM DMOG or **(C)** hypoxic induction at 0.2 % O_2 in a hypoxic chamber for 48 h each. CA IX expression was detected using M75. grey: HeLa cells induced to express CA IX, white: not-induced HeLa cells.

3.2.3 Binding characteristics of MSC 1 – 12 on human cell lines expressing CA IX

The selected Fab antibodies were tested for specific binding to human CA IX in flow cytometry. First Fab antibodies MSC 1 – 12 were tested on SKRC 17 cells transfected with the human *ca9* gene to over-express CA IX as well as on the not transfected parental cell line (**Figure 3.5 A**). All twelve Fab antibodies MSC 1 – 12 revealed a human CA IX-specific binding pattern. They specifically bound to cell lines transfected with the *ca9* gene but not to the parental cell line. Binding was considered specific if geometric mean fluorescence intensity (GMFI) on cell lines expressing CA IX was at least three times as big as for the control antibodies ESC 11 and ESC 14. Control Fab antibodies ESC 11 and ESC 14 did not recognize either cell line.

As a model for pVHL-deficiency, renal cell lines SKRC 1, SKRC 52 and SKRC 59 cells were used. SKRC 1 does express CA IX only at a very low level, whereas SKRC 59 and SKRC 52 show intermediate and high levels of CA IX expression, respectively. In flow cytometry, Fab antibodies MSC 1 – 12 did not bind to SKRC 1 expressing only low levels of CA IX, but they bound specifically to both SKRC 52 and SKRC 59 cells, while control Fab antibodies ESC 11 and ESC 14 did not (**Figure 3.5 B**). Binding on SKRC 52 led to higher GMFI than flow cytometry on SKRC 59, corresponding to higher expression levels of CA IX in SKRC 52 cells.

Binding of Fab antibodies MSC 1 – 12 to CA IX expressed on HeLa cells chemically induced in with DMOG was analyzed by flow cytometry (**Figure 3.5 C**). All Fab antibodies bound specifically to HeLa cells induced to express CA IX, while binding on not induced cells was much lower. Control Fab antibodies ESC 11 and ESC 14 did not bind to HeLa cells, regardless of their CA IX expression.

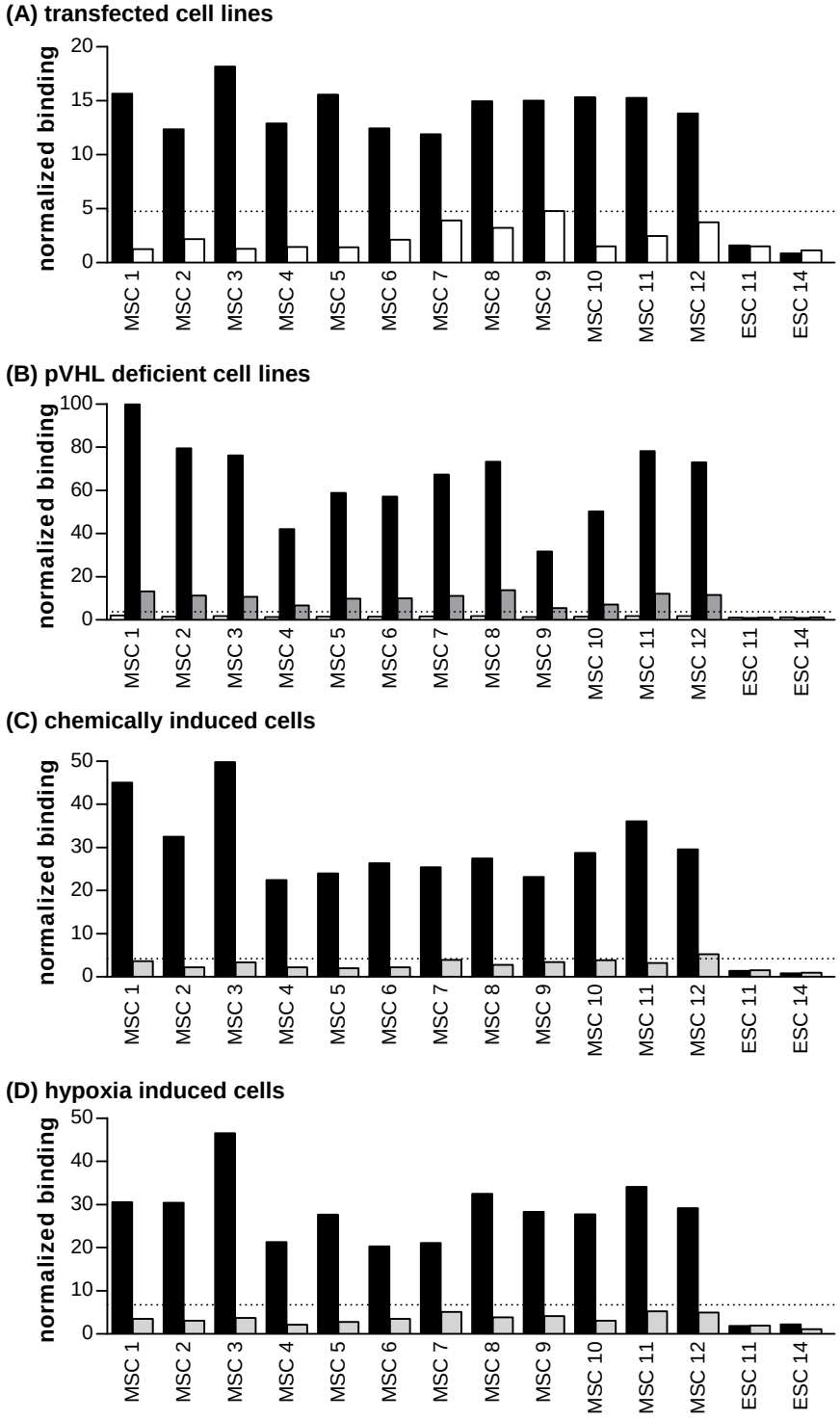

Figure 3.5: Binding characteristics of Fab antibodies MSC 1 – 12 on human cell lines. Binding of Fab antibodies MSC 1 – 12 as well as control Fab antibodies ESC 11 and ESC 14 was tested by flow cytometry on **(A)** transfected SKRC 17 MW1 cl4 (black) vs. parental SKRC 17 (white) cell lines (n = 4), **(B)** pVHL deficient cell lines SKRC 1 expressing low (white), SKRC 52 high (black) or SKRC 59 intermediate (grey) amounts of CA IX ($n \geq 4$), **(C)** chemically induced (black) or not induced (grey) HeLa cells (n = 5) and **(D)** HeLa cells induced in a hypoxic chamber (black) or under normoxia (grey) (n = 3). Geometric mean fluorescence intensity (GMFI) was calculated and normalized to the staining cascade. Mean values of all experiments are shown. The dotted line indicates significant binding, where GMFI is three times higher than for controls ESC 11 and ESC 14.

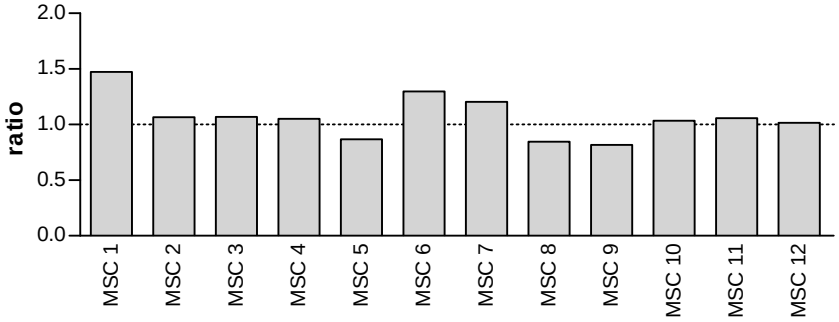

Figure 3.6: Ratio showing binding of Fab antibodies on human CA IX induced chemically or by hypoxia. The ratio of GMFI on HeLa cells expressing CA IX after chemical induction to GMFI on HeLa cells expressing CA IX after hypoxic induction was calculated. The dotted line indicates a ratio of 1.

The most physiological model simulating expression of CA IX in cancer tissue with limited oxygen supply is provided by HeLa cells induced to express CA IX in a hypoxic chamber. In flow cytometry, MSC 1 – 12 bound specifically to hypoxia induced HeLa cells, while binding to not induced cells was minimal and control antibodies did not bind at all (**Figure 3.5 D**).

Over all human cell lines analyzed, MSC 3 revealed the highest binding to human CA IX followed by MSC 1 and MSC 11. Lowest but nevertheless specific binding was observed for MSC 4.

Since CA IX is thought to have an active conformation under hypoxic conditions only, antibodies might show a difference in binding behaviour on cell lines expressing CA IX due to hypoxia or due to other factors, e.g. chemical induction or pVHL deficiency. However, if ratios of GMFI on chemically induced to hypoxia induced HeLa cells were calculated, ratio were around one for all Fab antibodies showing no significant difference in binding to CA IX expressed by chemical or hypoxic induction as calculated using an unpaired, two-sided T-test (**Figure 3.6**). In case that no difference could be observed due to short-time expression of the active conformation, one Fab antibody, MSC 8, and its corresponding IgG (see **3.2.11 IgG production of selected antibodies**) was titrated on HeLa cells (data not shown) and SKRC 52 cells (**Figure 3.7 A** and **B**) induced in a hypoxic chamber or under normoxic conditions. On HeLa cells no EC_{50} value could be calculated, since saturation levels were not reached (data not shown). On SKRC 52 cells, EC_{50} was in the same range on cells induced under normoxic or hypoxic conditions (**Figure 3.7 C**). For MSC 8 Fab, EC_{50} on cells induced under hypoxic conditions was 22.1 µg/ml compared to 24.6 µg/ml on cells induced under normoxic conditions. For MSC 8 IgG, EC_{50} values were 1.4 µg/ml and 1.6 µg/ml for hypoxic and normoxic conditions, respectively.

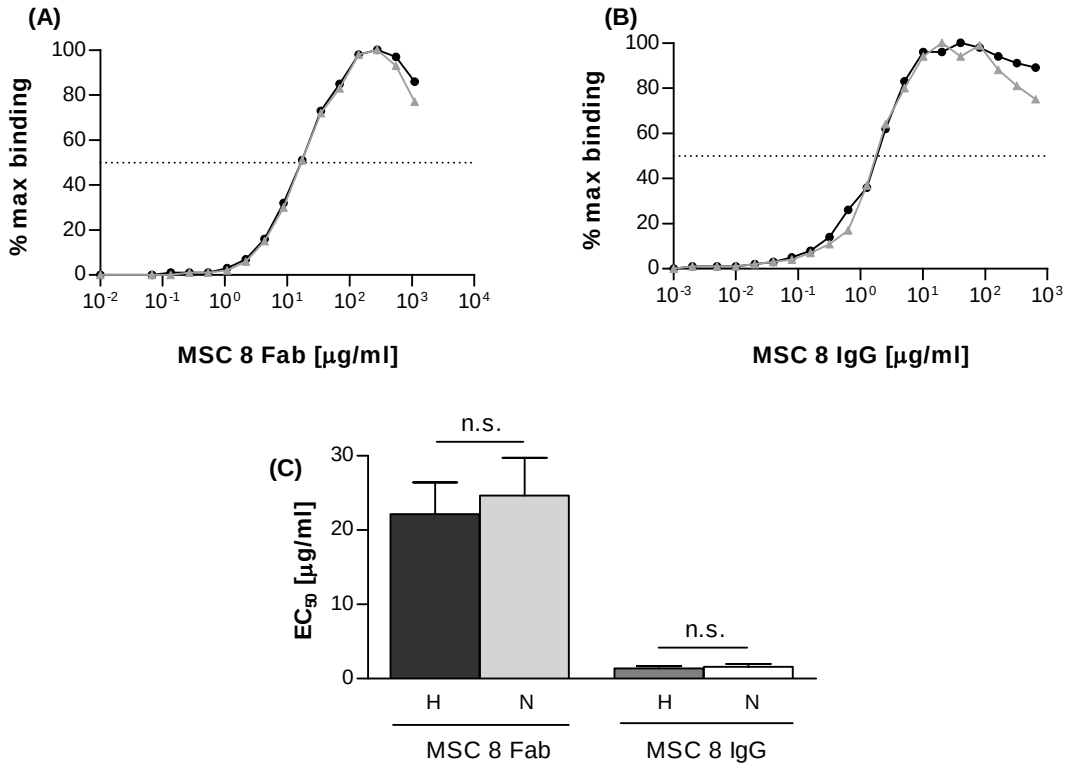

Figure 3.7: Titration of MSC 8 Fab and MSC 8 IgG on SKRC 52 cells induced under normoxic vs. hypoxic conditions. One representative titration for **(A)** MSC 8 Fab (n = 9) and **(B)** MSC 8 IgG (n = 4) on SKRC 52 cells induced under hypoxic (black) or normoxic (grey) conditions is shown. The dotted line represents half maximal binding. **(C)** EC_{50} values were determined and significant differences were determined using a paired, two-sided T-test. Mean values with SEM are shown.

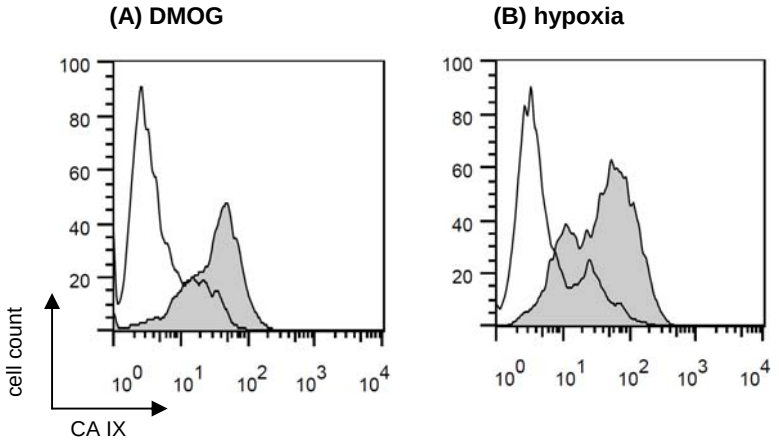

Figure 3.8: Induction of CA IX expression in C51 cells. Optimal conditions for induction of CA IX expression in C51 cells were found for **(A)** chemical induction with 2 mM DMOG or **(B)** hypoxic induction at 0.2 % O_2 in a hypoxic chamber for 48 h. CA IX expression was detected using M-100 antibody. Grey: C51 cells induced to express CA IX, white: not-induced C51 cells.

3.2.4 Induction of CA IX expression in murine cell lines

Since cross-reactivity with murine CA IX is favourable for later mouse experiments, selected Fab antibodies were tested for cross-reactivity to murine CA IX. On murine cell lines, murine CA IX can be induced either chemically with DMOG or under hypoxic conditions in a hypoxic chamber. Pre-tests showed that for murine cell lines CA IX induction was much weaker than in HeLa cells. Optimal conditions were reached using 2 mM DMOG for 48 h (**Figure 3.8 A**) or induction in a hypoxic chamber at 0.2 % O_2 for 48 h (**Figure 3.8 B**).

3.2.5 Binding characteristics of MSC 1 – 12 on murine cell lines expressing CA IX

The Fab antibodies were tested by flow cytometry on murine C51 (**Figure 3.9 A**) and CT26 (**Figure 3.9 B**) cells induced chemically with DMOG. Only MSC 1 and MSC 3 showed specific binding. Since CA IX expression in murine cell lines was much weaker than in human cell lines, binding was considered specific if GMFI of probes was at least twice the GMFI of control antibodies. The other Fab antibodies did not bind to murine CA IX. Binding of MSC 7, MSC 9, MSC 11 and MSC 12 on C51 was not specific although higher than for control antibodies ESC 11 and ESC 14. Specific binding of MSC 1 and MSC 3 to murine CA IX was confirmed by flow cytometry on hypoxia induced C51 (**Figure 3.9 C**). As on C51 chemically induced, binding of MSC 7, MSC 9, MSC 11 and MSC 12 was not specific although higher than for control antibodies ESC 11 and ESC 14. Flow cytometry on CT26 induced under hypoxia confirmed cross-reactivity of MSC 3 while binding of MSC 1 was not specific compared to controls ESC 11 and ESC 14 (**Figure 3.9 D**). Over all cell lines and conditions tested, MSC 3 showed highest binding to murine CA IX followed by MSC 1.

Like for human CA IX, murine CA IX might show a different conformation under hypoxic conditions leading to possible differences in binding behaviour of cross-reactive antibodies. Therefore, ratios of GMFI on chemically induced to hypoxia induced cells were calculated. On C51, ratios were around one for all Fab antibodies showing no significant difference in binding to CA IX expressed by chemical or hypoxic induction as calculated using an unpaired, two-sided T-test (**Figure 3.10 A**). On CT26 cells in contrast, MSC 1 as well as MSC 3 bound significantly better to CA IX expressed after chemical induction than to CA IX expressed under hypoxic conditions (**Figure 3.10 B**).

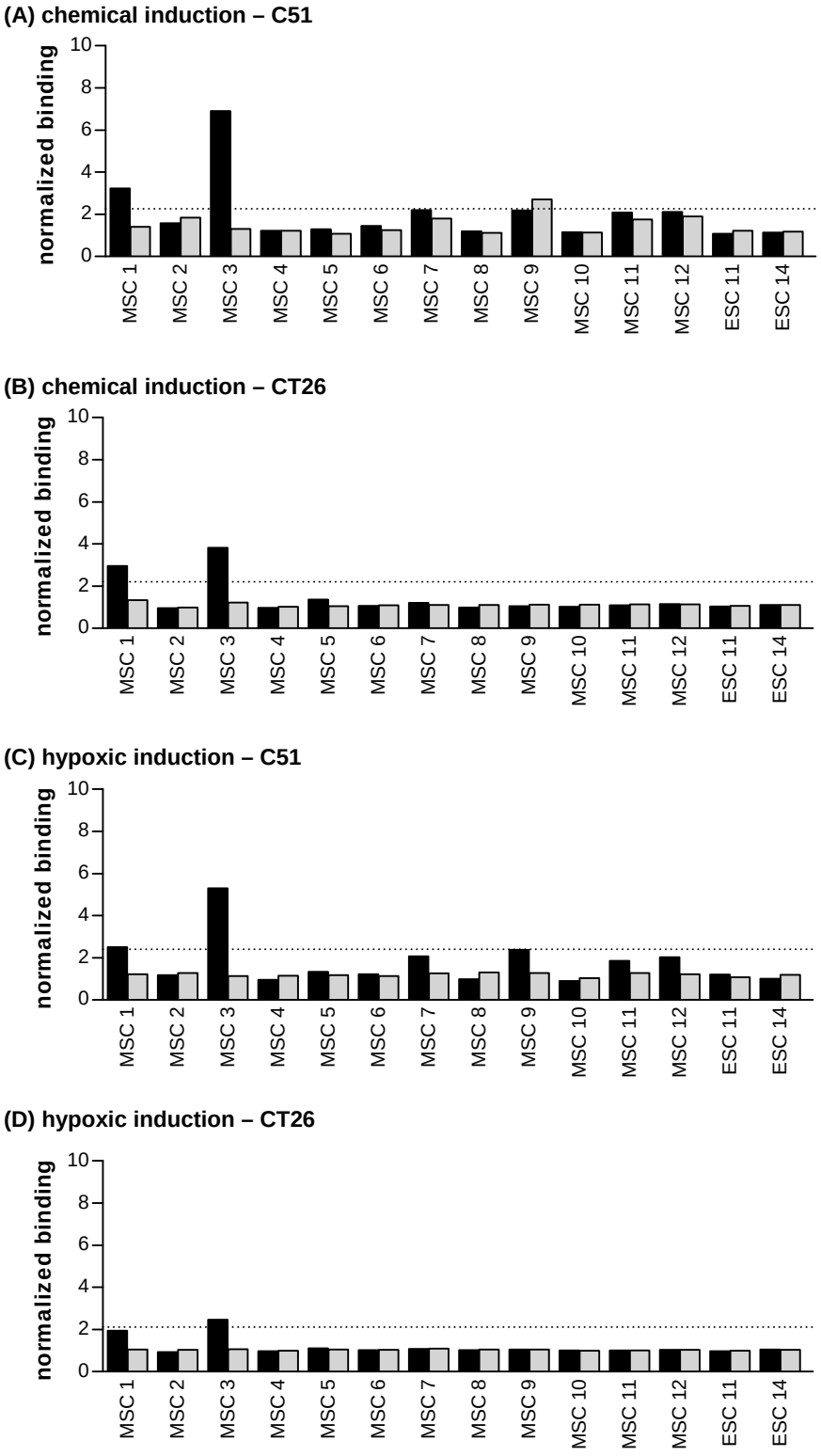

Figure 3.9: Binding characteristics of Fab antibodies MSC 1 – 12 on murine cell lines. Binding of Fab antibodies MSC 1 – 12 was tested by flow cytometry on **(A)** C51 cells (n = 4) and **(B)** CT26 cells (n = 3) induced with 2 mM DMOG (black) or not induced (grey) as well as **(C)** C51 cells (n = 5) and **(D)** CT26 cells (n = 6) induced in a hypoxic chamber (black) or under normoxic conditions (grey). Geometric mean fluorescence intensity (GMFI) was calculated and normalized to the staining cascade. The dotted line indicates significant binding, where GMFI is two times higher than for controls ESC 11 and ESC 14.

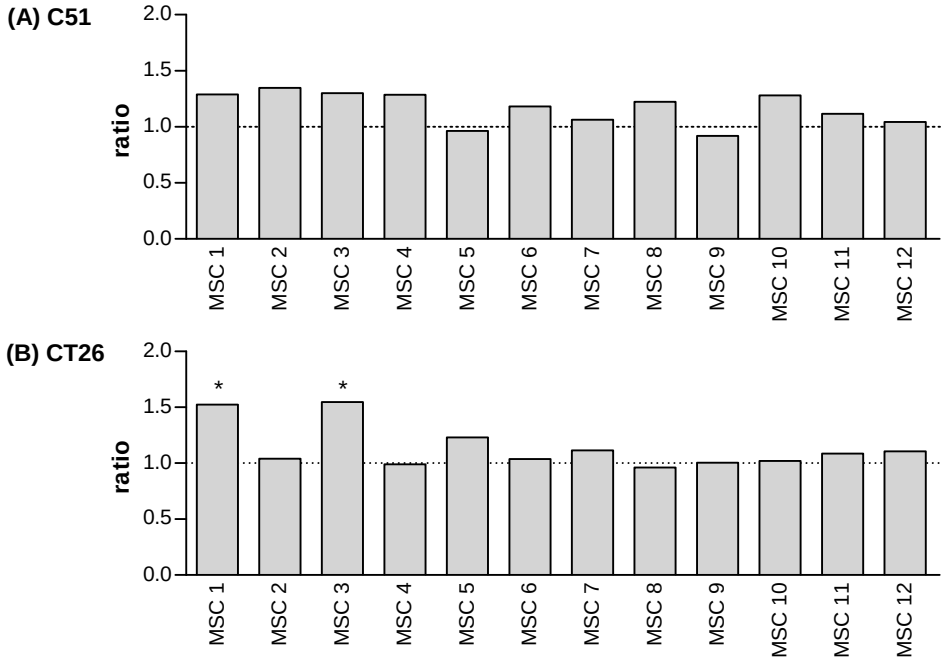

Figure 3.10: Ratio showing binding of Fab antibodies on murine CA IX induced chemically or by hypoxia. The ratio of GMFI on murine cells expressing CA IX after chemical induction to GMFI on murine cells expressing CA IX after hypoxic induction was calculated for **(A)** C51 or **(B)** CT26. The dotted line indicates a ratio of 1. Significance was calculated using an unpaired, two-sided T-test. P-value: * < 0.05.

3.2.6 Binding characteristics of MSC 1 – 12 on recombinant CA IX

Fab antibodies MSC 1 – 12 were selected by phage display on recombinant human CA IX. Since binding of Fab antibodies on recombinant protein might differ from the one on CA IX expressed on cell lines, binding of MSC 1 – 12 was analyzed in ELISA on recombinant human (rhCA IX) and recombinant murine CA IX (rmCA IX). All twelve Fab antibodies bound specifically to rhCA IX (**Figure 3.11 A**). Binding was considered specific if absorbance at 450 nm (A_{450}) was at least twice the value for control Fab antibodies ESC 11 or ESC 14. Interestingly, compared to other Fab antibodies MSC 8 Fab showed only weak although specific binding to rhCA IX in ELISA whereas binding in flow cytometry was equivalent to the one of other Fab antibodies. Significance of binding was calculated using a paired, two-sided T-test (**Table 3.1 A)**. Binding of all twelve Fab antibodies on rhCA IX was significant. In ELISA on rmCA IX MSC 1, MSC 3, MSC 5, MSC 7 and MSC 9 bound specifically to recombinant murine CA IX (**Figure 3.11 B**). For specific binders significance was calculated using a paired, two-sided T-test. While binding of both MSC 1 and MSC 3 was significant, binding of MSC 5, MSC 7 and MSC 9 was not significant (**Table 3.1 B**). Apart from MSC 8 showing different binding behaviour on recombinant compared to naturally expressed human CA IX, no differences in binding could be detected. ELISA thus confirmed binding data obtained by flow cytometry. All binding data are summarized in **Table 3.2**.

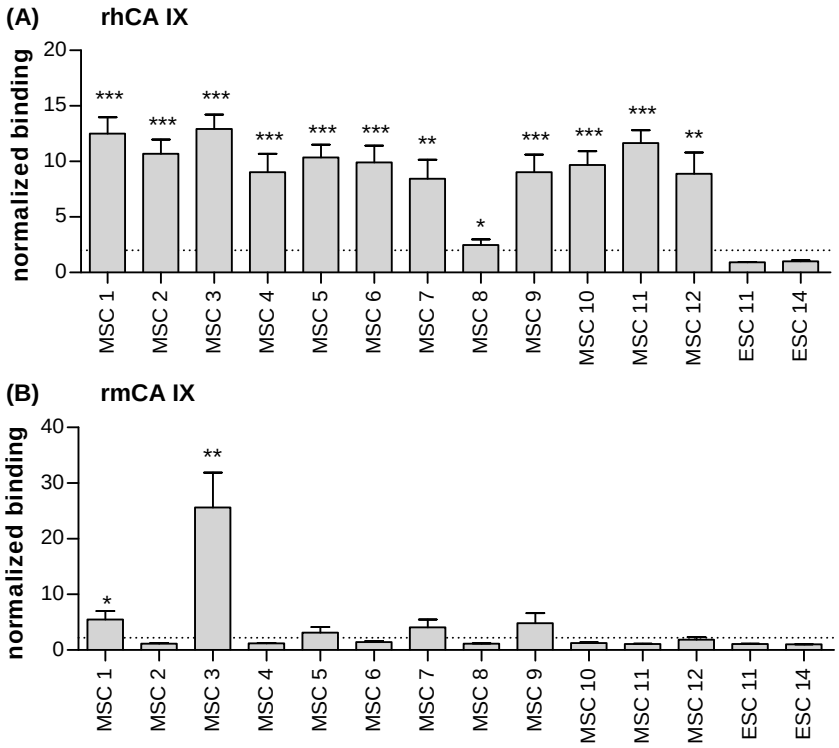

Figure 3.11: Binding characteristics of Fab antibodies in ELISA on recombinant CA IX. Binding of Fab antibodies MSC 1 – 12 was analysed in ELISA on **(A)** rhCA IX or **(B)** rmCA IX. Experiments were repeated at least four times in triplicates. Signals were normalized to the staining cascade. For specific binders significance was calculated using a paired, two-sided T-test. P-values compared to ESC 11 are shown: *** < 0.001, ** < 0.01, * < 0.05.

Table 3.1: P-values for MSC 1 – 12 in ELISA on recombinant CA IX. P-values of MSC 1 – 12 compared to the control Fab antibodies ESC 11 and ESC 14 were calculated on **(A)** human and **(B)** murine recombinant CA IX using a paired, two-sided T-test. T-tests were calculated only if binding was considered specific. P-values < 0.05 are considered significant. n.s. not significant, light grey < 0.05, grey < 0.01 and dark grey < 0.001, - no specific binding.

	(A) human CA IX		**(B) murine CA IX**	
	ESC 11	**ESC 14**	**ESC 11**	**ESC 14**
MSC 1	< 0.001	< 0.001	0.0152	0.0122
MSC 2	< 0.001	< 0.001	-	-
MSC 3	< 0.001	< 0.001	0.0018	0.0017
MSC 4	< 0.001	< 0.001	-	-
MSC 5	< 0.001	< 0.001	n.s.	n.s.
MSC 6	< 0.001	< 0.001	-	-
MSC 7	0.0011	0.0011	n.s.	n.s.
MSC 8	0.0105	0.0096	-	-
MSC 9	< 0.001	< 0.001	n.s.	n.s.
MSC 10	< 0.001	< 0.001	-	-
MSC 11	< 0.001	< 0.001	-	-
MSC 12	0.0016	0.0018	-	-

Table 3.2: Summary of binding characteristics of MSC 1 – 12 Fab antibodies. Binding characteristics of MSC 1 – 12 Fab antibodies in flow cytometry and ELISA on human and murine CA IX are indicated. Binding to human CA IX was analyzed in flow cytometry on **(A)** transfected, **(B)** pVHL deficient and **(C)** induced human cell lines and **(D)** in ELISA on rhCA IX. Binding to murine CA IX was analyzed **(E)** in flow cytometry on induced murine cell lines and **(F)** in ELISA on rmCA IX. Binding was considered specific in flow cytometry on human cell lines if GMFI > 3x GMFI of controls, on murine cell lines if GMFI > 2x GMFI of controls and in ELISA if A_{450} > 2x A_{450} of controls. + : specific binding; (+) : specific but not significant binding; - : not-specific binding.

	A	**B**			**C**		**D**	**E**				**F**
	SKRC 17 MW1 c14	SKRC 1	SKRC 52	SKRC 59	HeLa + DMOG	HeLa Hypoxia	rhCA IX	C51 + DMOG	CT26 + DMOG	C51 Hypoxia	CT26 Hypoxia	rmCA IX
MSC 1	+	-	+	+	+	+	+	+	+	+	-	+
MSC 2	+	-	+	+	+	+	+	-	-	-	-	-
MSC 3	+	-	+	+	+	+	+	+	+	+	+	+
MSC 4	+	-	+	+	+	+	+	-	-	-	-	-
MSC 5	+	-	+	+	+	+	+	-	-	-	-	(+)
MSC 6	+	-	+	+	+	+	+	-	-	-	-	-
MSC 7	+	-	+	+	+	+	+	-	-	-	-	(+)
MSC 8	+	-	+	+	+	+	+	-	-	-	-	-
MSC 9	+	-	+	+	+	+	+	-	-	-	-	(+)
MSC 10	+	-	+	+	+	+	+	-	-	-	-	-
MSC 11	+	-	+	+	+	+	+	-	-	-	-	-
MSC 12	+	-	+	+	+	+	+	-	-	-	-	-
ESC 11	-	-	-	-	-	-	-	-	-	-	-	-
ESC 14	-	-	-	-	-	-	-	-	-	-	-	-
M75	+	+	+	+	+	+	+	+	-	+	-	-
M-100	-	-	-	-	-	-	+	+	+	+	+	+

3.2.7 Specificity of Fab antibodies MSC 1 – 12

Many chemical compounds inhibiting CA IX function are known, while antibodies against CA IX used in clinics do not inhibit CA IX function. Nevertheless, those chemical drugs are unable to bind selectively to the CA IX isoform leading to a broad range inhibition of carbonic anhydrase isoforms and a lot of side-effects. Selectivity on the other hand is one of the advantages of antibodies. Antibodies are able to discriminate between very similar targets and thus to selectively bind one isozyme over another.

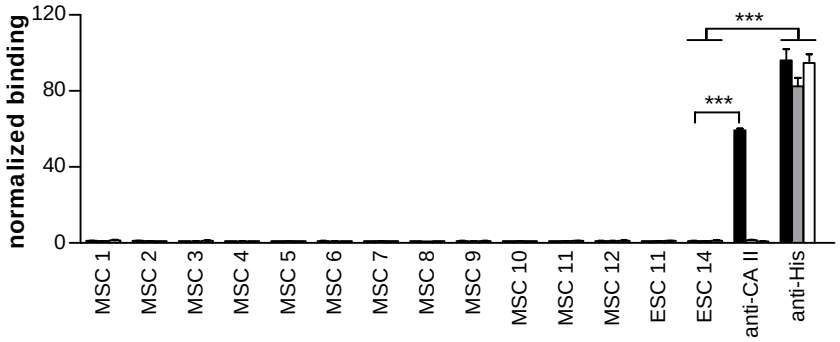

Figure 3.12: Selectivity of Fab antibodies MSC 1 – 12. Fab antibodies MSC 1 – 12 were tested in an ELISA on the most widely expressed isoform CA II which is present in the cytosol (black) and the two extracellular isoforms CA XII (grey) and CA XIV (white) showing high homology to CA IX. Binding was normalized to the staining cascade. P-values: *** < 0.001 compared to control Fab antibodies ESC 11 and ESC 14.

In order to find antibodies combining these two features – selectivity and inhibition of CA IX function – the here selected antibodies were first tested in ELISA on different recombinant carbonic anhydrase isoforms to analyze, whether the here selected antibodies are indeed selectively binding CA IX (**Figure 3.12**). No binding to any of the other tested isoforms CA II, CA XII or CA XIV was observed. Coating of the plates with the corresponding carbonic anhydrase isoforms was confirmed with anti-His and for CA II in addition by using anti-CA II.

3.2.8 Fab antibodies MSC 1 – 12 recognise a sterical epitope

Fab antibodies MSC 1 – 12 were tested for their potential use in Western blot analysis on whole cell protein extracts from SKRC 17 MW1 cl4 cells as well as from SKRC 17 cells. None of the twelve tested Fab antibodies was able to recognise denatured CA IX protein (**Figure 3.13**) suggesting that they recognize a sterical epitope. In contrast, M75 did bind to two bands of 54 and 58 kDa corresponding to CA IX in whole cell protein extracts from SKRC 17 MW1 cl4 cells but not in those from SKRC 17 cells.

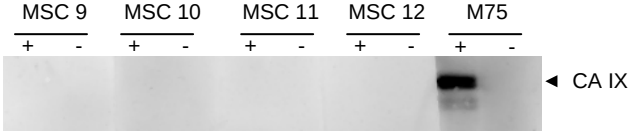

Figure 3.13: Western blot using MSC 1 – 12 to stain CA IX. Fab antibodies MSC 1 – 12 were tested in a Western blot analysis on whole cell protein extracts of SKRC 17 MW1 cl4 (+) and SKRC 17 (-) cells (n = 3). Four representative Fab antibodies MSC 9 to MSC 12 are shown. CA IX expression was confirmed using M75 antibody.

3.2.9 Affinity measurement of Fab antibodies on rhCA IX by surface plasmon resonance

Affinity measurements were performed on a low-density rhCA IX-coated chip using surface plasmon resonance (**Figure 3.14**). All Fab antibodies showed significant binding to rhCA IX, with affinities ranging from 2 nM (MSC 11) to 66 nM (MSC 9) (**Table 3.3**).

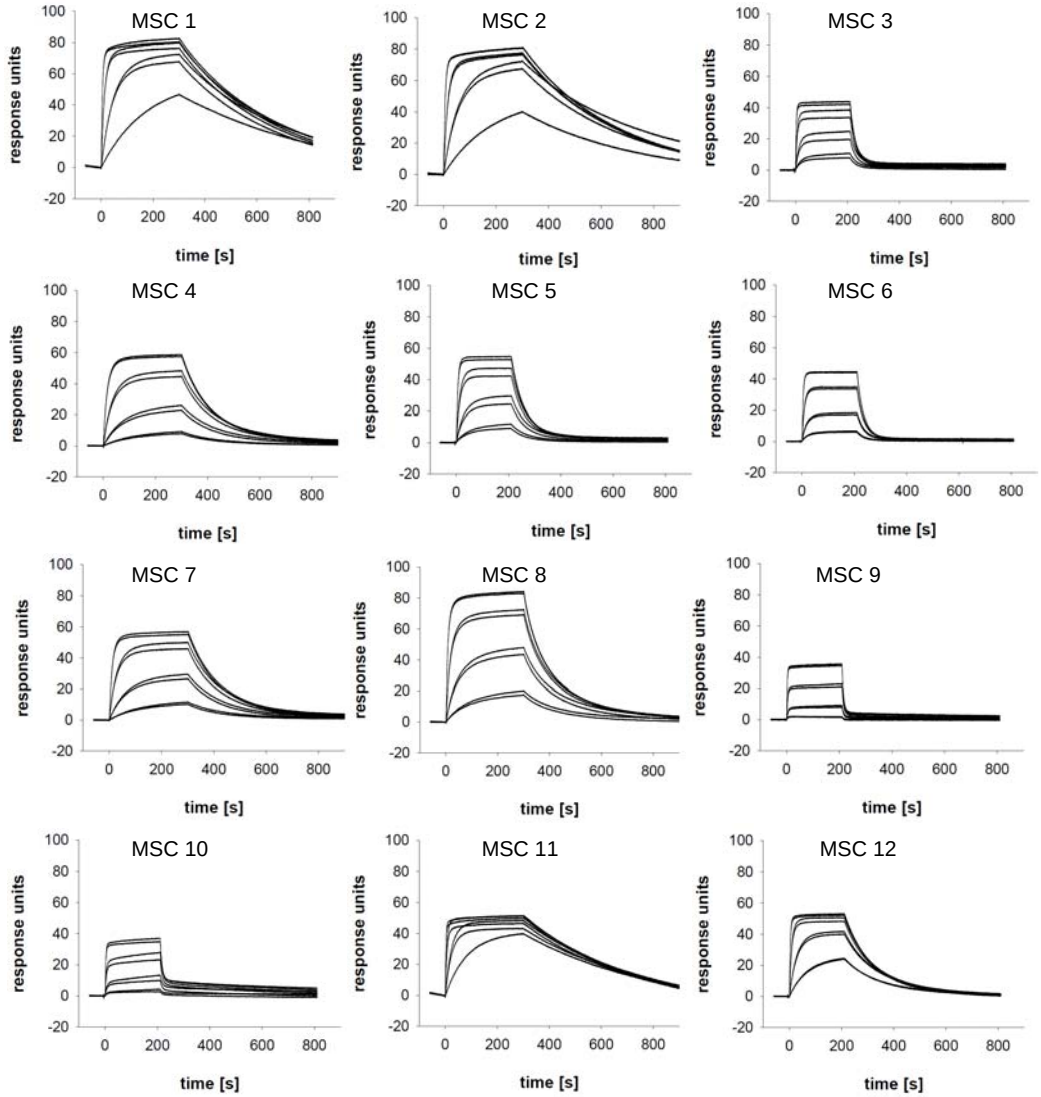

Figure 3.14: Affinity measurement of MSC 1 – 12 on rhCA IX. Affinity of Fab antibodies MSC 1 – 12 was tested using surface plasmon resonance on rhCA IX coated chips.

Table 3.3: Affinities of Fab antibodies MSC 1 – 12 on rhCA IX. Affinity of the selected Fab antibodies for rhCA IX was analyzed by surface plasmon resonance. Association and dissociation rate constants (k_a and k_d, respectively) were locally fit to a 1:1 binding model, assuming bulk contribution and affinities (K_D) were calculated.

	k_a [s^{-1}]	k_d [s^{-1}]	K_D [nM]
MSC 1	0.919	0.00301	3
MSC 2	0.732	0.00275	4
MSC 3	1.340	0.02549	19
MSC 4	0.394	0.01056	27
MSC 5	2.315	0.04009	17
MSC 6	0.846	0.03147	37
MSC 7	0.510	0.00974	19
MSC 8	0.856	0.01196	14
MSC 9	1.478	0.09798	66
MSC 10	0.468	0.00227	5
MSC 11	1.854	0.00311	2
MSC 12	1.822	0.01018	6

3.2.10 Affinity measurement of Fab antibodies on rmCA IX by Biacore

Affinity measurements were performed on a low-density rmCA IX-coated chip using surface plasmon resonance (**Figure 3.15**). Binding affinity to rmCA IX ranged from 4 nM to 163 nM and confirmed cross-reactivity of MSC 1, MSC 3, MSC 5, MSC 7, MSC 9 and MSC 12 to rmCA IX with MSC 3 being the best binder to the murine isoform (**Table 3.4**). For the other Fab antibodies affinities could not be determined due to too low binding to murine CA IX attended by too low response units.

Table 3.4: Affinities of Fab antibodies MSC 1 – 12 on rmCA IX. Affinity of the selected Fab antibodies for rmCA IX was analyzed by surface plasmon resonance. Association and dissociation rate constants (k_a and k_d, respectively) were locally fit to a 1:1 binding model, assuming bulk contribution and affinities (K_D) were calculated. Affinities of isoforms not listed in the table could not be determined due to too low binding to the murine isoform attended by too low response units

	k_a [s^{-1}]	k_d [s^{-1}]	K_D [nM]
MSC 1	0.050	0.00174	35
MSC 3	0.296	0.00125	4
MSC 5	0.049	0.00225	46
MSC 7	0.059	0.00196	34
MSC 9	0.042	0.00170	41
MSC 12	0.055	0.00273	50

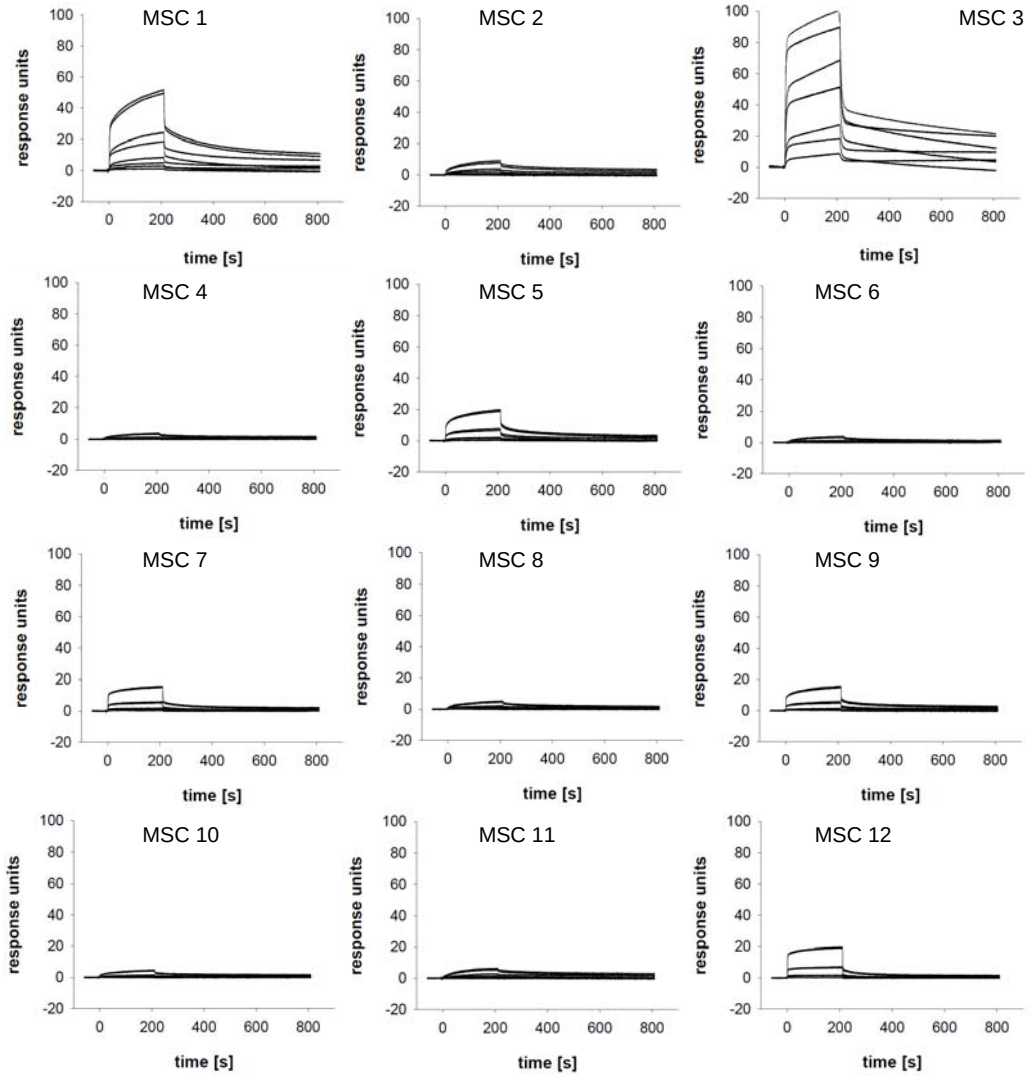

Figure 3.15: Affinity measurement of MSC 1 – 12 on rmCA IX. Affinity of Fab antibodies MSC 1 – 12 was tested using surface plasmon resonance on rmCA IX coated chips.

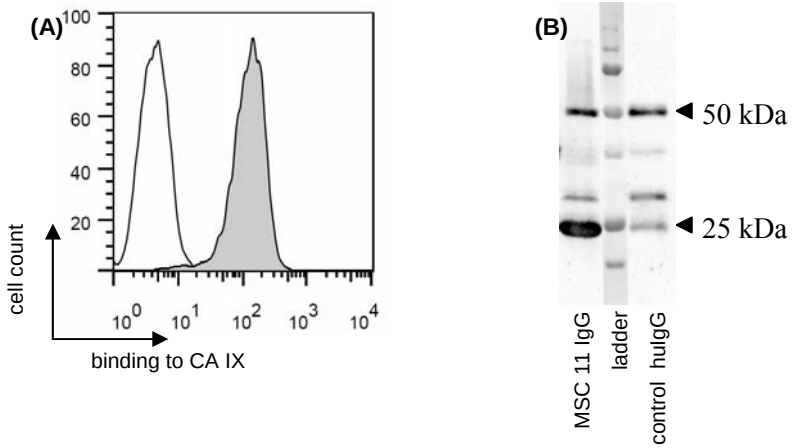

Figure 3.16: Production of pEE 12.4 MSC 11. (A) Specific binding of MSC 11 IgG to CA IX was confirmed in flow cytometry on SKRC 17 MW1 cl4. Grey: supernatants of one representative clone expressing MSC 11 IgG, white: staining cascade. **(B)** HC and LC of MSC 11 IgG were visualized in Western blot analysis and compared to a control huIgG. Purified supernatants from one representative clone are shown.

3.2.11 IgG production of selected antibodies

Selected Fab antibodies were cloned into an IgG format using the LONZA GS system pEE 12.4. MSC 3 and MSC 11 were chosen for their high affinity to human CA IX with MSC 3 showing in addition cross-reactivity to murine CA IX. MSC 8 was chosen for inhibiting CA IX function by up to 57 % in a biochemical assay on membrane fragments (see **3.3 Inhibition of CA IX function using MSC 1 - 12**). Correct cloning was confirmed by restriction digestion and subsequent sequencing. HEK 293 cells were transiently transfected with pEE 12.4 MSC 3, pEE 12.4 MSC 8 or pEE 12.4 MSC 11 and supernatants were tested for IgG production in Western blot analysis. Specific binding was confirmed in flow cytometry. pEE 12.4 MSC 11 was stably transfected in NSO cells and 400 clones were screened for IgG production in DotBlot and flow cytometry leading to the identification of 25 clones expressing MSC 11 IgG (**Figure 3.16 A**). HC and LC of IgGs were analyzed in Western blot analysis (**Figure 3.16 B**). For MSC 11 HC and LC a molecular weight of 50 and 25 kDa respectively was determined. For large scale production of IgGs, pEE 12.4 MSC 3 and pEE 12.4 MSC 8 were stably transfected in CHO cells by the Ludwig Institute of cancer research in Melbourne, Australia and IgGs were subsequently purified.

3.2.12 Tumour staining using MSC 3 IgG and MSC 11 IgG

MSC 3 IgG and MSC 11 IgG were used to stain tumour sections of C51 tumours (**Figure 3.17**). MSC 3 showed specific staining of tumour tissue corresponding to staining of the perfusion marker pimonidazole. Staining for MSC 11 was negative corresponding to the fact, that this antibody recognizes only human CA IX but not murine CA IX.

3.3 INHIBITION OF CA IX FUNCTION USING MSC 1 - 12

Up to date, G250 is the only anti-CA IX antibody used in the clinic. This antibody is very potent in tumour-targeting (Oosterwijk, Bander et al. 1993; Divgi, Bander et al. 1998) but therapeutic efficiency is disputed (Divgi, Bander et al. 1998; Bleumer, Knuth et al. 2004; Brouwers, Mulders et al. 2005). G250 as well as the other anti-CA IX antibody M75 are both not described to inhibit CA IX function. Inhibition of CA IX function is thought to have a therapeutic effect, since acidification of tumour environment and neutralisation of intracellular pH both triggered by CA IX function are thought to provide a survival advantage to tumour cells. Chemical drugs on the other hand are able to inhibit CA IX function but are not specific and inhibit also other isoforms. Selective and inhibitory compounds would be of great interest for tumour therapy. Therefore, selected antibodies were tested for inhibition of CA IX function.

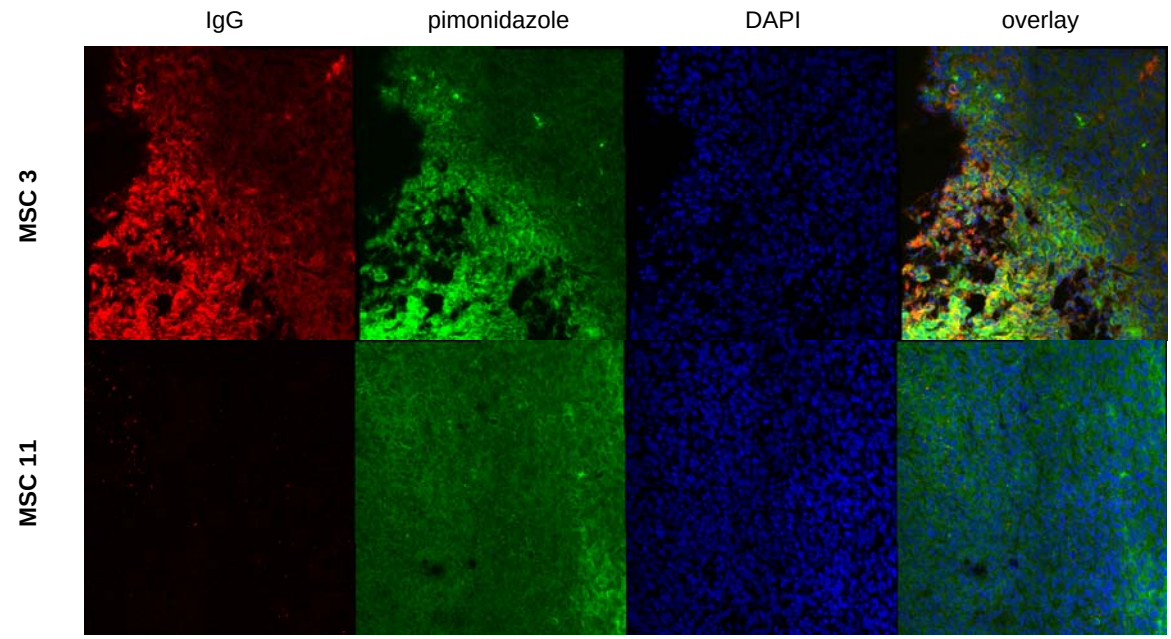

Figure 3.17: Immunofluorescence using MSC 3 IgG and MSC 11 IgG. Immunofluorescence of sections of C51 tumours was performed using MSC 3 IgG or MSC 11 IgG (red) in combination with the perfusion marker pimonidazole (green). Nuclei were stained using DAPI (blue).

3.3.1 Inhibition of CA IX function on membrane fragments using Fab antibodies

A first screen for the CA IX inhibiting activity of the selected Fab antibodies was performed on membrane-fragments extracted from HCT 116 cells expressing CA IX. Carbonic anhydrase activity was determined using a biochemical assay that measures CO_2 hydration by following the time-course of medium acidification. Sample time courses of medium pH were obtained with membrane-fragments from HCT 116-CA IX or HCT 116-EV cells, and with membrane-free buffer (**Figure 3.18 A**). Carbonic anhydrase activity in HCT 116-EV membranes was bigger than spontaneous hydration rate in membrane-free buffer but considerably lower than in HCT 116-CA IX membranes. Activity in HCT 116-EV membranes was in the same range as for HCT 116-CA IX cells where total carbonic anhydrase activity was blocked using acetazolamide (HCT 116-CA IX + ATZ), indicating that HCT 116-EV cells do not express significant surface carbonic anhydrase activity and that the carbonic anhydrase activity measured in HCT 116-CA IX membranes was primarily due to CA IX protein. The reaction constant was calculated and carbonic anhydrase activity was normalized to the values measured with buffer only (zero) and with control HCT 116-CA IX membranes (one) on the given day to compare data obtained on different days (**Figure 3.18 B**). The assay was repeated in the presence of 20 µg/ml Fab antibodies MSC 1 – 12, G250 IgG (Grabmaier, Vissers et al. 2000), anti-CA II IgG as a non-binding negative control and 100 µM acetazolamide, a broad-spectrum small-molecule CA inhibitor (**Figure 3.18**). Five out of the tested Fab antibodies (namely MSC 2, MSC 5, MSC 8, MSC 10 and MSC 12) were able to block

CA IX activity significantly while the other tested Fab antibodies as well as G250 were not able to reduce CA IX activity. All five inhibitory Fab antibodies led to partial inhibition of CA IX activity, with MSC 8 having the greatest inhibitory effect. The potency of MSC 2, MSC 5, MSC 10 and MSC 12 Fab antibodies was much lower and, therefore, they were not investigated further.

In order to see whether partial inhibition relies on too low Fab antibody concentrations, a dose response experiment was performed using higher concentrations of MSC 8 Fab (**Figure 3.19**). The dose response showed that concentrations of 20 µg/ml used in the first experiment are already more than ten times more than saturation levels. Saturation levels are reached with concentrations of 1 – 2 µg/ml leading to a maximal inhibition of CA IX activity by up to 57 %. Half-maximal inhibition (IC_{50}) was determined with concentrations around 0.33 µg/ml, which is equivalent to 6.5 nM for MSC 8 Fab antibody.

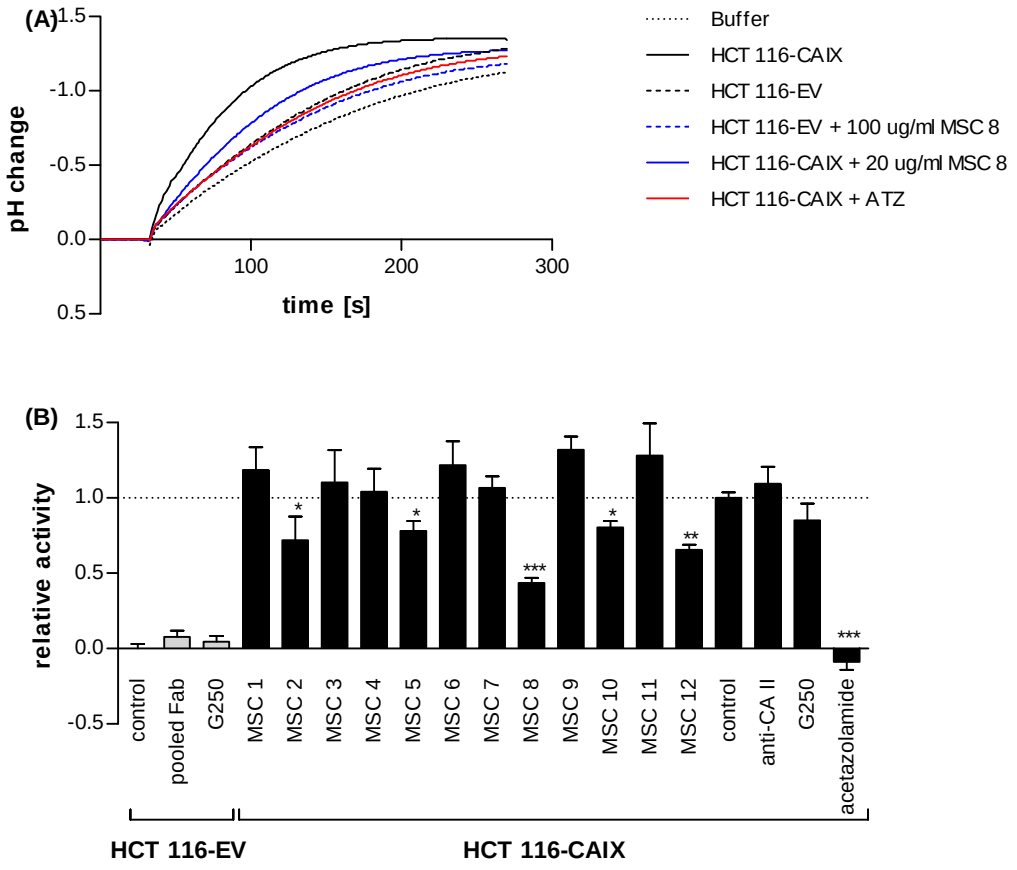

Figure 3.18: Inhibition of CA IX activity on membrane fragments using Fab antibodies. Fab antibodies MSC 1 – 12 were tested for inhibitory potential on membrane fragments expressing CA IX at a concentration of 20 µg/ml. **(A)** Time courses using membrane fragments of HCT 116-CA IX (continuous) or HCT 116-EV (dashed) are shown using only membrane fragments (black) or Fab antibody MSC 8 (blue). Spontaneous hydration rate was determined using buffer only (dotted). As control, total carbonic anhydrase activity was blocked with acetazolamide (red). **(B)** The reaction constant was calculated from the pH time-course and activity was normalized to HCT 116-EV (null) and HCT 116-CA IX membrane fragments alone (one). Black: HCT 116-CA IX membrane fragments; grey: HCT 116-EV membrane fragments.

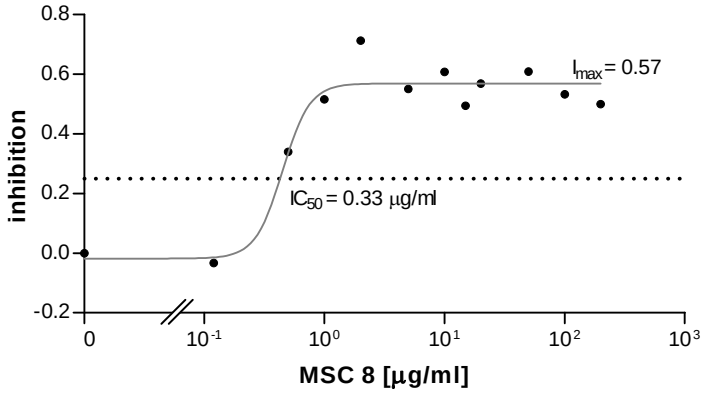

Figure 3.19: Dose response showing effect of MSC 8 Fab on CA IX activity. Concentrations of 0.1 µg/ml to 200 µg/ml MSC 8 Fab were tested for inhibition of CA IX activity on membrane fragments expressing CA IX. Reaction constants were calculated from the pH time-courses, normalized to HCT 116-EV and HCT 116-CA IX membrane fragments and percentage of maximal inhibition (I_{max}) was determined. Concentration at half-maximal inhibition (dotted line, IC_{50}) was calculated.

3.3.2 Inhibition of CA IX function on membrane fragments using MSC 8 IgG

Inhibition of CA IX function on membrane fragments of HCT 116 cells expressing CA IX or empty vector was repeated with MSC 3 IgG and MSC 8 IgG in order to see, if a bivalent IgG might be more potent in blocking CA IX activity than a monovalent Fab antibody (**Figure 3.20**). In agreement with previous experiments using Fab antibodies, inhibition of CA IX activity by MSC 8 IgG could be confirmed, whereas MSC 3 IgG showed no inhibition. A dose response experiment revealed a maximal inhibition of CA IX activity by up to 76 % using MSC 8 IgG (**Figure 3.21**). Although inhibition with MSC 8 IgG was higher, half-maximal inhibition (IC_{50}) was in the same range for both Fab antibody and IgG. An IC_{50} of 0.33 µg/ml was determined corresponding to 2.2 nM for MSC 8 IgG.

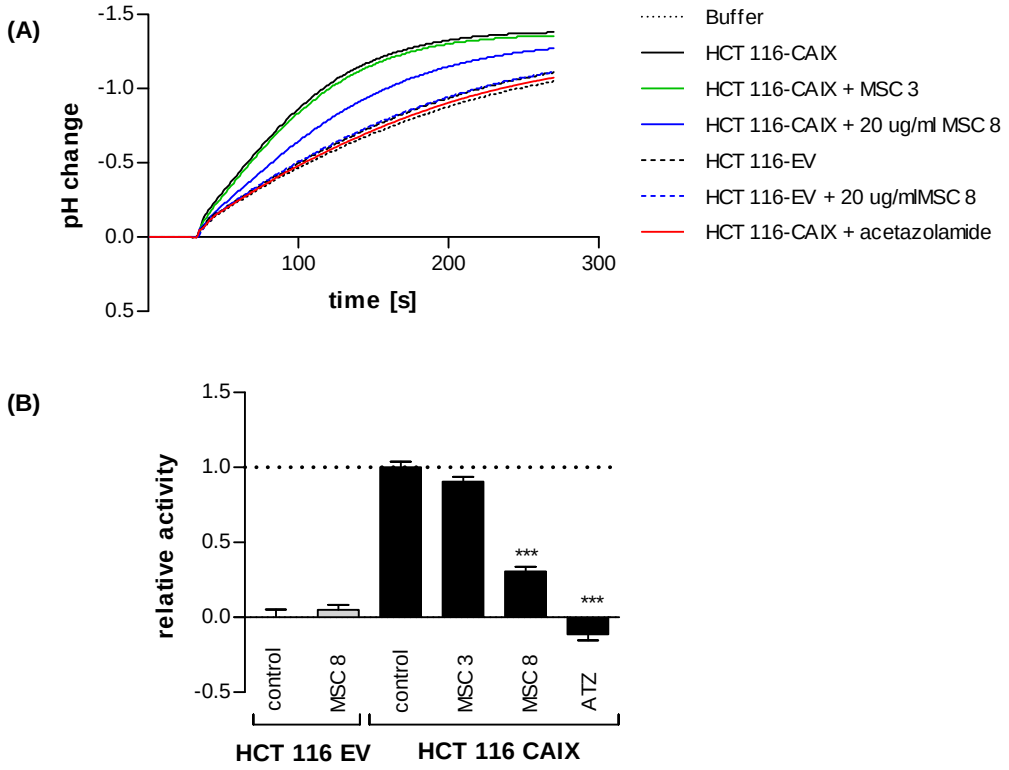

Figure 3.20: Inhibition of CA IX activity on membrane fragments using IgG. MSC 3 IgG and MSC 8 IgG were tested for inhibitory potential on membrane fragments expressing CA IX in order to confirm data obtained with Fab antibodies. **(A)** Time courses of CA IX activity with membrane fragments of HCT 116-CA IX (continuous) or HCT 116-EV (dashed) are shown, using only membrane fragments (black), MSC 3 IgG (green) or MSC 8 IgG (blue). Spontaneous hydration rate was determined using buffer only (dotted). As control, total carbonic anhydrase activity was blocked with acetazolamide (red). **(B)** The reaction constant was calculated from the pH time-course and activity was normalized to HCT 116-EV (null) and HCT 116-CA IX membrane fragments alone (one). P-value: *** < 0.001.

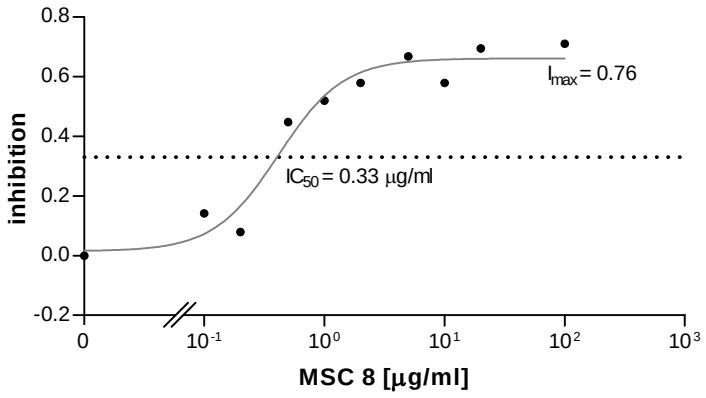

Figure 3.21: Dose response showing effect of MSC 8 IgG on CA IX activity. Concentrations of 0.1 µg/ml to 100 µg/ml MSC 8 IgG were tested for amount of inhibition on membrane fragments expressing CA IX. Reaction constants were calculated from the pH time-courses, normalized to HCT 116-EV and HCT 116-CA IX membrane fragments and percentage of maximal inhibition (I_{max}) was determined. Concentration at half-maximal inhibition (dotted line, IC_{50}) was calculated.

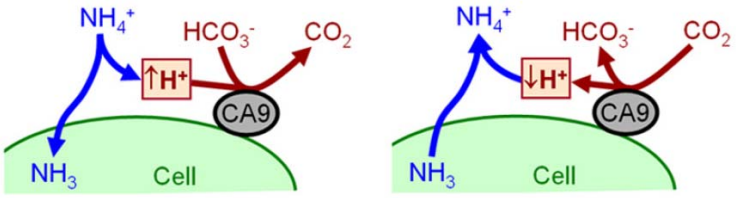

Figure 3.22: Schematic representation of the NH_3 flux across the membrane. NH_4^+ can not enter the cell in contrast to the non-ionized NH_3. Influx of NH_3 lowers pH_S while efflux elevates it. This change in pH is reduced by conversion of protons and hydrogen carbonate (provided by the CO_2/HCO_3^- buffer used) to water and carbon dioxide. The reaction is enhanced by carbonic anhydrase activity. From (Swietach, Patiar et al. 2009).

3.3.3 Measurement of CA IX activity on intact single cells

Measurement of CA IX activity on membrane fragments is a simple way to screen antibodies for possible inhibition of CA IX function. Nevertheless, this method has several drawbacks like being performed under non-physiological conditions with respect to the ionic composition, alkaline pH and low temperature of experimental media. In addition, CA IX is extracted from its native cellular environment. To provide more physiological conditions, CA IX activity was measured in the native cellular environment on intact single HCT 116 cells. For this, surface extracellular pH (pH_S) changes were determined after addition and subsequent removal of extracellular NH_4^+-containing solution driving a transmembrane NH_3 flux (**Figure 3.22**). NH_3 influx lowers pH_S depositing extracellular H^+-ions at the cell surface. Analogously, NH_3 efflux raises pH_S.

pH_S changes are reduced by the spontaneous reaction of H^+-ions with HCO_3^-, namely from the physiological CO_2/HCO_3^- buffer used. However, this reaction is strongly enhanced by extracellular carbonic anhydrase activity. The corresponding protocol and sample time-course measured in HCT 116-CA IX cells superfused with 5% CO_2/12 mM HCO_3^- buffer is shown in **Figure 3.23**. Changing the superfusate buffer displaced pH_s from the bulk extracellular pH of 7.2. These transient pH_S changes after addition or removal of extracellular NH_4^+-containing solution were considerably larger when CA IX was inhibited with the commonly used broad-range carbonic anhydrase inhibitor acetazolamide, illustrating the importance of carbonic anhydrase activity in pH buffering by CO_2/HCO_3^-.

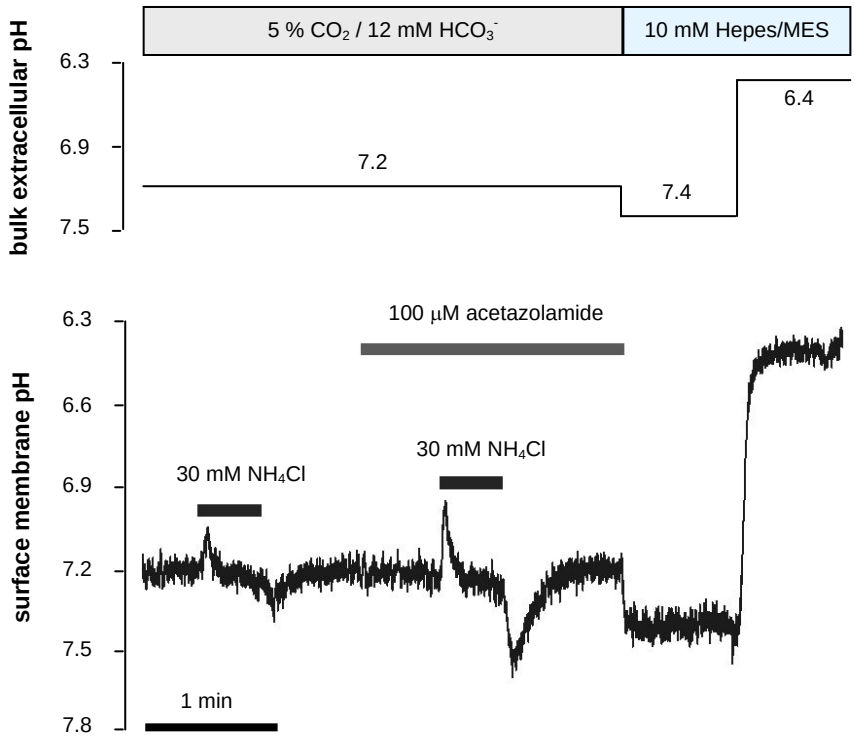

Figure 3.23: CA IX activity measurement on intact single cells. The experimental set-up is shown. The upper panel shows bulk extracellular pH and corresponding buffers. The lower panel shows addition and removal of ammonium chloride leading to transient pH_S changes which are thereafter compensated by spontaneous reaction of protons and hydrogen carbonate and by catalysis of the same reaction by CA IX. Spontaneous reaction is simulated by addition of the broad range inhibitor acetazolamide.

3.3.4 Inhibition of CA IX function on intact single cells

Antibodies were tested on HCT 116 cells expressing CA IX (HCT 116-CA IX) or empty vector (HCT 116-EV). HCT 116-CA IX cells had much smaller transient pH changes than HCT 116-EV cells (**Figure 3.24 A** and **B**). In HCT 116-CA IX cells, acetazolamide led to a strong increase of transient pH changes, whereas almost no increase in HCT 116-EV cells was observed, indicating only marginal expression of other extracellular isoforms. If preincubated with HCT 116-CA IX, only MSC 8 IgG (**Figure 3.24 C ii**) but not MSC 8 Fab (**Figure 3.24 C iii**) was able to increase transient pH changes and thus inhibit CA IX function. However, continuous addition of MSC 8 Fab to superfusate restored inhibition of CA IX activity (**Figure 3.24 C iv**). In contrast, MSC 3 IgG was not able to inhibit CA IX function (**Figure 3.24 C i**). In HCT 116-CA IX cells, transient pH changes were 42 % smaller than in ATZ treated control cells. MSC 8 IgG treated cells had transient pH changes only 16 % smaller than ATZ treated control. CA IX inhibition was calculated to be 48 % for MSC 8 Fab (when superfused continuously) and 61 % for MSC 8 IgG from the area under the curve (**Figure 3.24 D**).

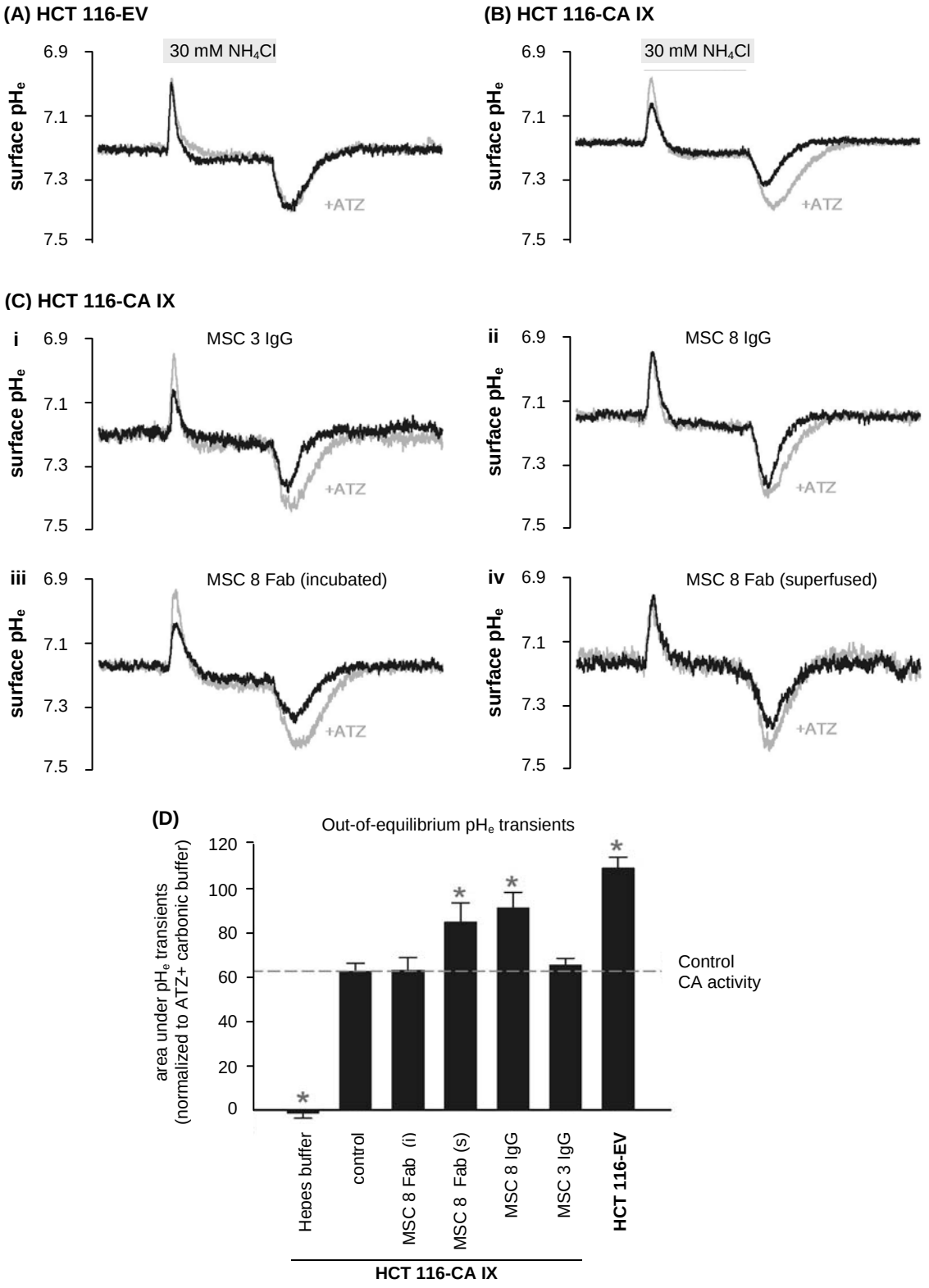

Figure 3.24: Influence of CA IX activity on pH_S. Transient pH_S changes were measured in **(A)** HCT 116-EV cells and **(B)** HCT 116-CA IX cells using only buffer (black) or inhibiting carbonic anhydrase activity with the broad range inhibitor acetazolamide (ATZ, grey). **(C)** Transient pH_S changes were measured in HCT 116-CA IX cells using **(i)** MSC 3 IgG, **(ii)** MSC 8 IgG or MSC 8 Fab **(iii)** incubated with the cells or **(iv)** added to the superfusate. **(D)** Areas under the curve were calculated and normalized to the measurement made in the presence of acetazolamide. (i): incubated, (s): superfused.

(A) SKRC 17 MW1 cl4

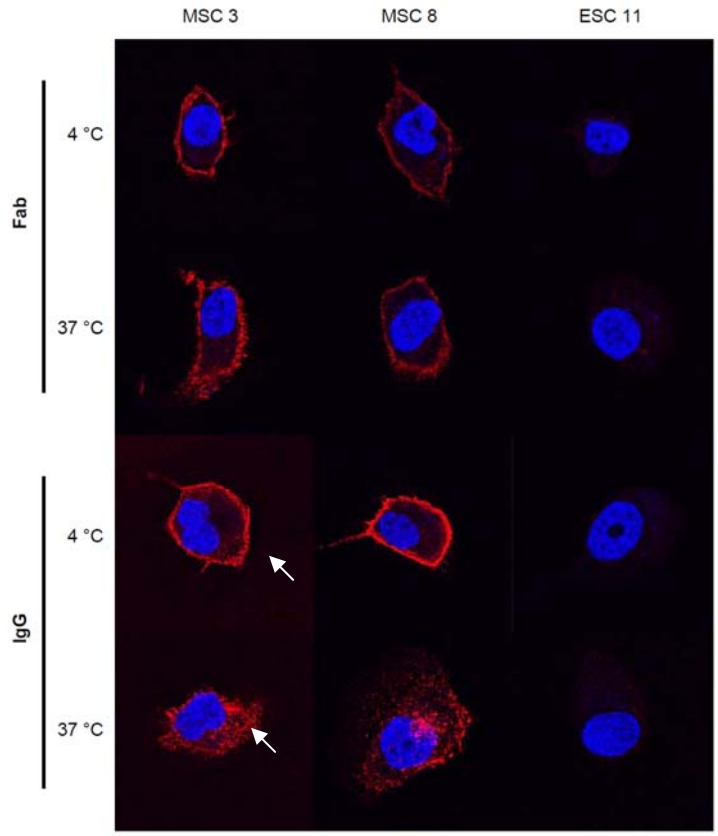

(B) HeLa

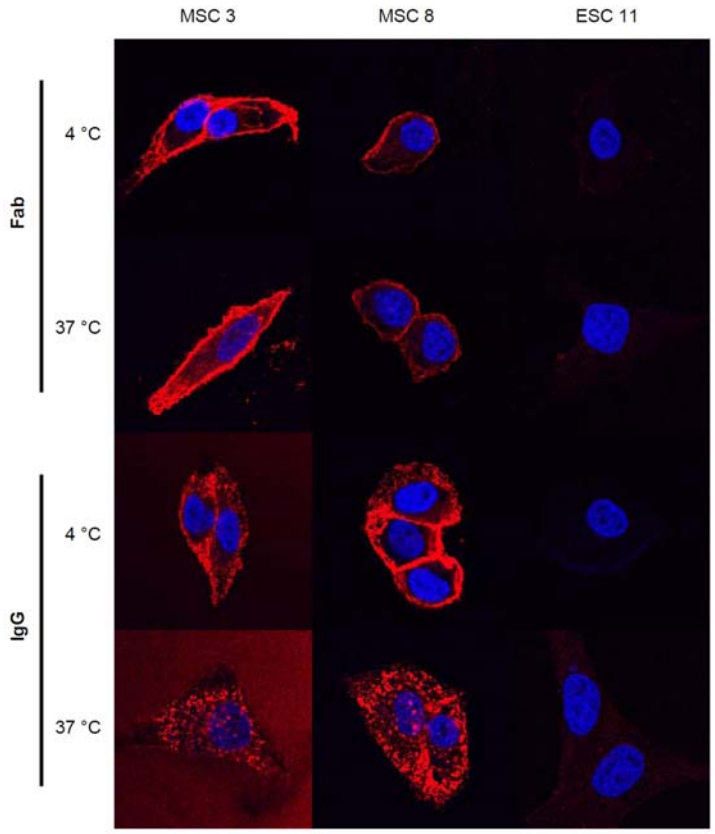

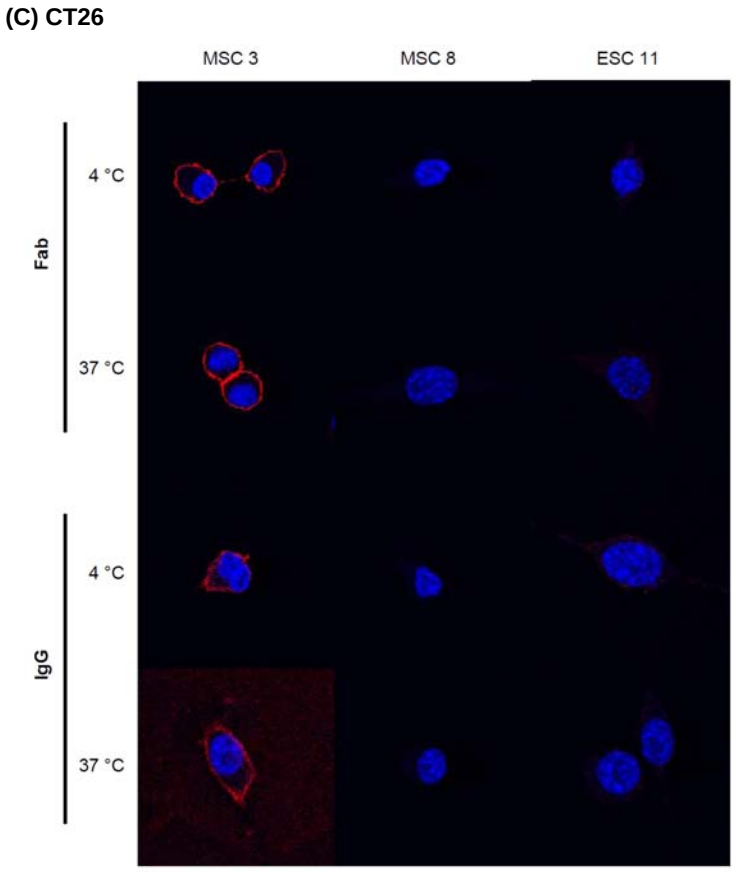

Figure 3.25: Internalization of CA IX. Internalization of CA IX was analyzed using Fab antibodies or IgGs on **(A)** SKRC 17 MW1 cl4 cells, **(B)** HeLa cells induced with 1 mM DMOG or **(C)** CT26 cells induced with 2 mM DMOG. For internalization MSC 3, MSC 8 or ESC 11 (red) were used, with the nuclei stained using DAPI (blue). White arrows in (A) indicate site of CA IX expression in one representative sample where at 4 °C expression is at the surface and at 37 °C in the cytosol.

3.4 PHYSIOLOGICAL EFFECTS OF THE SELECTED ANTIBODIES

3.4.1 Internalization of CA IX by MSC 3 IgG and MSC 8 IgG

Both antibodies were then tested for their potential to trigger internalization of bound CA IX protein. MSC 3 IgG as well as MSC 8 IgG led to internalization of CA IX on stably transfected SKRC 17 MW1 cl4 cells (**Figure 3.25 A**) and HeLa cells chemically induced with 1 mM DMOG for 48 h (**Figure 3.25 B**) when incubated at 37 °C for 2 h. If incubation was performed at 4 °C, the cell membrane was stained and no internalization was observed. In contrast, the corresponding Fab antibodies MSC 3 and MSC 8 did not induce internalization, regardless of the incubation temperature. On murine CT26 cells chemically induced with 2 mM DMOG no internalization was observed (**Figure 3.25 C**). MSC 3 Fab and IgG both stained the cell membrane and did not induce internalization. For the not cross-reactive antibody MSC 8 no signal could be detected on CT26. Control antibody ESC 11 did not led to any signal on the tested cell lines.

3.4.2 Influence of selected antibodies on cell proliferation

Fab antibodies MSC 3, MSC 8 and MSC 11 as well as MSC 3 and MSC 8 IgG were tested for a possible anti-proliferative effect on different cell lines expressing CA IX constitutively or after hypoxic induction. When SKRC 52 cells were incubated for 3 days with 1 μM MSC 3 or MSC 8 Fab antibody cell number was not decreased compared to cell number when incubated with media without any additives (**Figure 3.26**). Cell number of SKRC 52 and HeLa cells induced in a hypoxic chamber at 0.2 % O_2 decreased significantly when incubating the cells for 24 acetazolamide compared to incubation with medium without any additives. In contrast neither MSC 3 nor MSC 8 IgG were able to do so at a concentration of 0.5 μM, which is more than ten times higher than the concentration of MSC 8 IgG needed for maximal inhibition of CA IX activity. In addition, none of the tested Fab antibodies or IgGs was able to influence proliferation of any of the other tested cell lines SKRC 17, SKRC 17 MW1 cl4 or MCF-7 cells induced under hypoxia (data not shown).Under harsh conditions of low pH were cells have been proposed to depend on CA IX function to survive (Chiche, Ilc et al. 2009), survival of SKRC 17 MW1 cl4 was not augmented compared to SKRC 17 cells (data not shown). Similarly, blocking by ATZ had no effect on cell survival, showing that survival under these conditions was indeed not CA IX dependent.

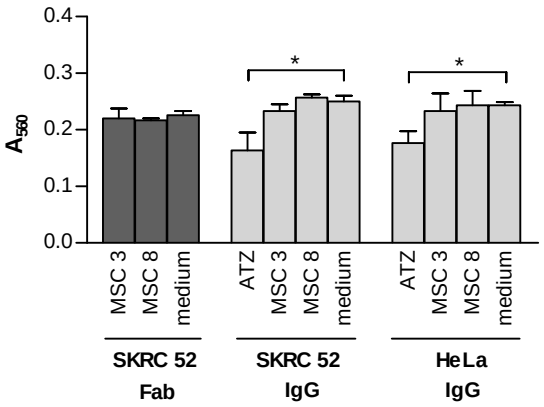

Figure 3.26: Proliferation assay. Survival of SKRC 52 cells and HeLa cells induced under hypoxia was analyzed using MSC 3 and MSC 8 Fab antibody (dark grey) or IgG (light grey) as well as acetazolamide (ATZ) and medium as control. Representative experiments analysed by crystal violet assay are shown. Samples were measured in triplicates. Results are shown as mean with standard deviation. Significance was calculated using a paired two-sided T-test. * : < 0.05.

3.5 COUPLING OF ANTIBODIES TO TOXIC MOIETIES

Coupling to toxic moieties can be used to combine antibody specific targeting with functional effects of a toxic moiety. MSC 3 and MSC 11 were chosen for their high affinity on human CA IX with MSC 3 showing in addition cross-reactivity to murine CA IX. To increase a possible anti-tumour effect, TNF was cloned into the pEE 12.4 vectors expressing the respective antibodies, creating an $F(ab)_2$ fragment coupled to TNF. $F(ab)_2$-TNF constructs were transiently expressed in HEK 293 cells and tested in Western blot (**Figure 3.27 A**) and in flow cytometry (**Figure 3.27 B**). All $F(ab)_2$-TNF constructs as well as the control MSC 3 IgG could be detected by an anti-hu-Fab-POX antibody in immuno blotting and anti-hu-Fab-PE in flow cytometry, whereas anti-huTNF and anti-muTNF stained only the $F(ab)_2$-TNF constructs containing the corresponding TNF.

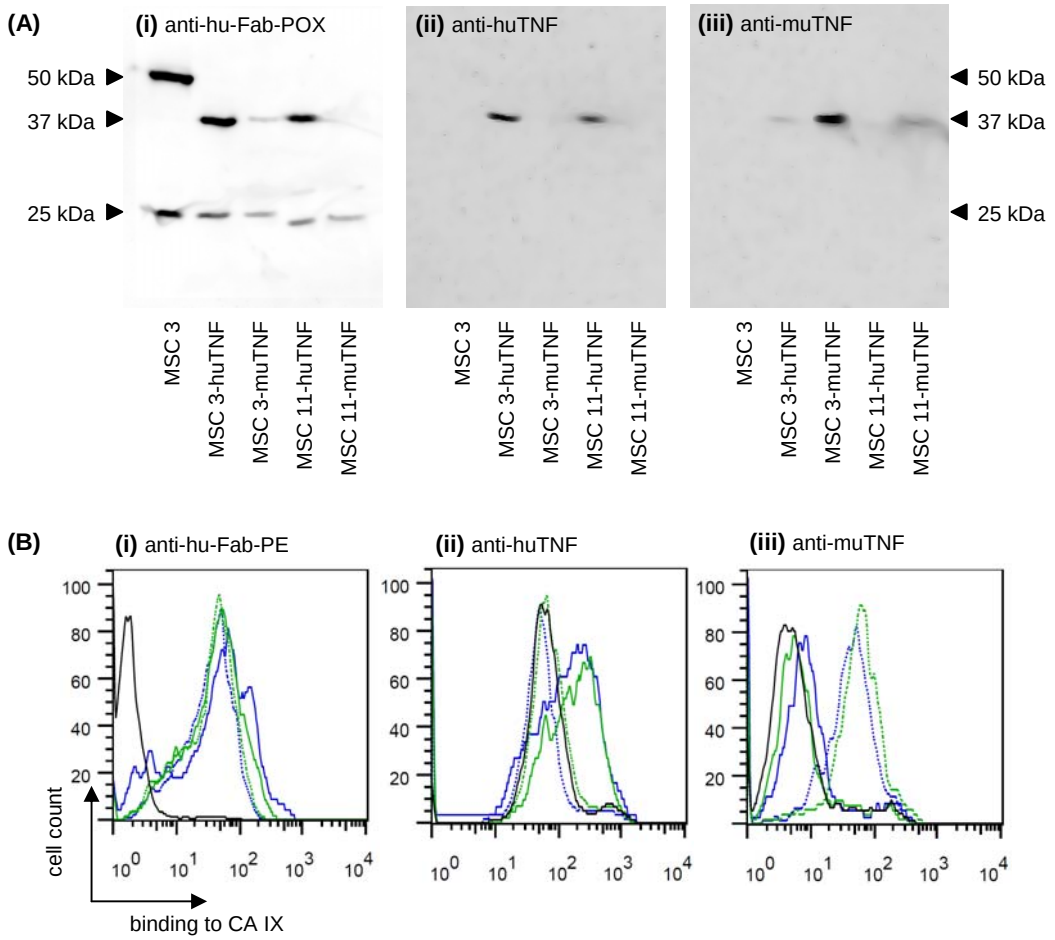

Figure 3.27: Confirmation of TNF-constructs. Transient expression of $F(ab)_2$-TNF constructs was validated in **(A)** Western blot analysis and **(B)** flow cytometry by staining with (i) anti-huFab-POX or anti-hu-Fab-PE, (ii) anti-huTNF and (iii) anti-muTNF. MSC 3 IgG served as a control. Flow cytometry: black: OptiMEM, blue: MSC 3 coupled to TNF green: MSC 11 coupled to TNF, solid line: huTNF, dotted line: muTNF.

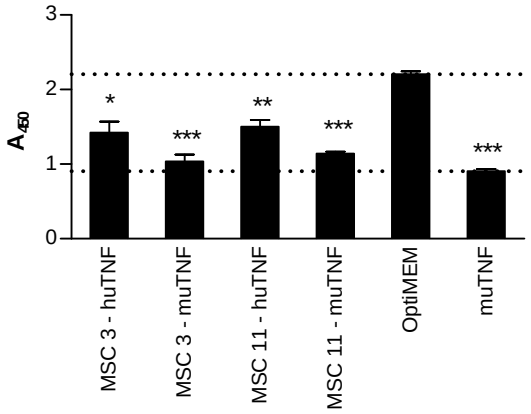

Figure 3.28: TNF-assay. Functionality of the $F(ab)_2$-TNF constructs was analyzed in a TNF-assay analyzing growth and survival of TNF sensitive Wehi S cells with variable doses of the $F(ab)_2$-TNF constructs. One representative measurements using undiluted supernatant of transient transfections is shown. Proliferation was compared to the one with OptiMEM (supernatants from not transfected HEK 293 cells, negative control) and muTNF (positive control), both represented with dotted lines. P-values were calculated compared to samples with OptiMEM of the same dilution using a paired, two-sided T-test: *** < 0.001, ** < 0.01, * < 0.05.

Functionality of the $F(ab)_2$-TNF constructs was confirmed by killing of TNF sensitive Wehi S cells in a dose dependent manner (**Figure 3.28**). $F(ab)_2$-TNF constructs were able to significantly inhibit survival of Wehi S cells when supernatant of HEK 293 cells transiently transfected with $F(ab)_2$-TNF constructs was added undiluted. Inhibition was in the same range as with recombinant muTNF.

4 DISCUSSION

4.1 STRATEGIES TO SELECT NOVEL CA IX SPECIFIC ANTIBODIES

This thesis describes the identification and characterization of twelve novel anti-CA IX antibodies MSC 1 – 12, among those five antibodies inhibiting CA IX enzymatic activity. There exist several strategies to identify novel antibodies. Immunization of mice led to the identification of many different anti-CA IX antibodies, among them M75 and G250 (Oosterwijk, Ruiter et al. 1986; Pastorekova, Zavadova et al. 1992; Zat'ovicova, Tarabkova et al. 2003). In this thesis, phage display using a semisynthetic human Fab antibody phage library consisting of $3.7 \cdot 10^{10}$ different phages was chosen, which allows expressing selected Fab antibodies on the surface of phages or as soluble Fab antibodies (de Haard, van Neer et al. 1999). Phage display is much faster and more suited to select human antibodies than immunization of mice. Indeed, the murine antibody G250 had to be humanized in order to avoid induction of human anti-mouse antibodies (Velders, Litvinov et al. 1994). In addition, antibodies with special features can be specifically enriched by phage display, e.g. selectivity for one special isoform or inhibition of CA IX enzymatic activity (reviewed in (Carter and Merchant 1997)). The PG-region of CA IX is very immunogenic due to the fact that human CA IX and murine CA IX differ mainly in this part, while the rest of the protein is much more conserved (Gut, Parkkila et al. 2002). Thus, most of the antibodies selected by immunization of mice recognize the PG domain, because this method does not allow selecting antibodies against self or closely related antigens. In contrast, inhibitory antibodies are most likely to bind to the catalytic CA domain. Selection of such inhibitory antibodies approved our choice to use phage display.

Recently, two independent groups selected antibodies against CA IX by phage display. Xu and coworkers used a library consisting of $2.7 \cdot 10^{10}$ different single chain antibodies (Xu, Lo et al. 2010), which is in the same range as the library used here, while Ahlskog et al. used a smaller library consisting of $3 \cdot 10^{9}$ different single chain antibodies only (Silacci, Brack et al. 2005; Ahlskog, Schliemann et al. 2009). Using a large library increases the chance to identify new antibodies with the desired features. Indeed, five different antibodies inhibiting CA IX enzymatic activity were selected from our library and four from the library of Xu, while Ahlskog et al. were not able to identify an inhibitory antibody (Ahlskog, Schliemann et al. 2009; Xu, Lo et al. 2010).

Selection by phage display on peptides allows selecting for antibodies specifically binding to the active pocket of the protein. Since at the beginning of this thesis no crystal structure of CA IX was available, models of CA IX structure based on CA II (Alterio, Vitale et al. 2006) were used to select peptides that include amino acids shown to be involved in CA II-sulfonamide interaction or in binding to the Zn^{2+} ion necessary for catalytic function. However, none of the Fab antibodies

selected against those peptides was able to bind to naturally expressed CA IX (data not shown), because the peptides chosen lie within the active pocket of CA IX and, although accessible to chemical compounds as sulfonamides, they might not be accessible to the much larger Fab antibodies. Therefore, selection was performed on recombinant CA IX protein leading to the selection of the twelve distinct anti-CA IX Fab antibodies MSC 1 – 12. The yield is comparable to the one of Xu et al. identifiying 14 distinct antibodies from their library (Xu, Lo et al. 2010). Seven of the here selected Fab antibodies were encountered several times, with two found even 16 times each (**Figure 3.2 B**). Another five groups selected contained only one clone. This enrichment of certain phages is typical for later rounds of selection, since with each round of selection phages binding to the selection antigen are enriched (reviewed in (Smith and Petrenko 1997)). The selection protocol used favours enrichment of phages binding with high affinity to rhCA IX, by using decreasing amounts of antigen in subsequent selection rounds and stringent washing leading to the loss of phages binding with low affinity to rhCA IX. High affinity binding as found for the here selected antibodies is favourable for later use in the clinic, since such antibodies stay longer at the site of action due to more stable antibody-antigen interactions. Nevertheless, too stringent conditions might lead to the loss of potential binders (reviewed in (Smith and Petrenko 1997)). Therefore, it is important to reduce the number of selection rounds to a minimum. The fact that some phages were enriched and others were encountered only once suggests that the number of selection rounds used was optimal.

In this work, selection was performed on a recombinant protein composed of the whole extracellular part of CA IX. Xu et al. performed selection on CA IX containing paramagnetic proteoliposomes (Xu, Lo et al. 2010), while Ahlskog et al. used recombinant CA domain, to select for binders possibly inhibiting CA IX catalytic function (Ahlskog, Schliemann et al. 2009). Although the latter approach favours selection of antibodies binding to the catalytic domain, it showed to be more favourably to use the whole extracellular part of CA IX or even the whole protein, since those two approaches led to the identification of inhibitory antibodies. Using a recombinant protein consisting of the whole extracellular part reduces the amount of selected binder against the CA domain, but displays a more natural target. Although Ahlskog et al. could show that their recombinant protein is catalytically active (Ahlskog, Schliemann et al. 2009), the structure of the protein might be altered having an influence on binding of the selected antibodies to naturally expressed CA IX.

4.2 CHARACTERIZATION OF ANTI-CA IX ANTIBODIES

The selected Fab antibodies MSC 1 – 12 bound specifically to recombinant human CA IX, to human CA IX expressed constitutively by stable transfection or by pVHL deficiency as well as to human CA IX expressed after chemical induction or under conditions of low oxygen levels. Every test system has its own strong points (**Table 4.1**). Therefore, it is necessary to combine those methods. In this work, binding of MSC 1 – 12 on CA IX expressed in those four test systems was identical indicating that those Fab antibodies are well suited for use in RCC as well as in hypoxic tumours. Thus, those four test systems were equivalent. Nevertheless, one Fab antibody, MSC 8, showed different binding to recombinant and naturally expressed protein. While in flow cytometry binding was in the same range as for all other antibodies, binding in ELISA on rhCA IX was much weaker, although still significant. This could point to an epitope presented differently in the recombinant protein than on cell lines. Such differences could arise from differences in glycosylation, slightly changed conformation in the recombinant protein or differences in multimerization. Problems with multimerization seem to be an issue for CA IX, where the extracellular part was shown to build dimers (Alterio, Hilvo et al. 2009) while the full length protein was proposed to form trimers (Pastorekova, Zavadova et al. 1992; Svastova, Hulikova et al. 2004). In addition, coating of the recombinant protein to the plate might impair correct formation or accessibility of such an epitope. Since the K_D value of 14 nM for MSC 8 Fab to rhCA IX lies within the range as for the other antibodies, binding differences seem to be due to the coating procedure.

Table 4.1 Comparison of different test systems for CA IX expression. +/-: low levels of CA IX possible due to density mediated upregulation (Kaluz, Kaluzova et al. 2002).

	stable transfection	**pVHL-deficiency**	**chemical induction**	**hypoxic induction**
constitutive expression	yes	yes	no	no
negative cell line available	yes	no	+/-	+/-
formation of active conformation	no	no	no	yes
induction of other HIF-regulated genes	no	yes	yes	yes
cell lines	artificial	many RCC	most cell lines	most cell lines
main field of use	screening, antibody characterization	model for RCC	fast upregulation in many cell lines	model for hypoxic tumours

Immunoprecipitation of the recombinant protein by M75 reduced the possibility to select antibodies recognizing an already known epitope, because the epitope of M75 was not accessible to phages. Nevertheless, it might be possible to select phages recognizing the same epitope since the linear epitope of M75 consists of a six fold tandem repeat of six aa in the PG region of CA IX with a minimal epitope provided by PGEEDLP (Zavada, Zavadova et al. 2000). None of the Fab antibodies MSC 1 – 12 was able to detect CA IX in Western blot analysis, indicating that they do not recognize linear epitopes (**Figure 3.13**). The epitope of G250 on the other hand is not yet known although there is evidence, that it is a sterical one (Chrastina, Zavada et al. 2003). Competition assays (Anna Zortea, unpublished data) revealed that binding of Fab antibodies MSC 1 – 12 to human CA IX was not competitive with M75 or G250. These data show that the here selected antibodies MSC 1 – 12 indeed are recognizing new epitopes not overlapping with the ones of the two established CA IX antibodies M75 or G250.

None of the Fab antibodies showed a difference in binding under normoxic or hypoxic conditions (**Figure 3.6**). Therefore, epitopes within regions subject to conformational changes triggered by the absence of oxygen could be excluded. Not much is known about those conformational changes and, although the absence of oxygen per se seems to be needed (Dubois, Douma et al. 2007), also other factors might play a role. In addition, the time frame during which the hypoxic conformation is stable might be too short for detection of different binding behaviour of Fab antibodies on CA IX expressed under those two conditions. Dubois et al. suggested that the hypoxic conformation is lost after reoxygenation with a half life time of 30 min (Dubois, Douma et al. 2007). Nevertheless, fixation of cells after incubation with antibody under hypoxic conditions did not lead to any change, although loss of antibody binding due to conformational changes is avoided (**Figure 3.7**). This further supports the hypothesis that MSC 8 binds to a region that is not affected by conformational changes. Ongoing co-crystallization studies of MSC 8 with the extracellular part of CA IX will give more insights according to the epitope.

Table 4.2 Comparison of antibodies and chemical compounds.

	antibodies	**chemical compounds**
selectivity	high	low or absent
inhibition of CA IX function	up to 76 % (MSC 8 IgG)	yes (many compounds)
affinity	high (2-66 nM)	high-intermediate
size	intermediate (Fab antibodies) – large (IgG)	small
tissue penetration	intermediate	good
blood clearance	fast (Fab antibodies) – intermediate (IgG)	mostly very fast

4.3 COMPARISON OF ANTIBODIES AND CHEMICAL COMPOUNDS

To find the optimal therapeutic compound, factors as affinity and size of therapeutic compounds having an influence on tissue penetration and blood clearance as well as selectivity and inhibition of CA IX function have to be considered (**Table 4.2**).

Affinities of the selected Fab antibodies against recombinant human CA IX are in the range of 2 – 66 nM (**Table 3.3**), which is the usual range for monovalent Fab antibodies. The single chain antibodies described to inhibit CA IX function have similar affinities (1 – 100 nM) (Xu, Lo et al. 2010), while the affinity of the most broadly used sulfonamide acetazolamide is 25 nM (Casey, Morgan et al. 2004). Other commonly used sulfonamides in the clinic show affinities in the same range, e.g. 27 nM for the antiglaucoma agent methazolamide (Casey, Morgan et al. 2004). The here selected antibodies therefore have up to tenfold higher affinity than those commonly used sulfonamides. Since antibodies are bivalent, their affinity is supposed to be even higher than for Fab fragments due to increased avidity. The here selected compounds are supposed to show slower blood clearance than commonly used sulfonamides, since high affinity leads to longer retention of therapeutic compounds at the site of interest (reviewed in (Tabrizi, Bornstein et al. 2010)). In contrast, it is expected that accessibility to tumour tissue is much higher for small chemical compounds like sulfonamides than for antibodies due to their much lower molecular weight. Similarly, Fab antibodies are expected to have much better tissue penetrasion than IgGs (reviewed in (Tabrizi, Bornstein et al. 2010)). Tissue penetration and blood clearance are important for duration of therapeutic effect. Long lasting effects reduce the number of injections necessary. If effects last too long on the other hand, side effects on tissue sites expressing CA IX under normal conditions and not only in cancer tissue, e.g. in the gastrointestinal tract, might cause some problems. Comparison of different formats therefore is very important to find the optimal form for administration and therapeutic efficiency.

Selectivity for the CA IX isozyme is of great importance to guarantee targeted treatment and to avoid side effects as they are common using sulfonamides. This is especially important, since several carbonic anhydrase isoforms show high homology to CA IX (Opavsky, Pastorekova et al. 1996). The probably most important carbonic anhydrase isoform is CA II, which is expressed in the cytosol. Due to its broad expression in many tissues (Pan, Leppilampi et al. 2006), its high catalytic activity and its involvement in respiration, pH homeostasis, bone development and function (reviewed in (Pastorekova, Parkkila et al. 2004; Supuran 2004)), selectivity compared to CA II is a major issue, although its intracellular expression prevents binding of the here selected Fab antibodies in the tissue. This restricted binding to extracellular epitopes is one major advantage of antibodies. Most sulfonamides in contrast can pass the membrane and, thus, bind also to intracellular isoforms. Although binding of antibodies to intracellular isoforms is not an issue, there exist three transmembrane or membrane-tethered carbonic anhydrase isoforms. Two of them with

high homology to CA IX (36 and 37 %, respectively), namely the cancer-related CA XII that is much less restricted to tumour tissue than CA IX (reviewed in (Pastorekova and Pastorek 2004)) and CA XIV were addressed. In contrast to many sulfonamides, none of the selected Fab antibodies bound to any of the tested isoforms confirming the high selectivity provided by antibodies.

Chemical compounds on the other hand are very potent in inhibiting CA IX enzymatic activity. Many different sulfonamides inhibiting CA IX function are known, while neither G250 nor M75 have been described to do so. In contrast, five of the Fab antibodies selected in this work reduced CA IX activity partially in a biochemical assay performed on membrane-fragments (**Figure 3.18 B**), with maximal inhibition of CA IX activity by up to 57 % using MSC 8 (**Figure 3.19**). Recently, an independent group has reported single chain antibodies selected by phage display with inhibitory effects on human CA IX (Xu, Lo et al. 2010). Inhibitory potential was tested on soluble CA IX fusion protein leading to reduction of CA IX activity by up to 50 %, which is in the same range as for the Fab antibodies selected in this work. In contrast, when using the corresponding IgG, inhibition using MSC 8 was augmented to 76 % (**Figure 3.21**), leading to the highest inhibition reported to date for antibodies. This increase in inhibition seems to rely on antibody format coupled to higher avidity. Half-maximal inhibition doses of 6.5 nM for Fab antibody and 2.2 nM for IgG can be explained by the same fact. Although selected against the CA domain of CA IX, none of the antibodies selected by Ahlskog et al. was able to inhibit CA IX function (Ahlskog, Schliemann et al. 2009). The single chain antibodies as well as the Fab antibodies selected here are therefore the first antibodies described to inhibit CA IX enzymatic activity.

The inhibition assay of Xu et al. (Xu, Lo et al. 2010) was based on a similar approach as the assay used in this thesis, but inhibition on membrane fragments expressing CA IX used in this work might provide a more physiologically-accurate target for inhibition studies than inhibition of soluble fusion protein. Nevertheless, both assays are performed in a buffer system having a non-physiological composition and an alkaline pH. This alkaline pH as well as low temperature of experimental media is necessary to bring the kinetics of the reaction within the resolving power of the pH electrode. In addition, CA IX is extracted from its native cellular environment, which might also have an influence on protein activity in the tumour tissue. Since CA IX might undergo structural changes during preparation of membrane fragments, the interaction with antibodies could be influenced. Additionally, possible interactions with other proteins could be important for proper CA IX function in intact cells. Disruption of such interactions might readily take place during preparation of membrane fragments. Since such interactions could either enhance or inhibit CA IX function, this inhibition assay might lead to false positive or false negative results, although it is the standard assay to screen antibodies for a possible inhibitory effect. Therefore, experiments were performed in the native cellular environment of intact single HCT 116 cells instead of membrane fragments.

Previous studies showed that CA IX does not have any influence on single cell pH_i under physiological conditions (Swietach, Wigfield et al. 2008 9). However, CA IX is able to influence surface extracellular pH (pH_S) (Swietach, Patiar et al. 2009). MSC 8 is the first antibody shown to inhibit CA IX function on intact single cells. Inhibition with MSC 8 Fab antibody could only be achieved by addition of MSC 8 Fab to the superfusate, while for MSC 8 IgG preincubation of cells was sufficient (**Figure 3.24 D**). In the single-cell approach, cells are constantly superfused with antibody free buffer. While the bivalent MSC 8 IgG associated persistently with CA IX protein and reduced CA IX activity although unbound antibody was washed away with superfusion, monovalent MSC 8 Fab antibody was washed away and no lasting inhibitory effect was produced.

Spheroids can be used to simulate CA IX activity in tumour masses (Swietach, Vaughan-Jones et al. 2007; Swietach, Wigfield et al. 2008; Swietach, Patiar et al. 2009). MSC 8 Fab and MSC 8 IgG both were shown to have an effect on pH in spheroids (unpublished data), most likely due to inhibition of CA IX activity. The effect was only visible when spheroids were preincubated with antibodies indicating the time needed to penetrate into the spheroid core. This accessibility has to be taken into account for further experiments, since tumour tissue is often poorly vascularised and, therefore, accessibility might also be hampered.

Taken together, an IgG is the format of choice for MSC 8 due to higher avidity, predicted slower blood clearance and much higher inhibition rate. Although penetration is diminished with increasing size of therapeutical compounds, the example of G250 shows that an IgG can specifically accumulate in hypoxic tumour tissue (Divgi, Pandit-Taskar et al. 2007).

Although antibodies and chemical compounds both are able to inhibit CA IX catalytic activity, the mechanism of inhibition seems to differ. Carbonic anhydrase activity depends on Zn^{2+} in the active pocket. This Zn^{2+}–ion binds a water molecule, thereby facilitating its interaction with the carbon dioxide and formation of hydrogen carbonate and a proton (reviewed in (Supuran 2004)). Sulfonamides inhibit CA IX function by binding to the Zn^{2+}–ion, thereby preventing binding of a water molecule to the active pocket (Abbate, Casini et al. 2004; Weber, Casini et al. 2004; Di Fiore, De Simone et al. 2005; Menchise, De Simone et al. 2005; Alterio, Vitale et al. 2006; Di Fiore, Pedone et al. 2006). Fab antibodies on the other hand are too big to enter the active pocket and, therefore, have to inhibit CA IX function by other means. Beside binding to the active site and blocking the binding of the substrate, antibodies can impede binding of the substrate by sterical hindrance, trigger conformational changes of target proteins, or downregulate them by triggering internalization.

Sterical hindrance by blocking the entry of the educts to the active site is very complicated to achieve for such small molecules like water and carbonic dioxide. That might be a reason, why the antibodies only partially inhibited CA IX (**Figure 3.18** and **Figure 3.20**). Although single chain

antibodies, Fab antibodies and IgGs differ in their size with a Fab being approximately twice and an IgG six times as big as a single chain antibody, this difference might not reflect a difference in sterical hindrance, since the educts of CA IX are disappearing small compared to the different antibodies. Inhibition by the single chain antibodies selected by Xu and coworkers (Xu, Lo et al. 2010) and inhibition by Fab antibodies selected in this work are indeed in the same range which might point towards a similar mechanism of inhibition. Nevertheless, it is doubtful whether sterical hindrance of such small educts could lead to inhibition by up to 76 % for MSC 8 IgG (**Figure 3.21**).

Conformational changes due to antibody binding can impair binding of educts to CA IX or CA IX catalytic function itself. Furthermore, conformational changes of one CA IX molecule might change conformation of other CA IX molecules involved in the CA IX multimer leading to allosteric effects. Binding of antibodies to only one subunit could in addition be based on an epitope that is accessible just once in the multimer, possibly due to sterical hindrance by the antibodies themselves. In a dimeric complex as shown for the extracellular part of CA IX by crystallization (Alterio, Hilvo et al. 2009), only one binding site might be accessible for MSC 8. Nevertheless, this seems unlikely since the IgG led to higher inhibition than the Fab antibody although it is plausible that the three times bigger IgG will hamper binding to a second subunit much more than the Fab antibody. MSC 8 therefore is thought to inhibit CA IX function through conformational changes. Ongoing co-crystallization studies using MSC 8 and CA IX might give further insights in the exact mechanism of inhibition.

The IC_{50} of MSC 8 Fab (0.33 µg/ml, corresponding to 6.5 nM) is close to the K_D value of 14 nM determined by surface plasmon resonance, suggesting that the epitope-binding step displays the event that inhibits CA IX catalytic activity. This is supported by the fact that on single cells addition of MSC 8 to the superfusate without prior incubation leads to inhibition of CA IX (**Figure 3.24 C iv**). Inhibition therefore is fast and does not rely on a general antibody-mediated effect, like IgG-induced internalization of CA IX. This is demonstrated by inhibition of CA IX function on singe cells by MSC 8 Fab although the Fab antibody is not able to trigger internalization due to missing cross-linking. In addition, inhibition could be observed in the biochemical assay on membrane fragments, where no internalization can take place. Nevertheless, beside direct inhibition of CA IX activity, indirect mechanisms can be important. It is plausible that, by decreasing the amounts of CA IX available on the cell surface, internalization reduces CA IX activity and, thus, might further increase the effect of CA IX inhibition by MSC 8 leading to an even more potent inhibitor. In contrast, none of the single chain antibodies selected by Xu and coworkers shown to inhibit CA IX function in the same range as the here selected antibodies was able to trigger internalization (Xu, Lo et al. 2010).

Recently, an independent group selected an antibody triggering CA IX internalization on CA IX transfected cells and eliciting anti-cancer effects in mouse xenograft model of colorectal

carcinoma, although no CA IX inhibitory function was described (Zatovicova, Jelenska et al. 2010). Therefore, by combining CA IX inhibitory potential and triggering of internalization not only on transfected, but also on chemically induced cells, MSC 8 might be even more potent. In addition, antibodies can directly trigger the immune response, e.g. by antibody mediated cellular cytotoxicity, and, thus, MSC 8 IgG not only inhibits CA IX function but also might lead to long lasting anti-tumour effects.

4.4 POSSIBLE IMPLICATIONS OF THE SELECTED ANTIBODIES

Inhibition of CA IX activity is thought to impede tumour growth. Nevertheless, MSC 8 was not able to inhibit growth of SKRC 52 cells and HeLa cells induced under hypoxic conditions (**Figure 3.26**). This is in line with reports that CA IX does not influence pH_i in single cells under physiological conditions (Swietach, Wigfield et al. 2008) and that only under harsh conditions of low pH and in the absence of added extracellular hydrogen carbonate CA IX expression protects cells against cytoplasmic acidification, sustains ATP levels and promotes cell survival (Chiche, Ilc et al. 2009). In addition, CA IX function can be compensated by other extracellular carbonic anhydrases, e.g. CA XII (Chiche, Ilc et al. 2009). This report indicates that it might be necessary to use a mouse model providing the conditions found in tumour tissue to see an effect of inhibition of CA IX activity while *in vitro* no effect might be visible.

Cross-reactivity of MSC 1 and MSC 3 is optimal for testing antibodies in a mouse model, since a syngeneic mouse model can be used and possible side effects due to binding to CA IX expressed in normal tissue are easily detectable. Affinities of the selected Fab antibodies against recombinant murine CA IX were in the range of 4 – 50 nM (**Table 3.3**), which is in the same range as on human CA IX. A similar range of affinities is ideal to transfer therapy in a mouse models to humans. MSC 3 was able to specifically stain C51 tumour sections and staining using MSC 3 corresponded to a staining using the hypoxia marker pimonidazole. Overlapping signals of CA IX expression and pimonidazole have been reported in some cases, while in other tumour sections no correlation could be observed (Troost, Bussink et al. 2005; Ahlskog, Schliemann et al. 2009) and, therefore, is thought to be tumour specific. Nevertheless, the here selected antibody MSC 3 is very useful for staining of CA IX in tumour sections and, thus, has possible applications in biodistribution.

Another application of antibodies is the delivery of therapeutic moieties to target cells expressing an antigen of interest. One possibility for such a toxic moiety is TNF. Previous studies by Bauer et al. demonstrated specific accumulation and retention of a cG250-TNF construct at tumour sites in xenografted mice resulting in growth inhibition and improved progression free survival (Bauer, Oosterwijk-Wakka et al. 2009). In this work, $F(ab)_2$-TNF constructs were produced containing an $F(ab)_2$ part specifically binding to tumour-associated CA IX and a TNF part which kills TNF-

sensitive cells by a receptor mediated mechanism. TNF activity was confirmed by killing TNF sensitive Wehi S cells in a dose dependent manner (**Figure 3.28**). To further address specific accumulation of the constructs in tumour tissue mice experiments are needed.

Antibodies can not only be used to deliver therapeutic moieties to target cells. Internalization triggered by antibodies can be utilised to deliver radioactive moieties or cytotoxic compounds coupled to antibodies directly into the target cells. Once inside the cell, such compounds can accumulate and fulfil their respective function. MSC 3 IgG and MSC 8 IgG triggering internalization of CA IX are therefore promising tools for radioactive labelling or specific killing of CA IX positive cells.

In conclusion, the here selected antibodies are promising tools for tumour targeting and tumour therapy. They combine high specificity and inhibition of CA IX function. In addition they trigger internalization of CA IX which further reduces CA IX levels at the cell surface. Therefore, they might lead to enhanced therapy of solid tumours and extend beyond the use of already known antibodies or chemical compounds.

5 APPENDIX

5.1 SEQUENCES

5.1.1 CA IX DNA sequence

(EMBL Data Library, X66839)

gcccgtacac	accgtgtgct	gggacacccc	acagtcagcc	gcatggctcc	cctgtgcccc	60
agcccctggc	tccctctgtt	gatcccggcc	cctgctccag	gcctcactgt	gcaactgctg	120
ctgtcactgc	tgcttctgat	gcctgtccat	ccccagaggt	tgccccggat	gcaggaggat	180
tccccttgg	gaggaggctc	ttctggggaa	gatgacccac	tgggcgagga	ggatctgccc	240
agtgaagagg	attcacccag	agaggaggat	ccacccggag	aggaggatct	acctggagag	300
gaggatctac	ctggagagga	ggatctacct	gaagttaagc	ctaaatcaga	agaagagggc	360
tccctgaagt	tagaggatct	acctactgtt	gaggctcctg	gagatcctca	agaaccccag	420
aataatgccc	acagggacaa	agaaggggat	gaccagagtc	attggcgcta	tggaggcgac	480
ccgccctggc	cccgggtgtc	cccagcctgc	gcgggccgct	tccagtcccc	ggtggatatc	540
cgcccccagc	tcgccgcctt	ctgcccggcc	ctgcgccccc	tggaactcct	gggcttccag	600
ctcccgccgc	tcccagaact	gcgcctgcgc	aacaatggcc	acagtgtgca	actgaccctg	660
cctcctgggc	tagagatggc	tctgggtccc	gggcgggagt	accgggctct	gcagctgcat	720
ctgcactggg	gggctgcagg	tcgtccgggc	tcggagcaca	ctgtggaagg	ccaccgtttc	780
cctgccgaga	tccacgtggt	tcacctcagc	accgcctttg	ccagagttga	cgaggccttg	840
gggcgcccgg	gaggcctggc	cgtgttggcc	gcctttctgg	aggagggccc	ggaagaaaac	900
agtgcctatg	agcagttgct	gtctcgcttg	gaagaaatcg	ctgaggaagg	ctcagagact	960
caggtcccag	gactggacat	atctgcactc	ctgccctctg	acttcagccg	ctacttccaa	1020
tatgaggggt	ctctgactac	accgccctgt	gcccagggtg	tcatctggac	tgtgtttaac	1080
cagacagtga	tgctgagtgc	taagcagctc	cacaccctct	ctgacaccct	gtggggacct	1140
ggtgactctc	ggctacagct	gaacttccga	gcgacgcagc	ctttgaatgg	gcgagtgatt	1200
gaggcctcct	tccctgctgg	agtggacagc	agtcctcggg	ctgctgagcc	agtccagctg	1260
aattcctgcc	tggctgctgg	tgacatccta	gccctggttt	ttggcctcct	ttttgctgtc	1320
accagcgtcg	cgttccttgt	gcagatgaga	aggcagcaca	gaaggggaac	caaaggggt	1380
gtgagctacc	gcccagcaga	ggtagccgag	actggagcct	agaggctgga	tcttggagaa	1440
tgtgagaagc	cagccagagg	catctgaggg	ggagccggta	actgtcctgt	cctgctcatt	1500
atgccacttc	cttttaactg	ccaagaaatt	ttttaaaata	aatatttata	at	1552

5.1.2 CA IX amino acid sequence

(NCBI, Q16790.2 GI:83300925)

MAPLCPSPWL	PLLIPAPAPG	LTVQLLLSLL	LLVPVHPQRL	PRMQEDSPLG	GGSSGEDDPL	60
GEEDLPSEED	SPREEDPPGE	EDLPGEEDLP	GEEDLPEVKP	KSEEEGSLKL	EDLPTVEAPG	120
DPQEPQNNAH	RDKEGDDQSH	WRYGGDPPWP	RVSPACAGRF	QSPVDIRPQL	AAFCPALRPL	180
ELLGFQLPPL	PELRLRNNGH	SVQLTLPPGL	EMALGPGREY	RALQLHLHWG	AAGRPGSEHT	240
VEGHRFPAEI	HVVHLSTAFA	RVDEALGRPG	GLAVLAAFLE	EGPEENSAYE	QLLSRLEEIA	300
EEGSETQVPG	LDISALLPSD	FSRYFQYEGS	LTTPPCAQGV	IWTVFNQTVM	LSAKQLHTLS	360
DTLWGPGDSR	LQLNFRATQP	LNGRVIEASF	PAGVDSSPRA	AEPVQLNSCL	AAGDILALVF	420
GLLFAVTSVA	FLVQMRRQHR	RGTKGGVSYR	PAEVAETGA			459

5.1.3 huTNF

GGTACCCACACCGT***GGCCGGCC***TCTGCGCCTGGGCCCAGCTCTGTCCCACACCGCGGTCACATGGCACCTTTTCTCTTCCA
GCCTCCACCAAGGGCCCAAGCGTCTTTCCTCTGGCCCCCAGCAGCAAGTCTACCAGCGGCGGCACTGCCGCTCTGGGCTGT
CTGGTGAAGGACTACTTCCCCGAGCCCGTGACCGTCAGCTGGAACTCTGGCGCTCTGACCTCCGGCGTGCACACCTTCCCC
GCCGTGCTGCAGAGCAGCGGCCTGTACAGCCTGAGCAGCGTGGTGACCGTGCCCAGCAGCAGCCTGGGCACCCAGACCTAC
ATCTGCAACGTGAACCACAAGCCCAGCAACACCAAGGTGGACAAGAAGGTGGAGCCCAAGAGCTGCGACAAGACCCACACC
TGCCCCCCTTGCCCTGGCGGCGGAGGAAGCAGCAGCTCCAGGACCCCCAGCGACAAGCCCGTGGCCCATGTGGTGGCCAAC
CCCCAGGCCGAGGGCCAGCTGCAGTGGCTGAACAGAAGGGCCAACGCCCTGCTGGCCAACGGCGTGGAGCTGAGGGACAAC
CAGCTGGTCGTGCCAAGCGAGGGCCTCTACCTGATCTACAGCCAGGTGCTGTTCAAGGGCCAGGGCTGCCCCAGCACCCAC
GTGCTGCTGACCCACACCATCAGCAGGATCGCCGTGAGCTACCAGACCAAGGTGAACCTGCTGTCCGCCATCAAGAGCCCC
TGCCAGAGAGAGACCCCCGAGGGCGCCGAGGCCAAGCCTTGGTACGAGCCCATCTACCTGGGCGGCGTGTTCCAGCTCGAA
AAGGGCGACAGACTGAGCGCCGAGATCAACAGGCCCGACTACCTGGACTTCGCCGAGAGCGGCCAGGTGTACTTCGGCATC
ATCGCCCTGTGA***CTCGAG***CTC

GGCCGGCC FseI, CTCGAG XhoI

5.1.4 muTNF

GGTACCCACACCGT***GGCCGGCC***TCTGCGCCTGGGCCCAGCTCTGTCCCACACCGCGGTCACATGGCACCTTTTCTCTTCCA
GCCTCCACCAAGGGCCCAAGCGTGTTCCCTCTGGCCCCCAGCAGCAAGAGCACCTCTGGCGGCACAGCTGCTCTGGGCTGC
CTGGTGAAGGACTACTTCCCCGAGCCTGTGACTGTGAGCTGGAACAGCGGCGCTCTGACCTCCGGCGTGCACACTTTCCCT
GCCGTCCTGCAGAGCAGCGGCCTGTACAGCCTGAGCAGCGTGGTGACCGTGCCCAGCAGCAGCCTGGGCACCCAGACCTAC
ATCTGCAACGTGAACCACAAGCCCAGCAACACCAAGGTGGACAAGAAGGTGGAGCCCAAGAGCTGCGACAAGACCCACACC
TGCCCCCCTTGCCCTGGCGGCGGAGGAAGCGACGAGCCTGTCGCCCATGTGGTGGCCAACCATCAGGTGGAGGAACAGCTG
GAATGGCTGTCCCAGAGGGCCAACGCCCTGCTGGCCAACGGCATGGACCTGAAGGACAACCAGCTGGTCGTGCCCGCCGAC
GGCCTGTATCTGGTGTACTCTCAGGTGCTGTTCAAGGGCCAGGGCTGCCCCGACTACGTGCTGCTGACCCATACAGTGAGC
AGGTTCGCCATCAGCTACCAGGAAAAGGTCAACCTGCTGTCCGCCGTGAAGAGCCCCTGCCCCAAGGACACCCCCGAGGGC
GCCGAGCTGAAGCCTTGGTACGAGCCCATCTACCTGGGCGGCGTGTTCCAGCTCGAAAAGGGCGACCAGCTGTCTGCCGAG
GTGAACCTGCCCAAGTACCTGGACTTCGCCGAGAGCGGCCAGGTGTACTTCGGCGTGATCGCCCTGTGA***CTCGAG***CTC

GGCCGGCC FseI, CTCGAG XhoI

5.2 ABBREVIATIONS

5.2.1 Commonly used abbreviations

A	adenine
aa	amino acid
ADCC	antibody dependent cellular cytotoxicity
AE	anionic exchanger
Amp	ampicillin
APS	ammonium persulfate
ATP	adenosintriphosphat
ATZ	acetazolamide
bp	base pair
BSA	bovine serum albumin
C	cytosine
CA	carbonic anhydrase
CA domain	carbonic anhydrase domain, catalytically active domain
CA IX	carbonic anhydrase IX
CDR	complementarity determining region
DAPI	4',6-Diamidino-2-phenylindole
dH_2O	deionised water
DMEM	Dulbecco's modified eagle medium
DMOG	dimethyloxaloylglycin
DMSO	dimethyl sulfoxide
DNA	desoxyribonucleic acid
dNTP	deoxyribonucleotide
DTT	dithiothreitol; IUPAC: (*2S*,*3S*)-1,4-Bis-sulfanylbutane-2,3-diol
E. coli	Escherichia coli
EDTA	ethylenediaminetetraacetic acid
ELISA	enzyme linked immuno sorbant assay
EtBr	ethidium bromide; IUPAC: 3,8-Diamino-5-ethyl-6-phenylphenanthridinium bromide
EtOH	ethanol
Fab	fragment, antigen binding
FAP	fibroblast activation protein
FBS	fetal bovine serum
Fc	fragment, crystallisable
FITC	Fluorescein isothiocyanate
G	guanine
GMFI	geometric mean fluorescence intensity
HC	heavy chain
HEK	human embryonic kidney
Hepes	2-[4-(2-hydroxyethyl)piperazin-1-yl]ethanesulfonic acid
HEPES	4-(2-hydroxyethyl)-1-piperazineethanesulfonic acid
HIF	hypoxia inducible factor

HIF-1	hypoxia inducible factor 1
HLH	helix-loop-helix
HRP	horseradish peroxidase
hu	human
IC domain	intracellular domain of CA IX
IFN	interferon
Ig	immunoglobulin
IgG	immunoglobulin G
IL	interleukin
IPTG	isopropyl-β-thiogalaktopyranoside
Kan	kanamycin
kb	kilo base pair
KCl	potassium chloride
kDa	kilo dalton
K-gluconate	potassium gluconate
LB	Luria-Bertani broth
LC	light chain
MCF-7	Michigan Cancer Foundation - 7
MDCK	Madin Darby canine kidney
MES	2-(*N*-morpholino)ethanesulfonic acid
mRNA	messenger ribonucleic acid
MSX	L-methionine sulphoximine
mu	murine
NCBI	National Center for Biotechnology Information
NGS	normal goat serum
nt	nucleotide
o/n	over night
OD	optical density at
ORF	open reading frame
PCR	polymerase chain reaction
PE	*R*-phycoerythrin
PEG	polyethylene glycol 6000
PFA	paraformaldehyde
pfu	plaque forming unit
PG domain	proteoglycan-like attachment domain of CA IX
pH_e	extracellular pH
pH_i	intracellular pH
pH_s	surface pH
PI3K	phosphatidylinositol 3-kinase
pVHL	von Hippel-Lindau protein
rhCA II	recombinant human carbonic anhydrase II
rhCA IX	recombinant human carbonic anhydrase IX
rhCA XII	recombinant human carbonic anhydrase XII
rhCA XIV	recombinant human carbonic anhydrase XIV
rmCA IX	recombinant mouse carbonic anhydrase IX

RNA	ribonucleic acid
RPMI	Roswell Park Memorial Institute *(cell culture medium)*
RU	response units
SDS	sodium dodecylsulfate
SDS-PAGE	sodiumdodecylsulfate polyacrylamid gel electrophoresis
T	thymine
TAE	tris-acetate-EDTA buffer
TEMED	tetramethylethylenediamine
Tet	tetracycline
TM domain	transmembrane domain of CA IX
TNF	tumour necrosis factor
Tris	tris(hydroxymethyl)aminomethane
TY	yeast tryptone
UV	ultraviolet
VHL	von Hippel-Lindau
β-OG	octyl β-D-glucopyranoside

5.2.2 Commonly used units

%	percent
% v/v	percent volume per volume
% w/v	percent weight per volume
°C	degree Celsius
d	day
g	gram
h	hour
l	litre
M	molar
mg	milliogram
ml	millilitre
mM	millimolar
mol	mole
nM	nanomolar
rpm	revolutions per minute
s	second
u	unit
µg	microgram
µl	microlitre
µM	micromolar

5.2.3 Chemical formula

$CaCl_2$	calcium chloride
$CoCl_2$	cobalt chloride / cobalt(II) chloride
H_2SO_4	sulphuric acid
HCl	hydrochloric acid
KCl	potassium chloride
KH_2PO_4	potassium dihydrogen phosphate
$MgCl_2$	magnesium chloride
Na_2HPO_4	disodium hydrogen phosphate
NaCl	sodium chloride
$NaHCO_3$	sodium bicarbonate; IUPAC: sodium hydrogen carbonate
NaOH	sodium hydroxide
NH4Cl	ammonium chloride

5.3 LIST OF FIGURES

5.4 LIST OF TABLES

6 BIBLIOGRAPHY

(2009). "Monoclonal Antibody Therapy (Rencarex®) in Treating Patients Who Have Undergone Surgery for Non-metastatic Kidney Cancer." 2010, from http://clinicaltrials.gov/ct2/show/NCT00087022.

Abbate, F., A. Casini, et al. (2004). "Carbonic anhydrase inhibitors: E7070, a sulfonamide anticancer agent, potently inhibits cytosolic isozymes I and II, and transmembrane, tumor-associated isozyme IX." Bioorg Med Chem Lett **14**(1): 217-223.

Ahlskog, J. K., C. Schliemann, et al. (2009). "Human monoclonal antibodies targeting carbonic anhydrase IX for the molecular imaging of hypoxic regions in solid tumours." Br J Cancer **101**(4): 645-657.

Alterio, V., M. Hilvo, et al. (2009). "Crystal structure of the catalytic domain of the tumor-associated human carbonic anhydrase IX." Proc Natl Acad Sci U S A **106**(38): 16233-16238.

Alterio, V., R. M. Vitale, et al. (2006). "Carbonic anhydrase inhibitors: X-ray and molecular modeling study for the interaction of a fluorescent antitumor sulfonamide with isozyme II and IX." J Am Chem Soc **128**(25): 8329-8335.

Alvarez, B. V., G. L. Vilas, et al. (2005). "Metabolon disruption: a mechanism that regulates bicarbonate transport." EMBO J **24**(14): 2499-2511.

Arsham, A. M., D. R. Plas, et al. (2002). "Phosphatidylinositol 3-kinase/Akt signaling is neither required for hypoxic stabilization of HIF-1 alpha nor sufficient for HIF-1-dependent target gene transcription." J Biol Chem **277**(17): 15162-15170.

Asikainen, T. M., A. Ahmad, et al. (2005). "Stimulation of HIF-1alpha, HIF-2alpha, and VEGF by prolyl 4-hydroxylase inhibition in human lung endothelial and epithelial cells." Free Radic Biol Med **38**(8): 1002-1013.

Barlow, J. H., N. Lowe, et al. (1987). "Human carbonic anhydrase I cDNA." Nucleic Acids Res **15**(5): 2386.

Bauer, S., J. C. Oosterwijk-Wakka, et al. (2009). "Targeted therapy of renal cell carcinoma: synergistic activity of cG250-TNF and IFNg." Int J Cancer **125**(1): 115-123.

Bleumer, I., A. Knuth, et al. (2004). "A phase II trial of chimeric monoclonal antibody G250 for advanced renal cell carcinoma patients." Br J Cancer **90**(5): 985-990.

Bleumer, I., E. Oosterwijk, et al. (2006). "A clinical trial with chimeric monoclonal antibody WX-G250 and low dose interleukin-2 pulsing scheme for advanced renal cell carcinoma." J Urol **175**(1): 57-62.

Brouwers, A. H., C. Frielink, et al. (2003). "Interferons can upregulate the expression of the tumor associated antigen G250-MN/CA IX, a potential target for (radio)immunotherapy of renal cell carcinoma." Cancer Biother Radiopharm **18**(4): 539-547.

Brouwers, A. H., P. F. Mulders, et al. (2005). "Lack of efficacy of two consecutive treatments of radioimmunotherapy with 131I-cG250 in patients with metastasized clear cell renal cell carcinoma." J Clin Oncol **23**(27): 6540-6548.

Carmeliet, P. and R. K. Jain (2000). "Angiogenesis in cancer and other diseases." Nature **407**(6801): 249-257.

Carter, P. and A. M. Merchant (1997). "Engineering antibodies for imaging and therapy." Curr Opin Biotechnol **8**(4): 449-454.

Casey, J. R., P. E. Morgan, et al. (2004). "Carbonic anhydrase inhibitors. Design of selective, membrane-impermeant inhibitors targeting the human tumor-associated isozyme IX." J

Med Chem **47**(9): 2337-2347.

Chiche, J., K. Ilc, et al. (2009). "Hypoxia-inducible carbonic anhydrase IX and XII promote tumor cell growth by counteracting acidosis through the regulation of the intracellular pH." Cancer Res **69**(1): 358-368.

Chrastina, A., J. Zavada, et al. (2003). "Biodistribution and pharmacokinetics of 125I-labeled monoclonal antibody M75 specific for carbonic anhydrase IX, an intrinsic marker of hypoxia, in nude mice xenografted with human colorectal carcinoma." Int J Cancer **105**(6): 873-881.

Davis, I. D., Z. Liu, et al. (2007). "A pilot study of monoclonal antibody cG250 and low dose subcutaneous IL-2 in patients with advanced renal cell carcinoma." Cancer Immun **7**: 14.

de Haard, H. J., N. van Neer, et al. (1999). "A large non-immunized human Fab fragment phage library that permits rapid isolation and kinetic analysis of high affinity antibodies." J Biol Chem **274**(26): 18218-18230.

De Simone, G., R. M. Vitale, et al. (2006). "Carbonic anhydrase inhibitors: Hypoxia-activatable sulfonamides incorporating disulfide bonds that target the tumor-associated isoform IX." J Med Chem **49**(18): 5544-5551.

Di Fiore, A., G. De Simone, et al. (2005). "Carbonic anhydrase inhibitors: X-ray crystal structure of a benzenesulfonamide strong CA II and CA IX inhibitor bearing a pentafluorophenylaminothioureido tail in complex with isozyme II." Bioorg Med Chem Lett **15**(7): 1937-1942.

Di Fiore, A., C. Pedone, et al. (2006). "Carbonic anhydrase inhibitors: Valdecoxib binds to a different active site region of the human isoform II as compared to the structurally related cyclooxygenase II "selective" inhibitor celecoxib." Bioorg Med Chem Lett **16**(2): 437-442.

Divgi, C. R., N. H. Bander, et al. (1998). "Phase I/II radioimmunotherapy trial with iodine-131-labeled monoclonal antibody G250 in metastatic renal cell carcinoma." Clin Cancer Res **4**(11): 2729-2739.

Divgi, C. R., N. Pandit-Taskar, et al. (2007). "Preoperative characterisation of clear-cell renal carcinoma using iodine-124-labelled antibody chimeric G250 (124I-cG250) and PET in patients with renal masses: a phase I trial." Lancet Oncol **8**(4): 304-310.

Doege, K. J., M. Sasaki, et al. (1991). "Complete coding sequence and deduced primary structure of the human cartilage large aggregating proteoglycan, aggrecan. Human-specific repeats, and additional alternatively spliced forms." J Biol Chem **266**(2): 894-902.

Dubois, L., K. Douma, et al. (2007). "Imaging the hypoxia surrogate marker CA IX requires expression and catalytic activity for binding fluorescent sulfonamide inhibitors." Radiother Oncol **83**(3): 367-373.

Ebert, B. L., J. D. Firth, et al. (1995). "Hypoxia and mitochondrial inhibitors regulate expression of glucose transporter-1 via distinct Cis-acting sequences." J Biol Chem **270**(49): 29083-29089.

Forsythe, J. A., B. H. Jiang, et al. (1996). "Activation of vascular endothelial growth factor gene transcription by hypoxia-inducible factor 1." Mol Cell Biol **16**(9): 4604-4613.

Fujikawa-Adachi, K., I. Nishimori, et al. (1999). "Human mitochondrial carbonic anhydrase VB. cDNA cloning, mRNA expression, subcellular localization, and mapping to chromosome x." J Biol Chem **274**(30): 21228-21233.

Gnarra, J. R., K. Tory, et al. (1994). "Mutations of the VHL tumour suppressor gene in renal carcinoma." Nat Genet **7**(1): 85-90.

Grabmaier, K., J. L. Vissers, et al. (2000). "Molecular cloning and immunogenicity of renal cell carcinoma-associated antigen G250." Int J Cancer **85**(6): 865-870.

Gut, M. O., S. Parkkila, et al. (2002). "Gastric hyperplasia in mice with targeted disruption of the carbonic anhydrase gene Car9." Gastroenterology **123**(6): 1889-1903.

Helmlinger, G., A. Sckell, et al. (2002). "Acid production in glycolysis-impaired tumors provides new insights into tumor metabolism." Clin Cancer Res **8**(4): 1284-1291.

Helmlinger, G., F. Yuan, et al. (1997). "Interstitial pH and pO2 gradients in solid tumors in vivo: high-resolution measurements reveal a lack of correlation." Nat Med **3**(2): 177-182.

Hewett-Emmett, D. and R. E. Tashian (1996). "Functional diversity, conservation, and convergence in the evolution of the alpha-, beta-, and gamma-carbonic anhydrase gene families." Mol Phylogenet Evol **5**(1): 50-77.

Hilvo, M., L. Baranauskiene, et al. (2008). "Biochemical characterization of CA IX, one of the most active carbonic anhydrase isozymes." J Biol Chem **283**(41): 27799-27809.

Hilvo, M., M. Tolvanen, et al. (2005). "Characterization of CA XV, a new GPI-anchored form of carbonic anhydrase." Biochem J **392**(Pt 1): 83-92.

Hockel, M. and P. Vaupel (2001). "Tumor hypoxia: definitions and current clinical, biologic, and molecular aspects." J Natl Cancer Inst **93**(4): 266-276.

Huang, L. E., Z. Arany, et al. (1996). "Activation of hypoxia-inducible transcription factor depends primarily upon redox-sensitive stabilization of its alpha subunit." J Biol Chem **271**(50): 32253-32259.

Huang, L. E., R. S. Bindra, et al. (2007). "Hypoxia-induced genetic instability--a calculated mechanism underlying tumor progression." J Mol Med **85**(2): 139-148.

Huang, L. E., J. Gu, et al. (1998). "Regulation of hypoxia-inducible factor 1alpha is mediated by an O2-dependent degradation domain via the ubiquitin-proteasome pathway." Proc Natl Acad Sci U S A **95**(14): 7987-7992.

Hulikova, A., M. Zatovicova, et al. (2009). "Intact intracellular tail is critical for proper functioning of the tumor-associated, hypoxia-regulated carbonic anhydrase IX." FEBS Lett **583**(22): 3563-3568.

Ivanov, S. V., I. Kuzmin, et al. (1998). "Down-regulation of transmembrane carbonic anhydrases in renal cell carcinoma cell lines by wild-type von Hippel-Lindau transgenes." Proc Natl Acad Sci U S A **95**(21): 12596-12601.

Jaakkola, P., D. R. Mole, et al. (2001). "Targeting of HIF-alpha to the von Hippel-Lindau ubiquitylation complex by O2-regulated prolyl hydroxylation." Science **292**(5516): 468-472.

Kaluz, S., M. Kaluzova, et al. (2002). "Lowered oxygen tension induces expression of the hypoxia marker MN/carbonic anhydrase IX in the absence of hypoxia-inducible factor 1 alpha stabilization: a role for phosphatidylinositol 3'-kinase." Cancer Res **62**(15): 4469-4477.

Kuroki, M., J. Huang, et al. (2006). "Possible applications of antibodies or their genes in cancer therapy." Anticancer Res **26**(6A): 4019-4025.

Lehtonen, J., B. Shen, et al. (2004). "Characterization of CA XIII, a novel member of the carbonic anhydrase isozyme family." J Biol Chem **279**(4): 2719-2727.

Li, G., M. Cuilleron, et al. (2003). "Rapid and sensitive detection of messenger RNA expression for molecular differential diagnosis of renal cell carcinoma." Clin Cancer Res **9**(17): 6441-6446.

Lilleby, W. and S. D. Fossa (2005). "Chemotherapy in metastatic renal cell cancer." World J Urol **23**(3): 175-179.

Liu, Z., F. E. Smyth, et al. (2002). "Anti-renal cell carcinoma chimeric antibody G250: cytokine enhancement of in vitro antibody-dependent cellular cytotoxicity." Cancer Immunol

Immunother **51**(3): 171-177.

Loiselle, F. B., P. E. Morgan, et al. (2004). "Regulation of the human NBC3 Na+/HCO3- cotransporter by carbonic anhydrase II and PKA." Am J Physiol Cell Physiol **286**(6): C1423-1433.

Mann, T. and D. Keilin (1940). "Sulphanilamide as a Specific Inhibitor of Carbonic Anhydrase." Nature **146**: 164-165.

Maxwell, P. H., M. S. Wiesener, et al. (1999). "The tumour suppressor protein VHL targets hypoxia-inducible factors for oxygen-dependent proteolysis." Nature **399**(6733): 271-275.

Menchise, V., G. De Simone, et al. (2005). "Carbonic anhydrase inhibitors: stacking with Phe131 determines active site binding region of inhibitors as exemplified by the X-ray crystal structure of a membrane-impermeant antitumor sulfonamide complexed with isozyme II." J Med Chem **48**(18): 5721-5727.

Montgomery, J. C., P. J. Venta, et al. (1987). "Nucleotide sequence of human liver carbonic anhydrase II cDNA." Nucleic Acids Res **15**(11): 4687.

Morgan, P. E., S. Pastorekova, et al. (2007). "Interactions of transmembrane carbonic anhydrase, CAIX, with bicarbonate transporters." Am J Physiol Cell Physiol **293**(2): C738-748.

Motzer, R. J., P. Russo, et al. (1997). "Renal cell carcinoma." Curr Probl Cancer **21**(4): 185-232.

Nagao, Y., J. S. Platero, et al. (1993). "Human mitochondrial carbonic anhydrase: cDNA cloning, expression, subcellular localization, and mapping to chromosome 16." Proc Natl Acad Sci U S A **90**(16): 7623-7627.

Nishimori, I., D. Vullo, et al. (2005). "Carbonic anhydrase inhibitors. The mitochondrial isozyme VB as a new target for sulfonamide and sulfamate inhibitors." J Med Chem **48**(24): 7860-7866.

Ohh, M., C. W. Park, et al. (2000). "Ubiquitination of hypoxia-inducible factor requires direct binding to the beta-domain of the von Hippel-Lindau protein." Nat Cell Biol **2**(7): 423-427.

Oosterwijk, E., N. H. Bander, et al. (1993). "Antibody localization in human renal cell carcinoma: a phase I study of monoclonal antibody G250." J Clin Oncol **11**(4): 738-750.

Oosterwijk, E., D. J. Ruiter, et al. (1986). "Monoclonal antibody G 250 recognizes a determinant present in renal-cell carcinoma and absent from normal kidney." Int J Cancer **38**(4): 489-494.

Opavsky, R., S. Pastorekova, et al. (1996). "Human MN/CA9 gene, a novel member of the carbonic anhydrase family: structure and exon to protein domain relationships." Genomics **33**(3): 480-487.

Pan, P., M. Leppilampi, et al. (2006). "Carbonic anhydrase gene expression in CA II-deficient (Car2-/-) and CA IX-deficient (Car9-/-) mice." J Physiol **571**(Pt 2): 319-327.

Parkkila, S., A. K. Parkkila, et al. (1994). "Distribution of the carbonic anhydrase isoenzymes I, II, and VI in the human alimentary tract." Gut **35**(5): 646-650.

Pastorek, J., S. Pastorekova, et al. (1994). "Cloning and characterization of MN, a human tumor-associated protein with a domain homologous to carbonic anhydrase and a putative helix-loop-helix DNA binding segment." Oncogene **9**(10): 2877-2888.

Pastorekova, S., S. Parkkila, et al. (2004). "Carbonic anhydrases: current state of the art, therapeutic applications and future prospects." J Enzyme Inhib Med Chem **19**(3): 199-229.

Pastorekova, S. and J. Pastorek (2004). Cancer-Related Carbonic Anhydrase Isozymes and Their Inhibition. Carbonic Anhydrase. Its Inhibitors and Activators. C. Supuran, CRC Press**:** 255-281.

Pastorekova, S., Z. Zavadova, et al. (1992). "A novel quasi-viral agent, MaTu, is a two-component

system." Virology **187**(2): 620-626.

Pore, N., Z. Jiang, et al. (2006). "Akt1 activation can augment hypoxia-inducible factor-1alpha expression by increasing protein translation through a mammalian target of rapamycin-independent pathway." Mol Cancer Res **4**(7): 471-479.

Rafajova, M., M. Zatovicova, et al. (2004). "Induction by hypoxia combined with low glucose or low bicarbonate and high posttranslational stability upon reoxygenation contribute to carbonic anhydrase IX expression in cancer cells." Int J Oncol **24**(4): 995-1004.

Raghunand, N., X. He, et al. (1999). "Enhancement of chemotherapy by manipulation of tumour pH." Br J Cancer **80**(7): 1005-1011.

Schofield, C. J. and P. J. Ratcliffe (2004). "Oxygen sensing by HIF hydroxylases." Nat Rev Mol Cell Biol **5**(5): 343-354.

Scozzafava, A., F. Briganti, et al. (2000). "Carbonic anhydrase inhibitors: synthesis of membrane-impermeant low molecular weight sulfonamides possessing in vivo selectivity for the membrane-bound versus cytosolic isozymes." J Med Chem **43**(2): 292-300.

Shafee, N., S. Kaluz, et al. (2009). "PI3K/Akt activity has variable cell-specific effects on expression of HIF target genes, CA9 and VEGF, in human cancer cell lines." Cancer Lett **282**(1): 109-115.

Shweiki, D., A. Itin, et al. (1992). "Vascular endothelial growth factor induced by hypoxia may mediate hypoxia-initiated angiogenesis." Nature **359**(6398): 843-845.

Silacci, M., S. Brack, et al. (2005). "Design, construction, and characterization of a large synthetic human antibody phage display library." Proteomics **5**(9): 2340-2350.

Sly, W. S. and P. Y. Hu (1995). "Human carbonic anhydrases and carbonic anhydrase deficiencies." Annu Rev Biochem **64**: 375-401.

Smith, G. P. and V. A. Petrenko (1997). "Phage Display." Chem Rev **97**(2): 391-410.

Steffens, M. G., O. C. Boerman, et al. (1999). "Phase I radioimmunotherapy of metastatic renal cell carcinoma with 131I-labeled chimeric monoclonal antibody G250." Clin Cancer Res **5**(10 Suppl): 3268s-3274s.

Sterling, D., B. V. Alvarez, et al. (2002). "The extracellular component of a transport metabolon. Extracellular loop 4 of the human AE1 Cl-/HCO3- exchanger binds carbonic anhydrase IV." J Biol Chem **277**(28): 25239-25246.

Sterling, D., R. A. Reithmeier, et al. (2001). "A transport metabolon. Functional interaction of carbonic anhydrase II and chloride/bicarbonate exchangers." J Biol Chem **276**(51): 47886-47894.

Stillebroer, A. B., P. F. Mulders, et al. (2010). "Carbonic Anhydrase IX in Renal Cell Carcinoma: Implications for Prognosis, Diagnosis, and Therapy." Eur Urol.

Stubbs, M., P. M. McSheehy, et al. (2000). "Causes and consequences of tumour acidity and implications for treatment." Mol Med Today **6**(1): 15-19.

Supuran, C. (2004). Carbonic Anhydrases: Catalytic and Inhibition Mechanisms, Distribution and Physiological Roles. Carbonic Anhydrase. Its Inhibitors and Activators. C. Supuran, CRC Press**:** 1-23.

Svastova, E., A. Hulikova, et al. (2004). "Hypoxia activates the capacity of tumor-associated carbonic anhydrase IX to acidify extracellular pH." FEBS Lett **577**(3): 439-445.

Svastova, E., N. Zilka, et al. (2003). "Carbonic anhydrase IX reduces E-cadherin-mediated adhesion of MDCK cells via interaction with beta-catenin." Exp Cell Res **290**(2): 332-345.

Swietach, P., S. Patiar, et al. (2009). "The role of carbonic anhydrase 9 in regulating extracellular and intracellular ph in three-dimensional tumor cell growths." J Biol Chem **284**(30):

20299-20310.

Swietach, P., R. D. Vaughan-Jones, et al. (2007). "Regulation of tumor pH and the role of carbonic anhydrase 9." Cancer Metastasis Rev **26**(2): 299-310.

Swietach, P., S. Wigfield, et al. (2008). "Tumor-associated carbonic anhydrase 9 spatially coordinates intracellular pH in three-dimensional multicellular growths." J Biol Chem **283**(29): 20473-20483.

Swietach, P., S. Wigfield, et al. (2008). "Cancer-associated, hypoxia-inducible carbonic anhydrase IX facilitates CO2 diffusion." BJU Int **101 Suppl 4**: 22-24.

Tabrizi, M., G. G. Bornstein, et al. (2010). "Biodistribution mechanisms of therapeutic monoclonal antibodies in health and disease." AAPS J **12**(1): 33-43.

Thiry, A., J. M. Dogne, et al. (2006). "Targeting tumor-associated carbonic anhydrase IX in cancer therapy." Trends Pharmacol Sci **27**(11): 566-573.

Triantafyllou, A., P. Liakos, et al. (2006). "Cobalt induces hypoxia-inducible factor-1alpha (HIF-1alpha) in HeLa cells by an iron-independent, but ROS-, PI-3K- and MAPK-dependent mechanism." Free Radic Res **40**(8): 847-856.

Troost, E. G., J. Bussink, et al. (2005). "Comparison of different methods of CAIX quantification in relation to hypoxia in three human head and neck tumor lines." Radiother Oncol **76**(2): 194-199.

Tureci, O., U. Sahin, et al. (1998). "Human carbonic anhydrase XII: cDNA cloning, expression, and chromosomal localization of a carbonic anhydrase gene that is overexpressed in some renal cell cancers." Proc Natl Acad Sci U S A **95**(13): 7608-7613.

Velders, M. P., S. V. Litvinov, et al. (1994). "New chimeric anti-pancarcinoma monoclonal antibody with superior cytotoxicity-mediating potency." Cancer Res **54**(7): 1753-1759.

Vince, J. W. and R. A. Reithmeier (1998). "Carbonic anhydrase II binds to the carboxyl terminus of human band 3, the erythrocyte C1-/HCO3- exchanger." J Biol Chem **273**(43): 28430-28437.

Wang, G. L., B. H. Jiang, et al. (1995). "Hypoxia-inducible factor 1 is a basic-helix-loop-helix-PAS heterodimer regulated by cellular O2 tension." Proc Natl Acad Sci U S A **92**(12): 5510-5514.

Wang, G. L. and G. L. Semenza (1993). "Desferrioxamine induces erythropoietin gene expression and hypoxia-inducible factor 1 DNA-binding activity: implications for models of hypoxia signal transduction." Blood **82**(12): 3610-3615.

Wang, G. L. and G. L. Semenza (1995). "Purification and characterization of hypoxia-inducible factor 1." J Biol Chem **270**(3): 1230-1237.

Wang, Y., X. Y. Wang, et al. (2008). "Carbonic anhydrase IX has chaperone-like functions and is an immunoadjuvant." Mol Cancer Ther **7**(12): 3867-3877.

Weber, A., A. Casini, et al. (2004). "Unexpected nanomolar inhibition of carbonic anhydrase by COX-2-selective celecoxib: new pharmacological opportunities due to related binding site recognition." J Med Chem **47**(3): 550-557.

Wykoff, C. C., N. J. Beasley, et al. (2000). "Hypoxia-inducible expression of tumor-associated carbonic anhydrases." Cancer Res **60**(24): 7075-7083.

Xu, C., A. Lo, et al. (2010). "Unique biological properties of catalytic domain directed human anti-CAIX antibodies discovered through phage-display technology." PLoS One **5**(3): e9625.

Yuan, Y., G. Hilliard, et al. (2003). "Cobalt inhibits the interaction between hypoxia-inducible factor-alpha and von Hippel-Lindau protein by direct binding to hypoxia-inducible factor-alpha." J Biol Chem **278**(18): 15911-15916.

Zat'ovicova, M., K. Tarabkova, et al. (2003). "Monoclonal antibodies generated in carbonic anhydrase IX-deficient mice recognize different domains of tumour-associated hypoxia-induced carbonic anhydrase IX." J Immunol Methods **282**(1-2): 117-134.

Zatovicova, M., L. Jelenska, et al. (2010). "Carbonic Anhydrase IX as an Anticancer therapy Target: Preclinical Evaluation of Internalizing Monoclonal Antibody Directed to Catalytic Domain." Curr Pharm Des.

Zavada, J., Z. Zavadova, et al. (2000). "Human tumour-associated cell adhesion protein MN/CA IX: identification of M75 epitope and of the region mediating cell adhesion." Br J Cancer **82**(11): 1808-1813.

Zhu, X. L. and W. S. Sly (1990). "Carbonic anhydrase IV from human lung. Purification, characterization, and comparison with membrane carbonic anhydrase from human kidney." J Biol Chem **265**(15): 8795-8801.

7 ACKNOWLEDGEMENTS

I would like to express my gratitude to all the people supporting me during my thesis. Special thanks go to:

- Prof. Dr. med. Christoph Renner who gave me the opportunity to work in his lab for the support and guidance during the past four years. It was a great chance to learn many new and interesting techniques.
- my supervisor Dr. med. Stefan Bauer who initiated this intriguing project, helped promoting this work and supported me during those years.
- my PhD committee Prof. Dr. Roland Wenger and Prof. Dr. med. Holger Moch for their time and valuable input in the project. I especially thank Prof. Dr. Roland Wenger for the opportunity to perform the hypoxic experiments in his lab.
- Dr. Daniel Stiehl and Patrick Spielmann for their kindness and the help with the hypoxic chamber. I appreciate the interesting scientific discussions I had with Dr. Daniel Stiehl.
- the whole lab of Oxford for the warm welcome in Oxford, where I had the chance to perform all the inhibitory assays with Dr. Pawel Swietach and Dr. Alzbeta Hulikova during two months. It was great to have the opportunity to work with them and learn so much about physiology. Thanks for the good collaboration.
- Dr. Stefan Schauer from the Functional Genomics Center Zurich who introduced me to surface plasmon resonance for his valuable advices.
- Dr. Steffi Lehmann for helping me with the immunofluorescence of tumour sections and for her friendship.
- Prof. Dr. med. Alexander Knuth, Prof. Dr. Egbert Oosterwijk, Prof. Dr. Andrew Scott, Prof. Dr. Gerd Ritter and Prof. Dr. Lloyd Old from the Ludwig Institute for Cancer Research for the good collaboration.
- Dr. Hiroyoshi Nishikawa (Mie, Japan) and Prof. Dr. Markus Rudin (Zurich, Switzerland) for providing cell lines and tumour sections.
- all former and current members of the lab for their help and the good time. I especially thank Dr. Thomas Wüest, who always took the time to help and to explain things, for sharing his experience, for the helpful discussions and his assistance revising my thesis. I'm very thankful to Nadia Jaouad, Petra Schuberth and Dr. Tanja Burckhart for their friendship.
- my family and especially my husband Samuel for their caring support and encouragement.

8 CURRICULUM VITAE

Name	MURRI-PLESKO
Vorname	Margarita Theresa
Geburtsdatum	28. Juli 1981
Heimatort	Winterthur ZH und Köniz BE

Ausbildung

Seit Nov. 2006	Doktorarbeit: „Selection and Characterization of Antibodies Blocking the Enzymatic Activity of the Tumour Associated Carbonic Anhydrase IX", Universität Zürich, Institut für Onkologie, Prof. Dr. med. C. Renner
2005 – 2010	Höheres Lehramt in Biologie und Chemie, ETH Zürich
Okt. 2005	Abschluss als Dipl. natw. ETH, ETH Zürich
2003 – 2005	Fachstudium Mikrobiologie, ETH Zürich
	Diplomarbeit: "Modificatios of the Semliki Forest Virus Replicon to Enhance Expression Efficiency", Universität Zürich, Institut für medizinische Virologie, PD Dr. J. Pavlovic
2001 – 2003	Grundstudium Biologie, chemische Richtung, ETH Zürich
1994 – 2001	Literargymnasium Rämibühl, Zürich
	Maturität Typus A

Publikationen

Murri-Plesko, M. T., A. Hulikova, et al. (2011). "Antibody inhibiting enzymatic activity of tumour-associated carbonic anhydrase isoform IX." Eur J Pharmacol.

Bauer, S., N. Adrian, et al. (2009). "Sequential cancer immunotherapy: targeted activity of dimeric TNF and IL-8". Cancer Immun **9**: 2.